Selected contributions in Physical Cosmology

Pier Stefano Corasaniti

Laboratoire Univers et Theories

CNRS, Observatoire de Paris & Université Paris Diderot

Président du Jury:	Prof. Jim BARTLETT
Rapporteurs:	Dr. Martin BUCHER
	Prof. Christian MARINONI
	Prof. Joe SILK
Examinateurs:	Dr. Jean-Michel ALIMI
	Dr. Philippe BRAX
	Dr. Hervé DOLE

Presented for the "Habilitation á Diriger des Recherches"

13 December 2013

Amphithéâtre Evry Schatzman

Observatoire de Paris, Meudon Campus

Acknowledgements

I am greateful to all people around the globe that over these many years I had the fortune to encounter and who have enriched my research. A special thanks to my close collaborators Jean-Michel Alimi and Yann Rasera, it is with them that I walk the paths that explore the invisible universe, without their dedication most of these routes will still be unknown. I am thankful to all the members of the jury for the time they have dedicated to me. If they have been asked to participate is because in different occasions and at different times I have discussed with them and had the chance to learn from them. Most of all I owe my wonderful wife, my two beautiful girls and my parents a debt of gratitude for their love, support and patience that allow me to pursue my bizarre endeavours.

Université Paris Diderot, Paris 7

Selected contributions in Physical Cosmology

Pier Stefano Corasaniti

Submitted for the "Habilitation á Diriger des Recherches"

May 2013

Abstract

This document contains a summary of my research activity, career achievements and student project supervision. My work has been mainly driven by the quest for Dark Energy in the Universe, a topic that is central to modern cosmology and which I believe has much deeper connections with other open problems in theoretical physics and extra-galactic astrophysics. Pursuing such an ambitious quest has naturally led me to investigate a large variety of topics in Cosmology. Because of this a complete presentation of the work done since my doctorate would have demanded a too lengthy dissertation. Hence, in the spirit of the HDR, I preferred to limit the discussion to a few selected works, focusing particularly on those which have involved the supervision of undergraduate and graduate students.

To the memory of my grandmother Rosina

Foreword

The reader who has no experience of the French Higher Education system might wonder what "Habilitation à Diriger des Rercherches" (HDR) stands for. In several countries the PhD is the ultimate academic degree necessary to pursue an academic career. In others including France, Germany, Switzerland, Sweden to mention a few, the HDR "is the highest academic qualification a scholar can achieve"[1]. If the HDR is an academic degree for PhDs only, then what does it entitle to?

In France holding a PhD does not certificate the ability of fully mastering all aspects of research work. This is why PhD holders still need to proof their aptitude to "diriger des recherches", which can be translated as supervising, running and managing research projects. Proof comes from the very ultimate academic degree, the HDR, established in 1984 by the "Savary law" and subsequently regulated by a series of decrees in 1988, 1992, 1995 and 2002. The HDR is an academic degree that allows the holder to officially supervise PhD students. It is mandatory for full professor positions at universities and, though not formally required for Research Director (DR) positions at CNRS, it is certainly an added value. In fact, as member of the "Comité Nationale" of Section 17 of CNRS I can tell you that one is better off having it than not. The HDR is not only the ultimate academic degree in France, but also the ultimate academic career certification. Quite interestingly though, the rules to obtain the HDR appear to be rather inconsistent across different institutions. Moreover, legal code only gives a list of recommendations about the content of the HDR application. More or less everything is left to the interpretation of local

---

[1]Citation from http://en.wikipedia.org/wiki/Habilitation

administrators. The advantage of applying for the HDR at Paris 7 is that at least their requirements are clearly stated on their website. One needs to submit a document which contains a summary of the scientific activity or one or more published papers. This can be in a format that includes a CV, a summary of student project supervision, description of the research and its originality, future perspectives and a list or copies of national and international publications. At this point if you are still confused about what this document should contain do not panic. As stated in the "Circulaire" 89-004 in application to the decree of 23 November 1988, the HDR is not a PhD or better still it is not a second PhD. So I can tell you what this document is certainly not: a PhD thesis. It is not intended to be a PhD thesis and it will not be one. Nevertheless, you should still find sufficient information that can demonstrate I have the ability to "diriger des recherches".

Contents

Curriculum Vitae

Current Position

- CNRS senior research scientist (CR1) at *'Laboratoire Univers et Theories'* (LUTH) of the Astronomical Observatory of Paris.

Positions Held

- 2006 - 2007: Postdoctoral research at Laboratoire Universe et ses Theories (LUTH), Astronomical Observatory of Paris-Meudon. Director: Prof. Jean-Michel Alimi.

- 2003 - 2006: Postdoctoral research at the Institute for String Cosmology and Astroparticle Physics (ISCAP), Columbia University. Institute Directors: Prof. Brian Greene and Prof. Arlin Crotts.

Education

- 2000 - 2003: Ph.D. in Physics, University of Sussex, Brighton (UK). Advisor: Prof. E.J. Copeland. Thesis Title: *"Phenomenological Aspects of Dark Energy Dominated Cosmologies"*

- 1994 - 1999: *Laurea* in Physics, 110/110 magna cum laude, University of Rome I, Rome (Italy). Advisors: Prof. F. Occhionero and Prof. L. Amendola. Thesis Title: *"Simulation and detection of non-gaussian signals in the Cosmic Microwave Background radiation"*

Grants & Awards

- ERC-Starting Grant 5-yr project, "Exploring Dark Energy through Cosmic Structures" (EDECS), 1.5 M€ funded by the European Research Council, Brussels (Belgium), July 2011.

- Ogden Prize for top Ph.D. thesis in Cosmology awarded by the University of Durham (UK), July 2004.

- Tito Maiani Award for top *Laurea* thesis in Cosmology awarded by *Accademia dei Lincei* (Italian Academy of Science), June 2001.

Summary of Research Interests

- Dark Energy Phenomenology, Structure Formation and N-body Simulations, Cosmic Microwave Background, Cosmological Data Analysis, Test of Inflation, Extragalactic Astrophysics

- Bayesian Statistics, Monte Carlo Simulations, Computational Methods Applied to Cosmology, Biophysics and Finance

Participation to International Projects

- XMM-XXL Galaxy Cluster Survey Consortium

- Euclid-ESA Mission Consortium

- Dark Energy Universe Simulations (DEUS) Consortium

PhD students

- Linda Blot, "Cosmological Simulations of Clustered Dark Energy Models", 2012-present, Observatoire de Paris-Meudon, Paris

- Irene Balmes, "Gravitational Lensing Time Delays and Dark Matter Halo Structures in non-Standard Cosmologies", 2009-present, Observatoire de Paris-Meudon, Paris

- Ixandra Achitouv, "Dark Matter Halo Mass Function: Imprints of the Initial Density Field and Non-Linear Collapse", 2009-2012, University of Paris VII-Diderot, Paris (currently postdoc at U. Munich & MPA-Garching)

Funding

- *"Dark Energy Models and Cosmic Structures"*, 12 k€ funded by the "Actions Incitatives 2009" of the Paris Observatory. Coordinators: P.S. Corasaniti & Y. Rasera.

- *"Nature of Dark Energy and Gravitation on the Large Scales: Theory and Observations"*, 4 k€ funded by PNC-2009 of "Institut Nationale Science de l'Univers". Coordinator: P.S. Corasaniti.

- *"Probing Planck Scale Physics with Cosmological Observations"*, 7 k€ funded by EGIDE/Van-Gogh program for the French-Dutch cooperation 2008-2009. Coordinator: P.S. Corasaniti & K. Schaalm.

Services

- CNRS-National Committee Sec. 17

- Referee for Physics Review Letter, Physics Review D, Journal of Cosmology and Astroparticle Physics, Montly Notice Royal Astronomical Society

List of Publications and Preprints

34) I. Balmes, Y. Rasera, **P.S. Corasaniti** and J.-M. Alimi, *'Imprints of Dark Energy on Cosmic Structure Formation: III) Sparsity of Dark Matter Halos'*, to be published on MNRAS, arXiv:1307.2922.

33) I. Achitouv, Y. Rasera, R.K. Sheth and **P.S. Corasaniti**, *'Self-consistency of the Excursion Set Approach'*, submitted to PRL, arXiv:1212.1166.

32) I. Balmes and **P.S. Corasaniti**, *'Bayesian approach to gravitational lens model selection: constraining H_0 with a selected sample of strong lenses'*, Mont. Not. Astron. Soc. **431**, 1528 (2013), arXiv:1206.5801.

31) I. Achitouv and **P.S. Corasaniti**, *'Primordial Bispectrum and Trispectrum Contributions to the Non-Gaussian Excursion Set Halo Mass Function with Diffusive Drifting Barrier'*, PRD **86**, 083011 (2012), arXiv:1207.4796.

30) I. Achitouv and **P.S. Corasaniti**, *'Non-Gaussian Halo Mass Function and Non-Spherical Halo Collapse: Theory vs. Simulations'*, JCAP **02**, 002 (2012). Erratum, JCAP **07**, E01 (2012), arXiv:1109.3196.

29) **P.S. Corasaniti** and I. Achitouv, *'Excursion Set Halo Mass Function and Bias in a Stochastic Barrier Model of Ellipsoidal Collapse'*, Phys. Rev. D **84**, 023009 (2011), arXiv:1107.1251.

28) **P.S. Corasaniti** and I. Achitouv, *'Toward a Universal Formulation of the Halo Mass Function'*, Phys. Rev. Lett. **106**, 241302 (2011), arXiv:1012.3468.

27) M. Pierre, F. Pacaud, J.B. Juin, J.B. Melin, P. Valageas, N. Clerc, **P.S. Corasaniti**, *'Precision cosmology with a wide area XMM cluster survey'*, Mont. Not. Roy. Astron. Soc. **414**, 1732 (2011), arXiv:1009.3182.

26) J. Coutin, Y. Rasera, J.-M. Almi, **P.S. Corasaniti**, V. Boucher, A. Fuzfa, *'Imprint of Dark Energy on Cosmic Structure Formation: II) Non-universality of the halo mass function'*, Mont. Not. Roy. Astron. Soc. **410**, 1911 (2011), arXiv:1001.3425.

25) J.-M. Alimi, A. Fuzfa, V. Boucher, Y. Rasera, J. Courtin, **P.S. Corasaniti**, *'Imprints of Dark Energy on Cosmic Structure Formation: I) Realistic Quintessence Models'*, Mont. Not. Roy. Astron. Soc. **401**, 775 (2010), arXiv:0903.5490.

24) P.D. Meerburg, J.P. van der Schaar, **P.S. Corasaniti**, *'Signatures of Initial State Modifications on Bispectrum Statistics'*, JCAP 0905, 018 (2009), arXiv:0901.4044.

23) J. Larena, J.-M. Alimi, T. Buchert, M. Kunz, **P.S. Corasaniti**, *'Testing backreaction effects with observations'*, Phys. Rev. D**79**, 083011 (2009), arXiv:0808.1152.

22) **P.S. Corasaniti**, *'Slow-roll suppression of adiabatic instabilities in coupled scalar field-dark matter models'*, Phys. Rev. D**78**, 083538 (2008), arXiv:0808.1646.

21) **P.S. Corasaniti** and A. Melchiorri, *'Testing Cosmology with Cosmic Sound Waves'*, Phys. Rev. D**77**, 103507 (2008), arXiv:0711.4119.

20) **P.S. Corasaniti**, D. Huterer and A. Melchiorri, *'Exploring the Dark Energy Redshift Desert with the Sandage-Loeb Test'*, Phys. Rev. D**75**, 062001 (2007), astro-ph/0701433.

19) P. Zhang and **P.S. Corasaniti**, *'Cosmic Dust Induced Flux Fluctuations: Bad and Good Aspects'*, Astrophys. J. **657**, 71 (2007), astro-ph/0607635.

18) **P.S. Corasaniti**, *'The Impact of Cosmic Dust on Supernova Cosmology'*, Mont. Not. Roy. Astron. Soc. **372**, 191 (2006), astro-ph/0603883.

17) P. Mukherjee, D. Parkinson, **P.S. Corasaniti**, A. Liddle and M. Kunz, *'Model Selection as a science driver for dark energy survey'*, Mont. Not. Roy. Astron. Soc. **369**, 1725 (2006), astro-ph/0512484.

16) **P.S. Corasaniti**, M. LoVerde, A. Crotts and C. Blake, *'Testing Dark Energy with the Advanced Liquid-Mirror Probe of Asteroids, Cosmology and Astrophysics'*, Mont. Not. Roy. Astron. Soc. **369**, 798 (2006), astro-ph/0511632.

15) S. Das, **P.S. Corasaniti** and J. Khoury, *'Super-acceleration as Signature of Dark Sector Interaction'*, Phys. Rev. D**73**, 083509 (2006), astro-ph/0510628.

14) L. Pogosian, **P.S. Corasaniti**, C. Stephan-Otto, R. Crittenden, R. Nichol, *'Tracking Dark Energy with the ISW Effect: short and long-term predictions'*, Phys. Rev. D**72**, 103519 (2005), astro-ph/0506396.

13) C. Ungarelli, **P.S. Corasaniti**, R.A. Mercer, A. Vecchio, *'Gravitational Waves, Inflation and the Cosmic Microwave Background: Towards Testing the Slow-Roll Paradigm'*, Class. Quant. Grav. **22**, S955 (2005), astro-ph/0504294.

12) A. Cooray, **P.S. Corasaniti**, T. Giannantonio, A. Melchiorri, *'An Indirect Limit on the Amplitude of Primordial Gravitational Wave Background from CMB-Galaxy Cross-Correlation'*, Phys. Rev. D**72**, 023514 (2005), astro-ph/0504290.

11) **P.S. Corasaniti**, T. Giannantonio, A. Melchiorri, *'Constraining Dark Energy with Cross-Correlated CMB and Large Scale Structure Data'*, Phys. Rev. D**71**, 123521 (2005), astro-ph/0504115.

10) B.A. Bassett, **P.S. Corasaniti**, M. Kunz, *'The Essence of Quintessence and the Cost of Compression'*, Astrophys. J. **617**, L1 (2004), astro-ph/0407364.

9) **P.S. Corasaniti**, M. Kunz, D. Parkinson, E.J. Copeland and B. Bassett, *'The Foundations of Observing Dark Energy Dynamics with the Wilkinson Microwave Anisotropy Probe'*, Phys. Rev. D**70**, 083006 (2004), astro-ph/0406608.

8) **P.S. Corasaniti**, *'Phenomenological Aspects of Dark Energy Dominated Cosmologies'*, PhD Thesis, British Library Press, astro-ph/0401517. advisor: E.J. Copeland

7) N. Bartolo, **P.S. Corasaniti**, A. Liddle and M. Malquarti, *'Perturbations in Cosmologies with a Scalar Field and a Perfect Fluid'*, Phys. Rev. D**70**, 043532 (2004), astro-ph/0311503.

6) M. Kunz, **P.S. Corasaniti**, D. Parkinson and E.J. Copeland, *'Model-Independent Dark Energy Test with σ_8 Using Results from the Wilkinson Microwave Anisotropy Probe'*, Phys. Rev. D**70**, 041301 (2004), astro-ph/0307346.

5) **P.S. Corasaniti**, B. Bassett, C. Ungarelli and E.J. Copeland, *'Model-Independent Dark Energy Differentiation with the ISW Effect'*, Phys. Rev. Lett. **90**, 091303 (2003), astro-ph/0210209.

4) **P.S. Corasaniti** & E.J. Copeland, *'A Model Independent Approach to the Dark Energy Equation of State'*, Phys. Rev. D**67**, 063521, (2003), astro-ph/0205544.

3) **P.S. Corasaniti** & E.J. Copeland, *'Constraining the Quintessence Equation of State with SNIa and CMB peaks'*, Phys. Rev. D**65**, 043004 (2002), astro-ph/0107378.

2) **P.S. Corasaniti**, L. Amendola & F. Occhionero, *'Present Limit to Cosmic Bubbles from the COBE-DMR three point correlation function'*, Mon. Not. Roy. Astron. Soc. **323**, 677 (2001), astro-ph/0005575.

1) L. Amendola, **P.S. Corasaniti**, F. Occhionero, *'Time Variability of the Gravitational Constant and type Ia Supernovae'*, (1999), astro-ph/9907222.

Popular Science Articles

- L. Amendola & P.S. Corasaniti, *"Il codice genetico dell'Universo"*, l'Astronomia, n. 216 Gennaio 2001 (in italian)

Bibliometrics (SPIRES-archive statistics)

- number of published papers in peer-reviewed journals: 30

- number of top cited papers (> 100 citations): 6

- total number of citations: 1522

- h-index: 21

Parcours: brief history of my time

In 1998 I was an undergraduate student in the last year of the Physics program at the University of Rome "La Sapienza" looking for a science project upon which writing a dissertation thesis. This was the last obstacle between me and the dreamed "Laurea" degree (equivalent to a combined B. Sc. and M. Sc. program of the duration of 4 years) on a journey that began in 1994, almost 20 years ago. The Physics Department at "La Sapienza" had always been dominated by theoretical High Energy Physics, a tradition which can be traced all the way back to Enrico Fermi. During the first three years of studies, the particle physics environment had quite seriously disturbed my original interest for the cosmos. However, in 1998, the *annus mirabilis*, I had the chance to attend the cosmology lectures by Prof. Franco Occhionero and those on extra-galactic astrophysics by Prof. Francesco Melchiorri. They gave great overviews of the challenging problems that Cosmology had to offer to a young generation of physicists. Furthermore, they resonated with the excitement of an upcoming golden age of observations and experiments; those that over the past decade have revolutionized the field of Cosmology. These lectures were very inspiring in several aspects and decisive in directing my inexpert curiosity toward a career in Cosmology. Particularly, the encounter with Franco Occhionero and his closest collaborator Luca Amendola (now full professor at the University of Heidelberg) was a turning point in life. I always wanted to be a Physicist, but now among physicists I wanted to be a Cosmologist because there is nothing more exciting than aspiring to know *everything*!

That year the results of the measurements of luminosity distance to Supernova Type

Ia indicated for the first time that the cosmic expansion is accelerating, thus providing evidence for Dark Energy [1, 2]. But Dark Energy was yet to become the central topic of investigation in Cosmology. Although the Rome group and particularly Luca were quite responsive to this new field of investigation, the cosmological arena was dominated by different debates.

In the mid and late '90, observations of the CMB were not accurate enough to discriminate between the two competing scenarios which were thought to be responsible for seeding the cosmic structure formation. On the one side was the theory of Inflation and on the other the cosmological scenario with topological defects. Franco and Luca were contributing to this debate by investigating a class of inflationary models characterized by a stage of production of bubble-like defects amid the standard spectrum of nearly scale invariant adiabatic Gaussian fluctuations [3–5]. They were particularly interested in the possibility of detecting the signature that such bubbles left on the CMB and calculated the imprints in a series of papers with Carlo Baccigalupi [6, 7]. It was clear that besides measuring the CMB power spectrum (for which topological defect models predicted the absence of acoustic oscillations), searching for non-Gaussian signals was the way to test the topological defect hypothesis. Around that period a series of articles dedicated to testing non-Gaussianity through CMB bispectrum statistics appeared in the literature [8–10]. In particular in [8], the authors claimed the detection of a non-Gaussian signal at a specific multipole in the COBE data, which at that time contributed to render non-Gaussianity a hot topic, perhaps as much as it has become in recent years. So I had a project: compute the CMB bispectrum statistics in topological defect scenarios. This implied developing the numerical tools to Monte Carlo generate CMB maps using an algorithm developed by Paolo Natoli (HEALPIX had yet to be written) which I had to modify to account for the temperature anisotropies induced by topological defects, then compute the bispectrum statistics and finally confront the inferred distributions against the Gaussian case. The task was successfully completed by a mix of Fortran coding and Mathematica analysis algorithms on a Toshiba laptop. Along the way I managed to derive an analytical expression for the three-point correlation function generated by bubble-like defects on the CMB, that I used to infer observational bounds on the bubble scenario using the COBE data, a

study which we published a couple of years later [11]. The results were discussed in my Italian "Laurea" thesis *"Simulation and detection of non-Gaussian signals in the Cosmic Microwave Background radiation"* defended the 17th December 1999 and presented at the 9th Marcel Grossman Meeting in Rome in July 2000, my first big conference. Unfortunately, a few months later the hard disk of my distressed laptop, which had run 24/7 munching Monte Carlos for months in a raw at home or on crowded metros, buses, in the office and cafes, crashed. Having no backups one year worth of work was for ever lost. A sign that it was time to move onto new stuff. Nevertheless, I knew I gained something worth more than one year of work and valuable for the rest of my career. How to work on cosmological problems I learned it from Franco and Luca. In any quest I learned to have equal consideration for the theoretical aspects of the problem, the phenomenological consequences and the comparison with observational data. I also learned to always keep an interest on many subjects at the same time. Thanks to their approach I learned to explore problems in their entirety, rather than looking at them from a single perspective. Most importantly, they taught me to never be dogmatic but always to keep an open mind.

It was time to look for a PhD and I needed to expand my horizons and confront myself with research abroad. Willing to remain in Europe for the PhD, the choice fell inevitably on the Physics & Astronomy Department at the University of Sussex. Around the year 2000, Sussex was the ideal place to study Cosmology. It was a strongly motivated group of cosmologists, particle physicists, string theorists, numerical and observational astrophysicists. A few months after my arrival I started working with Ed Copeland and I become one of his many students. I owe to him as much as I do to Franco and Luca. I learned how to work from them, but what to work on I learned it from Ed. His guidance has led me to success. However, this would not have been possible without the amazing environment of the Sussex group. People had offices along the same (hospital-looking) corridor, shared working space in the computer center, had common seminars, had tea together at 3 pm and pints at 5 pm[2]. Exchanges were constant and systematically organized, including the weakly football match on Thursday morning at 10 am. There was no moment of the day

---

[2]Sussex campus on the hills outside Brighton is equipped with two pubs that facilitate any sort of (scientific) discussion.

that you would not hear an interesting conversation about Inflation, Dark Energy, Galaxy Clusters, CMB, Red Galaxies, D-branes and Ramond-Ramond charges etc etc. To me it really felt like being a kid going to the playground to play with other kids all day long. It made such an inspiring working place where I learned an incredible amount of Physics and had the opportunity to develop my own research program on a topic that was going to become central to Cosmology, the quest for Dark Energy. I graduated in the summer of 2003 with the thesis *"Phenomenological Aspects of Dark Energy Dominated Cosmologies"*.

I was finally the Cosmologist that I wanted to be. Dark Energy and CMB were my stuff and I was heading for a three years postdoc at Columbia University in New York. Not surprising my next destination was again a multi-disciplinary group lead by string theorist Brian Greene and astrophysicist Arlin Crotts, the "Institute of String, Cosmology and Astroparticle Physics" (ISCAP). Being in the US and especially at Columbia allowed me to come into contact with several area of research in theoretical cosmology and extragalactic astrophysics. I worked with several postdocs and students on the most diverse topics and interacted with leading scientists. So, if at Sussex I became the Cosmologist that I wanted to be, it is definitely at Columbia that I have realized myself professionally. In 2007, motivated by a growing curiosity on cosmological signatures of Dark Energy on the non-linear structure formation, I moved to the Observatory of Paris as a postdoc in the "Horizon Project". That same year I was recruited by the CNRS and permanently established my quarters at the "Laboratoire Univers et Theory" (LUTH). Here, thanks to collaboration with my colleagues and friends Jean-Michel Alimi and Yann Rasera, I have become involved in the study of cosmic structure formation using N-body simulations. This collaboration has quickly evolved in a team work that has convinced us of the necessity to form an independent cosmology group at the Observatory of Paris. Joining our diverse expertise has allowed us to tackle challenging projects such as the "Dark Energy Universe Simulation Series" (DEUSS) and the "Full Universe Runs" (DEUS FUR). As a result of this activity, in the summer of 2010 I have proposed a 5-years research project, "Exploring Dark Energy through Cosmic Structures" (EDECS) to the European Resarch Council call for ERC-Starting Grant and awarded with a 1.5 million euros grant. The project is dedicated to the realization of innovative numerical simulations to study the impact of

Dark Energy clustering on the non-linear cosmic structure formation. The project has started on April Fool 2012 and the funding will allow me to set up a small team consisting of 3 postdocs and 1 PhD student. It is a responsibility that I felt ready to embrace and now it is my utmost priority to lead this project and its contributors to success. However, for this to be possible I first need to get my HDR and in the next Chapters you should find all you need to decide whether I deserve the French ultimate academic degree, the HDR.

Over the past 10 years the quest of Dark Energy has lead me to work on several topics. Since this is not a PhD thesis, in order to keep the material as concise as possible and in line with HDR requirements I decided to limit the presentation to three selected topics which have involved the supervision of students. I will discuss the work I have done on non-minimally coupled Dark Energy models in Section 1 and in Section 2 the work on the cosmological implications of dust in the Intergalactic Medium, while I will describe work on the physical modeling of the dark matter halo mass function in Section 3. I added at the very end original copies of the published articles discussed Section 1, 2 and 3 respectively. Next, I will discuss my experience with student supervision.

Student Supervision

I have always devoted time to mentoring students. I have received a lot from my mentors and I feel an obligation to give to younger generations what I received before. I regularly engaged in the supervision of PhD thesis since I joined the CNRS. At the beginning I was puzzled as to what kind of supervisor would have been best to be. Then, I quickly realized that there is not right answer to this question. It would be too naive to say - be the supervisor that you would like to have had - because it implies that there exists a perfect supervisor for each one of us and that it is completely unreal. We all have different characters, interests and goals. Supervising students primarily concerns with human interaction. As one gets to know students with different personalities one learns how to deal with each one of them. Something that works for one, may not work for others. Of course this requires a lot of dedication, because supervising students may turn not to be the most pleasant voluntary job in the world, unless one is really motivated to help someone else to realize itself. There is the student that prefers to be left in peace, then after months it comes with a fully edited paper just asking for your approval. On the other hand there is the student who is unhappy if it does not stop on your office front door every morning to tell you about the great ideas that it just had while showering[3]. I think what is especially important is to be crystal clear from the beginning about what the expectations are and then find the ways to get the best out of each of person.

As a postdoc I had the fortune to work with some extremely brilliant and talented students such as Subinoy Das , Tommaso Giannantonio and Marilena Loverde (rigourously

---

[3]Mine do.

in alphabetical order). However, supervising student projects as a postdoc does not carry the same sense of responsibility of being a PhD advisor. The latter requires having a long term vision about the topics that a student should investigate, while at the same time matching them with the student's own interests and capabilities.

It is a risky choice that can have a tremendous impact on the future career of the student. Flexibility, perseverance and most of all student' commitment to hard work are necessary to minimize the risk of failure. In the end, for all the effort a supervisor can make, it is ultimately in students hands to take the responsibility of realizing itself in life. What the supervisor can do it is only to provide them with the best options and advises.

In France, the majority of scholarships are funded by the National Department of Science and Education. Every year, depending on Government Funding, doctoral schools are allocated a limited number of scholarships. Master students need to apply to schools and after selection the winners can register for a PhD program. Part of the evaluation process include the PhD project proposal that must have been already concerted with the sponsoring advisor. Because of this, prospect students start working with their future mentors already at the level of the Master during a few months internship. It is in this way that I have met a number of students that I supervised..ops (I cannot officially say that) I co-supervised in the past few years.

The first student who has contacted me for a Master intership project is Irene Balmes. In 2008 Irene was a student of Master 2 and I proposed her to use up to date measurements of gravitational lens time delays to infer constraints on the Hubble constant under different cosmological model assumptions. Irene impressed me for her fast learning pace and her skills, in a few weeks she set up the entire analysis software in Mathematica, reproduced the results of a paper in the literature that I gave her to study and performed the analysis. The project was simple, the results neat, but not enough for a publication. Nevertheless, there were many aspects that could have been further developped and which were worth to investigate in a PhD thesis. After one year leave for voluntary work in Benin, Irene started her PhD under my supervision. She has worked on the application of Bayesian model selection methods to model strong gravitational lens potentials of double image lenses using astrometry and time-delay measurements. While studying the relation between the

lens potential and the lens halo mass distribution I suggested her to look into the properties of halo profiles from N-body simulations. This has led her to perform an original analysis of the DEUSS halo catalogs. She is expected to discuss her thesis before Autumn of this year, as she will leave for her postdoc.

In the Spring 2009 another Master student knocked at my door, Ixandra Achitouv, who was looking for a Master 2 internship. In that period I become interested in understanding the physical processes that shape the halo mass function as we infer it from numerical simulations. Previous studies performed by our group showed that this carry a signature of Dark Energy. So, I suggested her to study the Excursion Set Theory and particularly a series of papers which introduced a path-integral formulation of the theory. She successfully defended her thesis last September 2012 on "Halo Mass Function of Dark Matter Halos: Imprints of the Initial Matter Density Field and the Non-Linear Collapse". She is currently postdoc at University of Munich. Her thesis has been a co-supervision with Jim Bartlett at Paris 7. In Section 3 I will discuss the work that we have carried out during her PhD. Finally, last September I offered a PhD scholarship funded through my ERC-StG to Linda Blot, who is working with me on coding the Dark Energy fluid equations in RAMSES/hydro solver to run simulations which will allow us to study the effects of Dark Energy clustering properties on the non-linear scales.

Chapter 1

Dark Energy Cosmology: Interaction, Super-Acceleration and Stability

1.1 Why not just Λ?

Over the past 15 years, measurements of the temperature and polarization anisotropies of the Cosmic Microwave Background (CMB) radiation [12], surveys of the large scale distribution of galaxies [13] and the determination of cosmic distances through observations of Supernova Type Ia (SN Ia) standard-candles [1, 2, 14] have provided precise estimates of the geometry, matter content, and state of expansion of the universe. On the one hand these measurements have confirmed the pillars of the Standard Model of cosmology, i.e. the Hot Big-Bang scenario. On the other hand, they have opened a new window on an unknown invisible sector that accounts for most of the total matter/energy budget of the universe.

We have now compelling evidence that the bulk of cosmic matter is non-luminous, with baryons contributing only for a few percent. Observations strongly indicate that matter in cosmic structures is primarily made of a Cold Dark Matter (CDM) component [15], which

accounts for roughly 25% of the total cosmic matter density. Most striking is the discovery that the remaining 70% consists of an exotic component, dubbed as Dark Energy (DE), which is thought to be responsible for the present accelerated phase of cosmic expansion.

The presence of a Cosmological Constant (Λ) in Einsteins equations of General Relativity (GR) provides the simplest, best-fitting solution to the available cosmological data, thus reconciling the Standard Model of cosmology with the observed accelerating phase. Contrary to ordinary matter fields, Λ behaves as an effective fluid with constant energy density (ρ_Λ) and negative pressure (p_Λ), with a characteristic ratio (equation of state) $w_\Lambda = -1$. Because of its negative pressure, Λ acts with a repulsive effect on the space-time expansion, thus if ρ_Λ dominates the cosmic energy budget it drives a stage of cosmic accelerated expansion. Current observations indicate that $\rho_\Lambda \approx 10^{47}\,\mathrm{GeV}^4$. However the smallness of this value has posed a puzzling problem to any attempt of identifying the physical origin of Λ.

All forms of energy contribute to the curvature of space-time, including that stored in quantum vacuum fluctuations of the matter fields in the universe. These vacuum energies behaves as a cosmological constant term in GR and can be computed in Quantum Field Theory (QFT). For a given cut-off scale $k_{cut-off}$, which sets the limit of validity of the QFT, the vacuum energy is $k_{cut-off}^4$. Thus, if QFT is assumed to be valid all the way to the Planck scale, the resulting vacuum energy density is ~ 119 orders of magnitude larger than the observed value of ρ_Λ. Even assuming the cut-off to be at the TeV scale, where exact super-symmetric cancelations of vacuum diagrams might take place, the discrepancy is still ~ 60 orders of magnitude. This leaves us with an unnatural fine-tuning of vacuum diagrams with a bare geometrical cosmological constant, that is the unsolved "Cosmological Constant Problem" (for a review see [16]). One possibility to solve this puzzle is the existence of an unknown symmetry that forces vacuum energies to vanish, thus DE would have a different origin. Alternatively, it has been proposed that such vacuum energy may decay over time [17], but in such a case the phenomenology will differ from that of a pure Cosmological Constant model. Thus, if we exclude untestable multi-universe explanations as well as anthropic selection arguments, all attempted solutions to the cosmological constant problem point toward a different explanation for the DE

phenomenon.

In principle, we could imagine Λ being another fundamental gravitational constant, such as Newtons constant, G. However, even in this case we will find ourselves with the unsettling question as to why gravity is ruled by two very different constants: G, which sets the local gravitational interactions (a multiplicative coupling constant), and Λ, completely different in nature (the only additive constant of Physics), which controls the global dynamics of the universe in a very coincidental way. In fact, its value seems to be precisely set such as to allow for a sufficient period of structure formation, as we observe it today. Therefore, is quite remarkable that the Standard Model (SM) of cosmology with Cosmological Constant, so called "concordance" ΛCDM, accounts so well for the data available thus far. In the lack of theoretical prejudice, we should therefore keep an open mind. Since the discovery of Dark Energy several hypotheses have been advanced.

We can distinguish three main approaches: a modification of Einstein gravity on cosmological scales, the existence of additional scalar degree of freedom beyond the Standard Model of Particle Physics, or a relaxation of the Cosmological Principle at small scales. The latter is indeed very persuasive since it does not require any new additional physics. On the other hand, it is extremely hard for these models to account for all cosmological observations so far collected. My personal view on this approach is that general relativistic effects due to the inhomogeneous matter distribution at small scales and late times may well be there, but are not sufficiently important such as to solely account for DE. Modified gravity scenarios are also an original possibility. Though, the formulations so far advanced suffer to a different extent of technical difficulties. The same is true for "quintessence" scalar field scenarios. A class of interesting scalar models has emerged from noticing that a relaxation of the Equivalence Principle may provide an alternative approach to solving the Dark Energy problem. In fact, if gravity possess other degrees of freedom which couple non-universally to the various matter species [18] or via density dependent screening mechanisms [19], then these may be responsible for the Dark Energy we observe today. Personally, I find these scenarios quite intriguing since they open up the possibility of an invisible richness in the dark sector, which can be tested in the upcoming future with fine observations of the cosmic structures.

1.2   Phantom Dark Energy or Dark Sector Interactions?

Observationally the quest for Dark Energy has primarily focused on inferring the value of the equation of state w_{DE}. This is because a measurement of $w_{DE} \neq -1$, would be indicative of a dynamical component rather than a Cosmological Constant. A variety of measurements constrain the dark energy equation in a range of values that extends in a "super-negative" region with $w_{DE} < -1$ (see e.g [14,20,21]). A fluid with such an equation of state, usually referred as "phantom" Dark Energy, violates the Weak Energy Condition [22]. Because of this self-consistent theoretical formulations of phantom Dark Energy models have prooven extremely difficult (see e.g. [16]). However, such a measurement refers to the properties of an effective fluid, can there be other physical interpretations which do not require the existence of phantom fields?

In 2004, Huey and Wandelt [23] showed that if one consider a Dark Energy component in the form of a scalar field coupled to a matter species than the resulting cosmic expansion is similar to that of a phantom Dark Energy dominated cosmology. However, in their specific formulation the Dark Matter density becomes negligibly small beyond $z > 1$, thus requiring the introduction of an additional non-interacting Dark Matter species. This work raised a number of interesting questions. Is phantom cosmic dynamics a generic feature of coupled dark matter/quintessence models? Are there any constraints on the scalar field dynamics or the form of the scalar interaction to mimic a super-accelerating universe?

At that time I was postdoc at Columbia University and Justin Khoury also postdoc in the group was pondering similar questions inspired by his work on the Chameleon cosmology. Finding an answer made a neat project suitable for a student and Subinoy Das, who at that time was an undergraduate student at Columbia University, accepted the task. The project was developed over a few months period of close collaboration between the three of us. The results were published in [24].

We set the problem in the most general terms by considering a Yukawa-like interaction between a quintessence field ϕ and Dark Matter,

$$f(\phi/M_{\mathrm{Pl}})\bar{\psi}\psi\,, \tag{1.1}$$

where f is an arbitrary monotonic function of the scalar field ϕ, M_{Pl} is the Planck constant

and ψ is a Dirac spinor describing the Dark Matter particle. For simplicity we assumed no coupling with baryons such as to satisfy solar-system tests of gravity. Because of the field evolution, Dark Matter particles have a time-dependent mass, thus in a Friedman-Lemaitre-Robertson-Walker universe the dark matter energy density does not scale with the scale factor as a^{-3}, rather

$$\rho_{\mathrm{DM}} = \frac{\rho_{\mathrm{DM}}^{(0)}}{a^3} \frac{f(\phi/M_{\mathrm{Pl}})}{f(\phi_0/M_{\mathrm{Pl}})} \,, \tag{1.2}$$

where ϕ_0 is the field value today. By equating the corresponding Hubble equation to the standard one for non-interacting Dark Matter and Dark Energy with equation of state w_{eff} we obtained the relation

$$w_{\mathrm{eff}} = \frac{w_\phi}{1 - x} \,. \tag{1.3}$$

where

$$w_\phi = \frac{\dot{\phi}^2/2 - V(\phi)}{\dot{\phi}^2/2 + V(\phi)} \,, \tag{1.4}$$

with $V(\phi)$ the scalar self-interaction potential and

$$x \equiv -\frac{\rho_{\mathrm{DM}}^{(0)}}{a^3 \rho_\phi} \left[\frac{f(\phi/M_{\mathrm{Pl}})}{f(\phi_0/M_{\mathrm{Pl}})} - 1 \right] . \tag{1.5}$$

If $f(\phi_0/M_{\mathrm{Pl}})$ increases with time then $x \geq 0$. Thus, today we have $w_{\mathrm{eff}} = w_\phi > -1$, however in the near past when $0 < x < 1$ we can have $w_{\mathrm{eff}} < -1$. We have shown explicitly that this occur in the case of a coupled model with $f(\phi/M_{\mathrm{Pl}}) = \exp(\beta\phi/M_{\mathrm{Pl}})$ and scalar potential $V(\phi) = M^4 (M_{\mathrm{Pl}}/\phi)^\alpha$, and generally it is true for any "tracker" potential provided $\beta > 0$. In such a case, the scalar field decays into Dark Matter particles, thus transfering energy from the field to Dark Matter, while the coupling function stabilizes the runaway self-interaction potential. Hence, the scalar field evolves in an effective potential characterized by a minimum which moves toward large field values as the system evolves. The minimum is an attractor solution of the system with the scalar field slow-rolling around it. This is the so called "adiabatic" regime. We showed that for natural coupling values, $\beta \sim \mathcal{O}(1)$ (order of gravitational strength) and assuming a nearly flat scalar potential, the cosmic dynamics resemble that of a phantom Dark Energy model with a constant $w_{\mathrm{eff}} \approx -1.2$. In this case differences in the luminosity distance are of order of 2% up to

$z = 2$. On the other hand, we showed that such models can leave a distinctive imprint in the cosmic structure formation. In fact, the scalar interaction alters the gravitational of collapse of Dark Matter density fluctuations in a scale dependent manner. This is because the field mediates a scalar fifth force between DM particles with finite range that for an inverse-power law potential has given by

$$\lambda = V_{,\phi\phi}^{-1/2} = \sqrt{\frac{\phi^{\alpha+2}}{\alpha(\alpha+1)M^4 M_{\text{Pl}}^\alpha}} \, . \tag{1.6}$$

Hence, matter perturbations on scales larger than λ evolve as in the uncoupled case, while those on smaller scales feel a gravitational interaction that is $1 + 2\beta^2$ stronger. This has important phenomenological implications since it implies a more efficient DM clustering on the non-linear scales.

1.3 Adiabatic stability of linear density fluctuations

Several works in the literature have pointed out that coupled models suffer of instabilities, with scalar field fluctuations becoming unstable at early times and inducing a non-linear regime of gravitational collapse of the Dark Matter density perturbations on the large scales deep in the matter-dominated era. This immediately rules out these models unless the amplitude of the scalar coupling is constrained to be unnaturally small. In 2008, I decided to study this problem in greater detail. In fact, from a numerical analysis of the system I was aware of the presence of instabilities (which I initially thought to be of numerical origin). However, these occurred only for certain dynamical regimes of the scalar field which were not attractor solutions of the system. This contrasted with works in the literature that claimed exponentially unstable growing modes to be a generic features of coupled models. Even the analysis by Trodden et al. [25] or that of Majerotto et al. [26] where not fully convincing. The former suggested that since in the adiabatic regime the system behaves as a single adiabatic fluid for which the square of the adiabatic sound speed, $c_a^2 = \dot{p}_T/\dot{\rho}_T$, equals the square of the sound speed of pressure perturbations in the fluid rest frame, $c_s^2 = \delta p_T/\delta\rho_T$, the one that controls the clustering properties of the fluid, then having found that $c_a^2 = \dot{p}_T/\dot{\rho}_T \propto -\beta$ implies the presence of large scales Jeans-like

instabilities for $\beta > 1$. In the analysis of Majerotto et al. [26] the perturbations were studied in a gauge invariant formalism in the case of Dark Matter coupled to a generic Dark Energy fluid with constant equation of state, w_{DE}. However, their equations become singular for $w_{DE} \to -1$ which corresponds to the behavior of the scalar field equation of state in the adiabatic regime. Thus, the instabilities they found for $w_{DE} \neq -1$ referred to a different dynamical regime of the system, not the adiabatic one.

The issue deserved a clarification which I set to discuss in [28]. Rather then assuming the adiabaticity of the system I first considered the linear equations for the coupled scalar field and Dark Matter perturbations in the synchronous gauge (the choice of the gauge turns out to be irrelevant), then I derived the linear perturbation equations for the total fluid and evaluated the expressions for the sound speeds in the adiabatic regime approximation to find

$$c_{aT}^2 = -\beta \frac{\dot{\phi}}{3H} \,, \tag{1.7}$$

and

$$c_{sT}^2 = -\frac{1}{1 - \frac{1}{\beta} \frac{\delta_{DM}}{\delta\phi}} \,. \tag{1.8}$$

In the adiabatic regime $3H\dot{\phi} \approx 0$ due to the slow-roll dynamics of the field, thus the term $\dot{\phi}/3H$ is negligibly small compared to β. This implies that $c_{aT}^2 < 0$, however, the absolute value is exponentially small even for $\beta \sim \mathcal{O}(1)$. Similarly, since in the matter-dominated era the scalar field is subdominant compared to Dark Matter, $\delta\phi/M_{\rm Pl} \ll \delta_{DM}$, thus $c_{sT}^2 \approx \beta\delta\phi/\delta_{DM} \approx 0$ and never negative (the system starts with adiabatic initial conditions, for which $\delta\phi$ and δ_{DM} have the same sign). This implies that during the adiabatic regime the system behaves as an adiabatic fluid to very good approximation since $c_{aT}^2 \approx 0^-$ and $c_{sT}^2 \approx 0^+$. Hence, even in the case of $\beta \gg 1$ instability cannot occur on large-scales because they are suppressed by the slow-roll dynamics of the field. The numerical study of the coupled equations of the system along the adiabatic attractor solution of the field confirms these conclusions.

Finally, by solving numerically the system I was able to study also the case of non-attractor solutions, for which analytical formula of the relevant quantities cannot be derived. In particular I found that instabilities occurs only for initially large scalar field
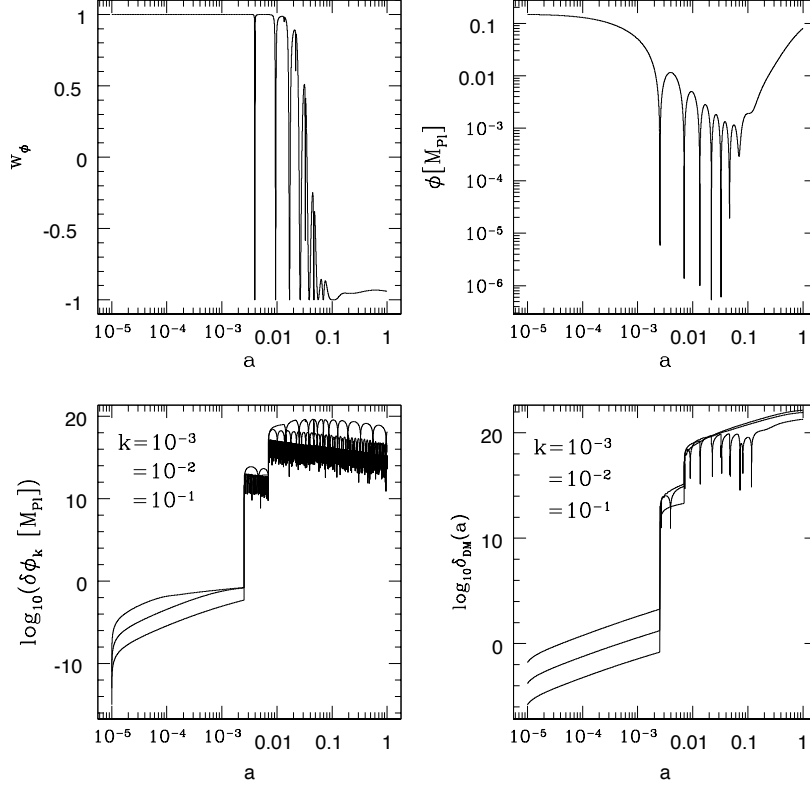
Figure 1.1: Evolution of ϕ (top right panel), w_ϕ (top left panel), $\delta\phi$ (bottom left panel) and δ_{DM} (bottom right panel) for $k = 0.001, 0.01$ and 0.1.

values, corresponding to $\phi_i > \phi^i_{min}$ (Figure 1.1). In such a case the field rolls down a steep part of the effective potential, quickly acquires kinetic energy which is then dissipated through large damped oscillations whose frequency increase as the amplitude diminishes. As shown in [27], this is a proxy for the presence of scalar field instabilities as in the case of pre-heating. Here, because of the energy transfer from the scalar field to Dark Matter, the instabilities of the field perturbations are transmitted to that in the Dark Matter component, causing an exponential growth of the perturbations on the linear scales. During this oscillatory regime of the homogeneous part of the scalar field evolves with an average equation of state $w_\phi > -1$, which recover the results of Majerotto et al. [26].

Chapter 2

Cosmological Implications of Inter-Galactic Dust

2.1 Luminosity Distance and Dust Extinction

Cosmic distance measurements to Supernova Type Ia are a sensitive probe of the cosmic expansion history over a time period which sees the emergence of the Dark Energy phenomenon. Their use as cosmic standard candles relies on the presence of correlated features light-curve features which allow a standardization of high-redshift observations using a local calibrated sample.

The luminosity distance to a supernova at redshift z is given by

$$m_B(z) = \mathscr{M}_B + 5 \log H_0 d_L(z), \tag{2.1}$$

where $m_B(z)$ is the apparent SN magnitude in the B-band, $\mathscr{M}_B = M_B - 5 \log H_0 + 25$ is the "Hubble-constant-free" absolute magnitude. The peak luminosity-decline rate correlation of SN light-curves is the most prominent feature used to standardize SN data [29, 30]. However, it is only in the past ten years or so that the origin of this empirical relation has become clearer (see e.g. [31, 32]).

The most accredited scenario of SN Ia is the explosion of a degenerate C/O White Dwarf at the Chandrasekar mass limit due to the accretion of mass from an evolved

companion star. The photons that we observe today as SN Ia are the decay product of Ni synthesized during the explosion. Improvements in the physical modeling of the explosive phase through high-resolution simulations have shown that one parameter family of light-curves may arise if the propagation of the burning flame undergoes a transition from subsonic deflagration to supersonic detonation. The earlier the transition the greater the amount of Ni synthesized. This cause both higher peak-luminosity, higher density and higher temperatures which increase the opacity of the gas thus allowing for a slower energy release which delays the decrease of the SN light-curve.

Current observations are characterized by a dispersion about the standard-candle relation of $\sim 0.15\,\mathrm{mag}$ [33]. Whether larger statistical sample may reduce such dispersion by an order of magnitude is still debated, since it is not clear that at that level of accuracy SN Ia remains standard-candles. Errors may well become dominated by astrophysical systematics.

Present SN Ia data are marginally informative on Dark Energy provided external constraints on the cosmic matter density are included. Even in such a case the interpretation of Dark Energy parameter inference requires careful consideration (see e.g. [34, 35]). The effect of systematic uncertainties on future SN data had been considered only at the level of parametric studies which assumed unphysical redshift dependent off-sets [36, 37].

During my last postdoctoral year at Columbia University I was particularly involved in estimating the performance of the ALPACA survey and consequently become interested in quantifying the effect of astrophysical systematics [38] on the future SN surveys. Extinction by a diffuse dust component in the Inter-Galactic Medium (IGM) is one of such systematics. Here, I will briefly summarize the most salient points of my analysis and refer the reader to the original article for more details [39].

Dust particles are present in the interstellar medium causing the absorption of nearly $30 - 50$ per cent of the light emitted by stars in the Galaxy. In contrast, very little is known about the presence of a diffuse dust in the IGM. The existence of such component has been speculated upon for years; at the time I worked on this project no direct evidence of IGM dust was available. Nevertheless, the presence of metal lines in the X-ray spectra of galaxy clusters (see e.g. [40]) and in high-redshift Lyman α clouds left this hypothesis

still viable [41, 42]. This situation has changed in recent years, thank to a number of observations that have provided the first direct evidence of dust particles in the IGM. As an example [43] obtained the first detection of dust reddening in the Intra-Cluster Medium (ICM), while angular cross-correlation studies of large samples of background distant quasars with foreground galaxies provided evidence of reddening signature of diffuse dust on scales ranging from 20 kpc up to several Mpc [44, 45], we will return on this work more in detail in the next Section.

The conditions in the IGM are unfavorable to the formation of dust grains. Dust forms in stellar environments inside galaxies, nonetheless several mechanisms (stellar winds, SN explosions, etc.) can expel grains from formation sites in the IGM. As an example, simulations have shown that grains can efficiently diffuse over considerable distance (up to several hundred kiloparsec over one billion years) [46]. The presence of diffuse dust in the IGM has several consequences. From the point of view of galaxy formation the large scale motion of dust provides mass exchange between galaxies and the IGM. On the other hand, this component may play an important role in regulating the thermal equilibrium of the IGM and contribute to the metal pollution of the medium. IGM dust particles also contribute to the extinction of SN Ia photons, however, different from grains in the interstellar medium, IGM dust particles have undergone several selection processes that have altered their original size distribution. Because of this, the galactic extinction law is hardly justifiable for IGM dust. In particular, due to sputtering with the hot gas in the IGM it is expected that the population of dust grain is primarily made of large particles in the range $\sim 0.05\,\mu$m to $\sim 0.1\,\mu$m. In such a case the extinction law tends to flatten since scattering on large grains tends to be independent of the wavelength of light-rays, thus the absence of reddening does not guarantee that incoming photons have freely propagated.

Constraints on the IGM dust density have been inferred from several indirect measurements. As an example Aguirre & Haiman [47] have inferred an upper bound on the cosmic dust density of $\Omega_d \lesssim 10^{-5}$ at $z \lesssim 0.2$ from the FIRAS/DIRBE limits on the far-infrared background emission. This is because dust particles absorb UV-photons from star forming galaxies and remit in the far-infrared. Similar bounds where inferred from the thermal structure of the IGM [48] as well as direct constraints on the scattering of IGM grain along

the line-of-sight of luminous X-ray source [49].

In the presence of dust extinction Eq. (2.1) becomes

$$\tilde{m}_B(z) = m_B(z) + A_B(z), \tag{2.2}$$

where $A_B(z)$ is the B-band extinction. In order to evaluate this term it is first necessary to model the evolution of the IGM dust density. Following the work of Inoue & Kamaya [50] this can be obtained assuming that the abundance of IGM dust evolves proportionally to the cosmic mean metallicity. The latter can be inferred assuming that the amount of metals released in the IGM is proportional (on average) to the cosmic Star-Formation-History (SFH). In such a case if we assume that metals are instantaneously ejected from newly formed stars, the metal ejection rate per unit comoving volume at redshift z can be written as $\dot{\rho}_Z(z) = \dot{\rho}_{\mathrm{SFR}}(z) y_Z$ where $\dot{\rho}_{\mathrm{SFR}}$ is the star formation rate and y_Z is the mean stellar yield. If y_Z is constant, it follows that the mean cosmic metallicity is given by:

$$Z(z) = \frac{y_Z}{\Omega_{\mathrm{b}} \rho_c} \int_z^{z_S} \dot{\rho}_{\mathrm{SFR}}(z') \frac{dz'}{H(z')(1+z')}, \tag{2.3}$$

where Ω_b is the baryon density, ρ_c is the current critical density, $H(z)$ is the Hubble rate and z_S redshift at which star formation began. Finally, assuming a constant dust-to-gas ratio $\mathscr{D}$ of the IGM, the mass fraction of dust to the total metal mass is given by $\chi = \mathscr{D}/Z$, and the differential number density of dust particles in a unit physical volume reads as

$$\frac{dn_{\mathrm{d}}}{da}(z) = \chi \frac{Z(z)\,\Omega_{\mathrm{b}}\rho_c(1+z)^3}{4\pi a^3 \varrho/3} N(a), \tag{2.4}$$

where ϱ is the grain material density and $N(a)$ is the grain size distribution normalized to unity.

The amount of cosmic dust extinction on a source at redshift z observed at the rest-frame wavelength λ integrated over the grain size distribution is then given by:

$$\frac{A_\lambda(z)}{\mathrm{mag}} = 1.086\pi \int_0^z \frac{c\,dz'}{(1+z')H(z')} \int a^2 Q_m^\lambda(a, z') \frac{dn_{\mathrm{d}}}{da}(z')da, \tag{2.5}$$

where c is the speed of light and $Q_m^\lambda(a, z')$ is the extinction efficiency factor which depends on the grain size a and complex refractive index m of the grain material. This factor can be computed by solving numerically the Mie equations for spherical grains. From Eq. (2.5)
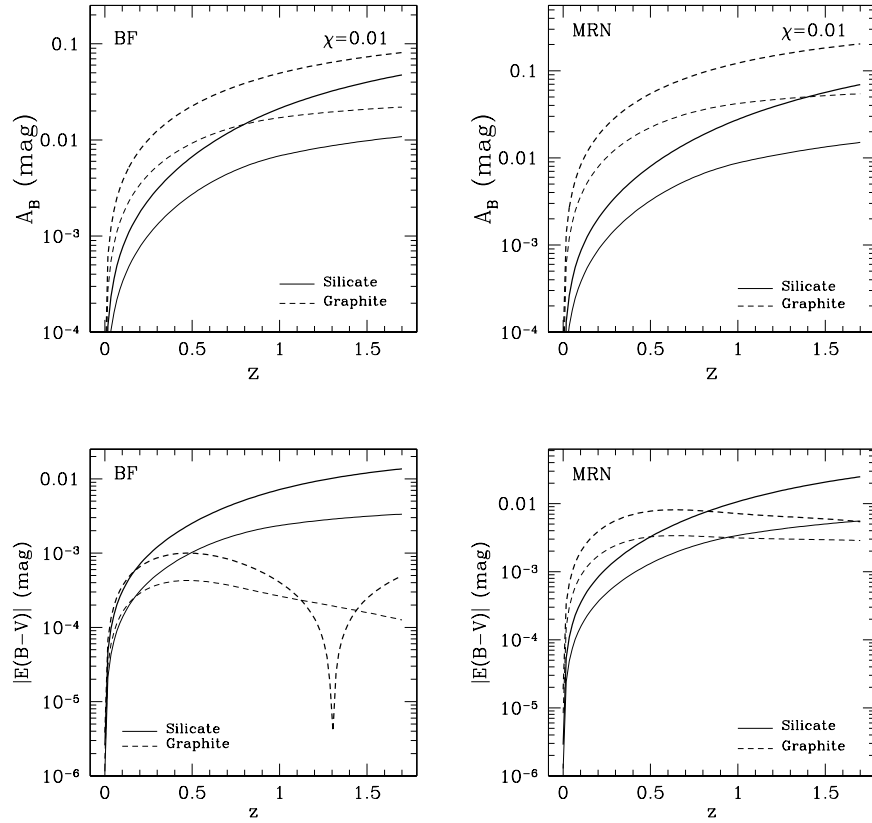
Figure 2.1: Cosmic gray dust extinction in the B-band (upper panels) and color excess (lower panels) as function of redshift of the source for BF (left panel) and MRN (right panel) grain size distributions in the range $0.02 - 0.15\,\mu m$. Solid and dash lines correspond to silicate and graphite grains respectively. Thick (thin) lines correspond to high (low) SFH models.

we can infer that the extinction at a given redshift depends on the dust properties and the metal content of the IGM. More specifically, for a given cosmological background a model of dust is specified by the grain composition, size distribution and material density, the mean interstellar yield, the star formation history and the IGM dust-to-total-metal mass ratio.

In Figure 2.1 we plot the extinction in the B-band (upper panels) and the color B-V (lower panels) for a standard LCDM model in the case of Silicate and Graphite grains respectively, for two different grain size distribution: uniform as resulting from the study of dust migration (left panels) and power law as in the case of the Milky Way (right panels). At the time of my analysis it was unclear whether the Star-Formation-Rate at high-redshift ($z > 1$) declined (low-SFH) or flattened (high-SFH), the extinction for these two scenarios is also shown in Figure 2.1. The current consensus is that SFR declines at high-redshift [51].

Notice that extinction can raise up to $0.1\,\mathrm{mag}$ at $z \sim 1.5$, while reddening would require photometric measurements better than 1% accuracy. In order to quantify the impact on the Dark Energy parameter inference from future SN searches, assuming Eq. (2.2) I generated synthetic samples of few hundreds SN Ia per redshift bin up to $z \sim 2$ for a fiducial LCDM model and different IGM dust models which are consistent with current astrophysical constraints. By running a blind Markov Chain Monte Carlo (MCMC) likelihood analysis using Eq. (2.1) I then inferred the DE model parameters. The results have shown that a systematic bias at more than 2σ compared to a dust-free universe. Indeed, the presence of dust can mimic a time-varying DE component and shift the equation of state towards more negative values. This is because assuming no extinction SN appear to be farther away, hence to account larger luminosity distance at high redshifts requires a more negative value of w.

The conclusion of my analysis is that in the light of current astrophysical observations, extinction by IGM dust grains can be a relevant source of systematic bias for future SN data analysis. Nevertheless, several observations can provide us with the necessary information to account for its effect. As I will discuss in the next Section cross-correlation studies can provide a better insight on the IGM dust properties.

2.2 IGM Dust and Angular Cross-Correlations

The presence of IGM dust along the line-of-sight in the proximity of foreground galaxies alters the flux of background sources, causing fluctuations about the sample average. If dust is mostly concentrated in the halos surrounding the foreground galaxies and/or within galaxy clusters at low-z, one can expect flux fluctuations to increase as the background sources are at smaller angular separations from foreground objects. Consequently, IGM dust induce correlations between flux fluctuations of background sources relative to foreground objects. Cosmic magnification by weak gravitational lensing can also generate angular correlations between independent samples. However, at optical wavelengths this effect is opposite to the flux fluctuations induced by cosmic magnification[1]. In fact, the observed flux of a source at redshift z in the direction of the sky $\hat{n}$ is given by

$$F^{\mathrm{obs}}(\hat{n}, z) = F\mu\, e^{-\tau} \simeq F e^{-\bar{\tau}(z)} \left[1 + 2\kappa(\hat{n}, z) - \delta\tau(\hat{n}, z)\right] \ , \tag{2.6}$$

where the lensing magnification $\mu \simeq 1 + 2\kappa$ with κ the lensing convergence and the optical depth $\tau \equiv \bar{\tau} + \delta\tau$ with $\delta\tau$ the spatial fluctuations of the optical depth.

In 2006 a number of articles described how lensing magnification could be inferred by measuring the spatial correlation of supernova flux fluctuations [52, 53]. Pengjie Zhang proposed me to compare the amplitude of the dust induced correlations in SN samples to those generated by lensing magnification. The results of that work are published in [54] which I refer to for further details. Here, I will briefly sketch the key results of our work.

SN flux fluctuation correlations can be inferred from the estimator $\delta_F(\hat{n}, z) \equiv F^{\mathrm{obs}}/\bar{F}^{\mathrm{obs}} - 1$, where $\bar{F}^{\mathrm{obs}}(z) \simeq \bar{F} e^{-\bar{\tau}(z)}$ is the average flux of the SN sample [52]. From Eq. (2.6) we then have $\delta_F = 2\kappa - \delta\tau$, hence δ_F provides an estimate of the gravitational lensing only if fluctuations in the optical depth are negligible. In terms of the angular power spectrum we have

$$\frac{1}{4}C_{\delta_F}(l) = C_\kappa + \frac{1}{4}C_{\delta\tau} - C_{\kappa\delta\tau}, \tag{2.7}$$

where C_κ, $C_{\delta\tau}$, $C_{\kappa\delta\tau}$ are the angular power spectra of κ, $\delta\tau$, and the κ-$\delta\tau$ cross correlation.

---

[1]Hereafter, lensing magnification refers to both the cases of magnification ($\mu > 1$) and de-magnification ($\mu < 1$).

Using the Limber's approximation these read as:

$$\frac{l^2 C_\kappa}{2\pi} = \frac{\pi}{l} \left[\frac{3\Omega_m H_0^2}{2c^2} \right]^2 \int \Delta_\delta^2 \left(\frac{l}{\chi}, z \right) W^2(\chi, \chi_s) \chi d\chi \,, \tag{2.8}$$

$$\frac{l^2 C_{\delta\tau}}{2\pi} = \frac{\pi}{l} \left[\frac{1}{2.5 \log e} \right]^2 \int \Delta_{\delta_d}^2 \left(\frac{l}{\chi}, z \right) \left[\frac{d\bar{A}}{d\chi} \right]^2 \chi d\chi \,, \tag{2.9}$$

and

$$\frac{l^2 C_{\kappa\delta\tau}}{2\pi} = \frac{\pi}{l} \frac{3\Omega_m H_0^2}{5c^2 \log e} \int \Delta_{\delta\delta_d}^2 \left(\frac{l}{\chi}, z \right) W(\chi, \chi_s) \frac{d\bar{A}}{d\chi} \chi d\chi, \tag{2.10}$$

where Δ_δ^2 is the dimensionless non-linear matter spectrum and $\Delta_{\delta\delta_d}^2$ and $\Delta_{\delta_d}^2$ are defined analogously. The spatial distribution of IGM dust is not known, the simplest assumption is that dust traces the total mass distribution. In such case $\Delta_{\delta_d}^2 = b_d^2 \Delta_\delta^2$ and $\Delta_{\delta\delta_d}^2 = b_d \Delta_\delta^2$, where b_d is the dust bias.

Defining $\Sigma_L \equiv \frac{3}{2} \Omega_m \frac{H_0^2}{c^2} \int W(\chi, \chi_s) d\chi$, one has $\delta\tau/\kappa \sim b_d \bar{A}/\Sigma_L$, hence $C_{\delta\tau}/C_\kappa \sim b_d^2 (\bar{A}/\Sigma_L)^2$ and $C_{\kappa\delta\tau}/C_\kappa \sim b_d (\bar{A}/\Sigma_L)$. This indicates that cosmic dust contamination is negligible only if $\bar{A}(z) \ll \Sigma_L(z)$. For realistic IGM dust models discussed in the previous Section, the redshift evolution of extinction versus $\Sigma_L(z)$ is shown in Figure 2.2. Since A_B and Σ_L are comparable, dust extinction effects cannot be neglected in lensing measurements of SN flux correlation.

In [54] we proposed to use a combination of angular convergence power spectrum measurements and SN angular flux fluctuation correlation to quantify the dust contamination by the ratio $\eta \equiv |C_{\kappa\delta\tau} - C_{\delta\tau}/4|/C_\kappa \approx 0.7 b_d \bar{A}/\Sigma_L$, thus allowing to estimate $\bar{A}$ up to model uncertainties in b_d and measurement errors in C_{delta_F}.

On the other hand constraints on the amount of IGM dust can be inferred from the study of the galaxy-quasar correlation. For a given line-of-sight, dust extinction reduces the observed number of galaxies above flux F from $N(> F)$ to $N(> F \exp[\bar{\tau} + \delta\tau]) \simeq N(> F)[1 - \alpha(\bar{\tau} + \delta\tau)]$. Here, $\alpha = -d\ln N/d\ln F$ is the (negative) slope of the intrinsic galaxy luminosity function $N(> F)$ and we have assumed $\tau \ll 1$. Thus dust inhomogeneities induce a fractional fluctuation $-\alpha\delta\tau$ in the galaxy number density. Since $\delta\tau$ is correlated with the matter density field, dust extinction induces a correlation between foreground galaxies and background galaxies (quasars) such that $w_{fb}(\theta) = -\alpha\langle\delta\tau(\theta')\delta_g^f(\theta' + \theta)\rangle$. Here, δ_g^f is the foreground galaxy number overdensity. On the other hand, lensing induced
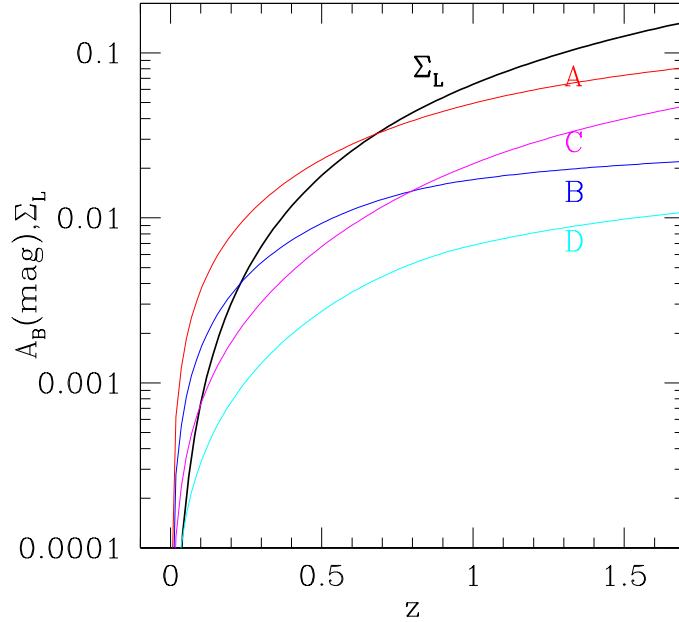
Figure 2.2: The lensing normalized matter surface density Σ_L and the B-band dust extinction A_B for different dust models.

fluctuations in galaxy number density are $2(\alpha - 1)\kappa$ [55], where the -1 term accounts for the fact that lensing magnifies the surface area and thus decreases the number density. Because of the different dependence on the slope α the signal of extinction and lensing can be separated simultaneously. Furthermore, while the lensing effect is wavelength independent, the cross-correlation is wavelength dependent with a small, but non-vanishing color slope even in the case of gray dust. In [54] we predicted for one our dust models with $\Omega_d = 10^{-6}$ a negative correlation with amplitude ~ 0.003 at $\theta = 0.01°$. quite remarkably this coincides with the characteristics of the quasar-galaxy correlation measured by Menard et al. [44, 45] from the analysis of the SDSS which have provide the first clear indication of dust in the IGM.

Chapter **3**

Dark Energy and Non-linear Dark Matter Collapse

3.1 Non-linear scales and DE signatures

How Dark Energy alters the formation and evolution of cosmic structures? Are there observational features that can shed light onto the nature of this exotic phenomenon? These are the key questions that have motivated the bulk of my research since my doctorate.

At large scale Dark Energy leaves a distinct imprint on the temperature anisotropies of Cosmic Microwave Background radiation. CMB photons crossing overdense regions during the accelerating phase are perturbed by the time variation of the potential wells. This generates temperature fluctuations which are imprinted on the large angular scales of the CMB [56]. This is the so called Integrated Sachs-Wolfe effect which has been detected through cross-correlation measurements of CMB maps with galaxy surveys [57] as originally proposed by [58] and which provide complementary constraints on DE [59,60]. Dark Energy clustering can also affect the Dark Matter power spectrum on the very large scales. In the simplest scenario a Quintessence-like component is homogeneous on sub-horizon scales, while a constant perturbation mode may exist only near horizon scale, thus causing a small excess of power on the large scale clustering of Dark Matter compared to the small scales. The effect is of order of a few percent and as such it is hardly

detectable even with future galaxy survey data due to cosmic variance. On the other hand a fully inhomogeneous DE component alter the Dark Matter clustering proportionally to $(1+w)\Omega_{DE}/\Omega_m$ [61], where w is the DE equation of state, Ω_{DE} and Ω_m are the cosmic DE and matter densities respectively. Thus, for $w > -1$ the DM clustering is enhanced, while for $w < -1$ is suppressed.

At small scales the late time gravitational collapse of Dark Matter perturbations becomes non-linear. The onset of mode couplings alters the matter power spectrum on non-linear scales. Furthermore, as the collapse proceeds Dark Matter particles are bounded into virialized structures, the halos. These are the building blocks of the cosmic structure formation, since it is inside these objects that cooling baryonic gas falls in to form the stars and galaxies that we observe today. Whether DE leaves a clear imprint also on these scales has been subject of active investigation. Two arguments may suggest a negative answer to this quest. Firstly, Dark Energy comes to dominate the cosmic energy budget at late time and its effect are dominant only on the large scales. Secondly, we may expect that the non-linear regime would erase any dependence on initial conditions and linear growth history. Due to the non-linear dynamics of the system, this evolutionary regime of structure formation is mostly studied through N-body simulation experiments. Early studies of the non-linear clustering of Dark Matter in Quintessence cosmologies found results that seemed to support these arguments (see e.g. [62, 63]). However, none of these works performed neither a systematic study of the problem nor possessed the numerical accuracy to detect the feeble DE signatures. As an example a result that has been very influential in suggesting the idea that the non-linear clustering of Dark Matter is independent not only of Dark Energy, but of the underlying cosmological model concerned the halo mass function inferred from N-body simulations [64]. This particular study found that when properly scaled to account for the mean matter density and the variance of the linear density field the number density of Dark Matter halos can be expressed in terms of a universal fitting formula which does not dependent on the underlying cosmology to within 20% accuracy.

The research program that Jean-Michel Alimi, Yann Rasera and myself have set at LUTH aims to asses the impact of DE on the non-linear structure formation through a

systematic and detailed physical analysis based on the use of accurately designed N-body simulations. The bulk of this work is still ongoing, nevertheless in the past three years we have obtained some important results that falsify the arguments against the presence of DE effect on non-linear scales.

In [65] we have shown that DE dependent modifications of the Dark Matter power spectrum occurs on non-linear scales above the stable clustering regime. These are a manifestation of the fact that the non-linear regime carries a memory of the past linear growth. In fact, we find that relative to the standard LCDM case deviations of the non-linear matter power spectrum are correlated with the integral of the growth factor of the underlying DE model relative to that of the LCDM. Again this is because above the stable clustering scales the non-linear regime does not erase information on the linear growth phase as shown in [66]. Similar conclusions where inferred from the numerical study by the Durham group led by Elise Jennings [67].

In [68] we have tackled the issue of the "universality" of the mass function and indentified the conditions for which an apparent universality may occurs. In particular, we find that models with nearly identical linear growth histories exhibit approximately identical mass functions to numerical precision. In contrast, models which do not share the same linear growth function predict different mass functions. As clearly shown by our study even when properly scaled the mass function still carries a characteristic imprint of the underlying DE model, which causes deviations from a universal behavior. We find such deviations to be correlated with the value of the linearly extrapolated critical density δ_c predicted by the spherical collapse model of the DE model under consideration. Using the Sheth-Tormen formula [69] which explicitly depends on this quantity to fit the numerical data reduces the amplitude of such deviations. Nevertheless, excess residuals at different redshifts still remains and which we find to be correlated with the values of the virial overdensity predicted by the spherical collapse model at that redshift. These results indicated that the entire shape of the mass function and not simply the exponential cut-off at the high-mass end carry cosmological information. It is this study that has lead me to further investigate the physicality of the halo mass function. A topic which in recent years I have worked on in collaboration with my student Ixandra Achitouv.

3.2   Halo Mass Function and Collapse Model

The seminal work by Press & Schechter (PS) [70] is the first attempt to derive the halo mass function from the statistical properties of the linear Dark Matter density perturbations. The basic idea behind the PS approach is that halos form in regions of the smoothed linear density field which lie above a critical linearly extrapolated density threshold of collapse, such as predicted from the spherical collapse model. Then, the number density of halos in the mass range $[M, M + dM]$ can be inferred from the fraction of mass elements in halos with mass $> M$, namely

$$\frac{dn}{dM} = \frac{1}{V}\frac{dF}{dM}, \tag{3.1}$$

where

$$F(M) = \int_{\delta_c}^{\infty} d\delta\, P(\delta, M), \tag{3.2}$$

with δ_c being the collapse threshold and $P(\delta, M)$ the probability distribution function of the linear density field smoothed over a scale R associated to a mass $M = \bar{\rho}V(R)$, where $\bar{\rho}$ is the mean matter density and $V(R) = \int W(x, R)\, d^3x$ the volume filtered by $W(x, R)$ the smoothing function in real space. In the case of a Gaussian random field with zero mean and variance $S \equiv \sigma^2(R)$, $P(\delta, S) = e^{-\delta^2/2S}/\sqrt{2\pi S}$ and Eq. (3.2) gives

$$F(M) = \frac{1}{2}\text{Erfc}\left[\frac{\delta_c}{\sqrt{2S}}\right]. \tag{3.3}$$

At this point is convenient to rewrite Eq. (3.1) as

$$\frac{dn}{dM} = \frac{\bar{\rho}}{M^2}\frac{d\log\sigma^{-1}}{d\log M}f(\sigma), \tag{3.4}$$

where we have factorized the contribution of the mean matter density and the variance of the smoothed linear density field, while the so called "multiplicity function" $f(\sigma) = 2\sigma^2 dF/dS$ encodes all information on the non-linear collapse of Dark Matter halos. From Eq. (3.2) one finds

$$f_{PS}(\sigma) = \frac{1}{\sqrt{2\pi}}\frac{\delta_c}{\sigma}e^{-\frac{\delta_c^2}{2\sigma^2}}, \tag{3.5}$$

the exponential cut-off in the above formula is consistent with the N-body mass function at the high-mass end, but overall Eq. (3.5) poorly reproduce results from N-body simulations. A key limitation of the PS approach is the miscounting of the number of regions which are

above the threshold at multiple scales, the so called "cloud-in-cloud" problem. Since the fraction of mass element in halos is obtained by indiscriminately integrating over density perturbations independently of the mass enclosed the formalism does not make difference whether a collapsed mass M_1 is embedded in a larger collapsed region $M_2 > M_1$. The PS approach wrongly counts both M_1 and M_2 as contributing to the mass function, while only M_2 should be considered.

The formulation of the Excursion Set theory by Bond et al. [71] encompasses the original Press-Schecther idea with a powerful mathematical formalism in which the computation of the mass function is reduced to solving a stochastic calculus problem. As shown in [71], at any point in space the density fluctuation field behaves as a stochastic variable obeying a Langevin equation as function of the smoothing scale:

$$\frac{\partial \delta}{\partial R} = \zeta(R) \ \& \ \zeta(R) = \frac{1}{(2\pi)^3} \int d^3k \delta(k) \frac{\partial \tilde{W}}{\partial R} e^{-ikx}, \tag{3.6}$$

where ζ is a noise term that depends on the form of the filter function (halo mass definition) and statistical properties of the linear density field. Halos are associated to random trajectories which first-cross the critical density threshold of collapse. It is the first-crossing requirement together with the introduction of a mass ordering through the pseudo-time dependence on R that solves the cloud-in-cloud problem.

The goal of the Excursion Set is to compute the probability distribution of random walks obeying Eq. (3.6) that have yet to cross the collapse threshold, $\Pi(\delta, \delta_c, S)$. This allows to compute the first-crossing distribution

$$\frac{dF}{dS} = -\frac{\partial}{\partial S} \int_{-\infty}^{\delta_c} \Pi(\delta, \delta_c, S) \, d\delta, \tag{3.7}$$

from which one can derive the multiplicity function, $f(\sigma)$.

In the case of uncorrelated Gaussian random walks the Excursion Set reduces to solving a simple diffusion problem and the multiplicity function matches the Press-Schechter result multiplied by a factor of 2, that is the so called Extended Press-Schechter. Hence, even after solving the cloud-in-cloud problem the Excursion Set prediction still fail to reproduce N-body simulation results. This is because assuming uncorrelated Gaussian random walks with a spherical collapse barrier is a too simplistic model of halo formation. In fact,

assuming that the random walks are uncorrelated implies that the smoothing function of the linear density field differs from the standard one (e.g. when computing σ_8), a spherical top-hat in real space. Hence, the computation of Eq. (3.4) is not coherent. However, in the case of a top-hat in real space the random walks are correlated and the computation of the multiplicity function cannot be performed analytically, thus requiring numerical Monte Carlo simulations. Another oversimplification concerns the spherical collapse threshold. As shown in a vast literature (see e.g. [72,73]) the Dark Matter collapse at small scales can be highly non-spherical and the collapse of a homogeneous ellipsoid may be a much better model to extrapolate the collapse threshold. As shown by Sheth et al. [74] in the ellipsoidal collapse model the linearly extrapolated collapse threshold is randomly distributed variable with mass dependent average. By numerically solving the first-crossing distribution of uncorrelated random walk for such barrier model Sheth et al. found that the inferred multiplicity function provides a good approximation of the Sheth-Tormen formula derived empirically to fit the GIF simulations [69] and as mentioned in the previous chapter the Sheth-Tormen fitting formula is capable of encoding some of the cosmology dependence of the N-body mass function. This clearly suggests that the parameters of Sheth-Tormen formula may have a direct physical meaning related to the collapse model, as well as to the mass definition of halos which depends on the smoothing function.

In 2009 in a series of papers [75], Maggiore and Riotto described how to derive self-consistent and fully analytical predictions for mass function using path-integral techniques. The application of this mathematical approach to the Excursion Set theory offers the opportunity to address several questions about the Dark Matter halo mass function and statistics of Dark Matter halos in general. I was particularly interested in two line of research. First, developing a clear analytical link between barrier model parameters (and their cosmology dependence) and the form of the mass function which in the long term can optimize the cosmological parameter inference from observational tests such as cluster number counts. Second, given the interest on the mass function as probe of primordial non-Gaussianity, it needed to be addressed how the non-spherical halo collapse affected the signature of primordial non-Gaussianity on the mass function. This made the subject of a doctoral thesis. At that time Ixandra Achitouv was looking for an internship in

Cosmology as part of the NPAC-School Master 2 program and I proposed her to study the articles by Maggiore and Riotto. Since I do not have the HDR I discussed with Prof. Jim Bartlett of Paris 7 about the possibility of a "co-tutelle" which would allow me to sponsor Ixandra application for a PhD scholarship and supervise her work. In the end everything worked out and Ixandra started her PhD in the Autumn 2009. In September 2012 she obtained her PhD with a thesis on "Dark Matter Halo Mass Function: Imprints of the Initial Density Field and Non-Linear Collapse".

Hereafter, I will just outline the basic idea of the path-integral approach to the Excursion Set theory and summarize the main results of our work. I leave the reader to the original articles for a detailed discussion.

As we have already mentioned the goal of the Excursion Set theory is to compute the probability distribution of random walks that do not cross the barrier. In the path-integral this computation is performed as an integral over all possible trajectories of the systems that obey such a constrain. More specifically, let us consider a stochastic variable Y varying over the time interval $[0, S]$ discretized in steps $\Delta S = \epsilon$ such that at $S_k = k\epsilon$ with $Y(S_k) = Y_k$ for $k = 1, ..., n$. Then, the transition probability from the starting point Y_0 to Y_n at $S = S_n$ of trajectories that never cross a boundary at $Y = 0$ is given by ensemble averaging of the random walks

$$\Pi_\epsilon(Y_0, Y_n, S_n) = \int_0^\infty dY_1 ... \int_0^\infty dY_{n-1} \, \mathscr{D}\lambda \, e^{i \sum_{i=1}^n \lambda_i Y_i} \langle e^{-i \sum_{i=1}^n \lambda_i Y_i(S_i)} \rangle, \qquad (3.8)$$

where the term with brakets is nothing else than the exponential of the partition function of the system, e^Z, where

$$Z = \sum_{p=1}^\infty \frac{(-i)^p}{p!} \sum_{i_1=1}^n ... \sum_{i_p=1}^n \lambda_{i_1} ... \lambda_{i_p} \langle Y_i(S_{i_1}) ... Y(S_{i_p}) \rangle_c, \qquad (3.9)$$

with $\langle Y_i(S_{i_1}) ... Y(S_{i_p}) \rangle_c$ the connected correlators of the random walks. Hence, a stochastic model is fully specified by the correlation functions. The markovian (uncorrelated) case corresponds to having the 2-point function being a δ-Dirac and all higher moments to be vanishing. If the amplitudes of the connected correlators are small compared to the markovian analog than one can compute $\Pi_\epsilon(Y_0, Y_n, S_n)$ as a perturbative expansion around the markovian solution. Maggiore & Riotto [75] have shown that in the case of standard
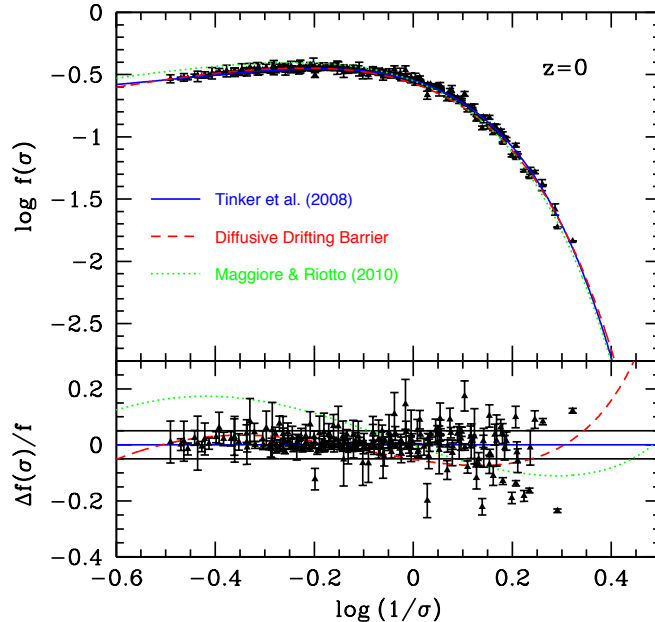
Figure 3.1: (Upper panel) Halo mass function at z = 0 given by the Tinker et al. fitting formula for $\Delta = 200$ (solid blue line), diffusing drifting barrier with $\beta = 0.057$ and $D_B = 0.294$ (red dashed line) and Maggiore & Riotto [75] with $D_B = 0.235$ (green dotted line). Data points are from [77]. (Lower panel) Relative difference with respect to the Tinker et al. fitting formula. The thin black solid lines indicates 5% deviations.

Gaussian LCDM model the 2-point correlation due to filtering the linear density field with a top-hat function in real space is small compared to that of a top-hat filter in Fourier space which generates uncorrelated random walks. This allowed them to infer perturbative corrections with respect to the Extended Press-Schechter formula and further extend the calculation to the case of a stochastic spherical collapse barrier.

In [76] we have derived analytical formulae of the halo mass function and bias for a stochastic barrier which captures the main features of the non-spherical collapse of halos. The computation has allowed us to show that on the one hand the deviations from the spherical collapse mainly suppress the mass function at small masses; on the other hand

a stochastic diffusion of the collapse condition affects the mass function at large and intermediate masses. By comparing the analytical formula with the mass function from simulations by Tinker et al. [77] we have found an unprecedented agreement to the level of numerical uncertainty of the simulations $\sim 5\%$ (see Fig. 3.1). Following this work, Ixandra has investigated the relation between the signature of the non-spherical collapse on the mass function and the imprint of primordial non-Gaussianity. The results, published in [78], have shown that also in the case of non-Gaussian initial conditions the path-integral calculation of the mass function agrees with results from non-Gaussian N-body simulations. Moreover we have found that the effect of the non-spherical collapse of Dark Matter shapes the mass function in a way that is degenerated with the effects induced by PNG, with the amplitude of the non-spherical collapse effects being larger for increases PNG amplitudes. This implies that reliable PNG constraints from cluster number counts can be inferred only if the imprint on the mass function of the non-spherical collapse of halo is properly accounted for.

The Excursion Set formalism relies on the idea that halos form out of any random points in the initial density field where the density inside a smoothed region centered on these points is above a non-linear collapse density threshold. In the work described above we have modeled this threshold with a statistical model. The reason being that it is impossible to know the exact density condition of non-linear collapse at every point of the density field, rather it is more plausible to access to its ensemble properties. Hence, if the Excursion Set is self-consistent, once the mass function has been found to be in agreement with that from N-body simulations, the regions in the initial conditions from which the N-body halos have formed, must have densities whose statistics is consistent with the statistical model of collapse used to predict the mass function. Ixandra has lead a project specifically dedicated to test the self-consistency of the Excursion Set using the vast simulation dataset from the "Dark Energy Universe Simulation Series" (DEUSS) project. In Achitouv, Rasera, Sheth, Corasaniti [79] we have analyzed a catalog of numerical halos. In order to be consistent with the basic assumption of the Excursion Set Theory, for each halo in the catalog we have drawn a random particle. Then, by tracing its location in the initial conditions we have measured the initial overdensity contained within a radius containing a mass equal
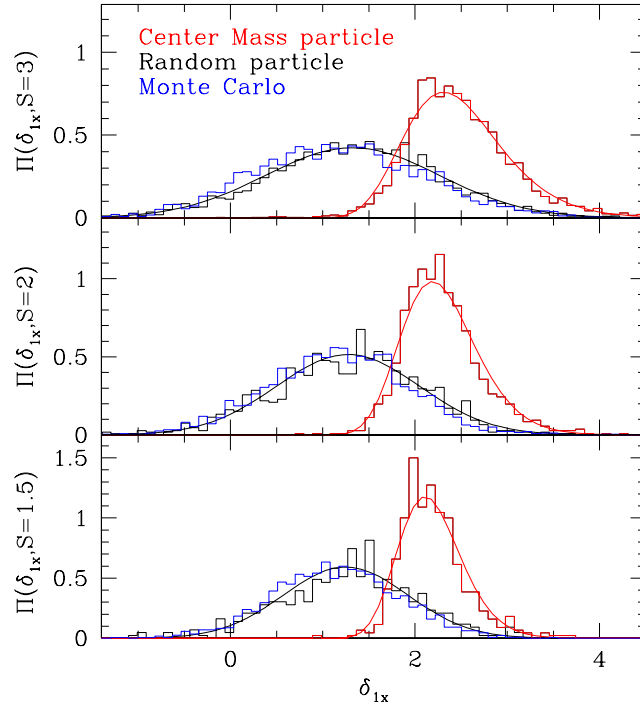
Figure 3.2: Distribution of first-crossing overdensities in Monte-Carlo simulations (blue histograms) and our theoretical prediction (smooth solid black curves), for parameters calibrated using the first-crossing distribution from DEUS simulations and the initial over-densities around randomly chosen halo particles (black histograms) at S = 1.5, 2 and 3. Red histograms, which are more sharply peaked, show the same measurement but around the halo centers of mass. In this case, smooth curves show the best-fitting Lognormal.

to that of the halo under consideration. By repeating this procedure for halos in the catalog we have been able to compute the distribution of halo overdensities in the initial conditions. The comparison with the prediction from the statistical model of collapse shows a remarkable agreement (see Fig. 3.2), which for the first time has demonstrated the self-consistency of the formalism.

Morale

In the previous chapters I summarized some of the work that I carried out in the past ten years in the field of Physical Cosmology. I am very keen of using this term because it is the title of a founding cosmology textbook by Jim Peebles which concisely expresses a Physics approach to question, model and understand the phenomena that characterize the Universe we live in.

I hope to have convinced the reader that although the topics presented here differs from one another, their study has been stimulated by a unifying endeavor: that of advancing the quest for Dark Energy. Whether concerning dust in the Inter-Galactic Medium or the non-linear gravitational collapse of Dark Matter shaping the halo mass distribution, understanding Dark Energy can only be attained by solving the myriads of puzzles that contribute to our ignorance of the cosmos.

There is today a widespread believe that the quest for Dark Energy resolves into measuring an equation of state parameter/s w (w_a). This, however, instills the tempting idea that once things get ready it will be sufficient to point all the guns (observations) on to the same target to kill the Dark Energy problem out of the astrophysical realm once and for all. Despite the limited size of this dissertation I hope to have been able to pass the reader my anti-conformist message: "understanding Dark Energy cannot be reduced to simply measuring a few parameters". What if w is the wrong parameter? Having measured its value to the third decimal digit would really provide us with the necessary knowledge to make sense of all other phenomena that occur in the Universe? In the end the stuff we are made of contributes to no more than 5% of the total content of the Universe, and still it

has taken more than 100 years from the discovery of quantum nature of photons to that of the Higgs boson to have a complete understanding of the laws that govern it. Pretending that we may settle the question on the invisible Universe in the next 20 years by simply measuring one or two parameters sounds like what the Ancient Greeks defined as $u\beta\rho\iota\varsigma$, and the history of physics has always implacably erased human hubris.

We have just come to perceive the existence of a vast Dark sector through its gravitational effects. Given how little we know about, it cannot be a priori excluded that such an invisible domain can manifests a complexity which today we are simply not able to appreciate. For this to be excluded there is still lots of unknown complex physics that needs to be disclosed.

Bibliography

[1] A.G. Riess et al., Astron. J. **116**, 1009 (1998)

[2] S. Perlmutter et al., Astrophysical J. **517**, 565 (1999)

[3] F. Occhionero and L. Amendola, Phys. Rev. D**50**, 4846 (1994)

[4] L. Amendola, C. Baccigalupi, R. Konoplich, F. Occhionero, S. Rubin, Phys. Rev. D**56**, 7199 (1996)

[5] F. Occhionero, C. Baccigalupi, L. Amendola, S. Monastra, Phys. Rev. D**56**, 7588 (1997)

[6] C. Baccigalupi, L. Amendola, F. Occhionero, L. Amendola, MNRAS **288**, 387 (1997)

[7] L. Amendola, C. Baccigalupi, F. Occhionero, L. Amendola, ApJ **492**, L5 (1998)

[8] P.G. Ferreira, J. Magueijo and K. Gorski, ApJ **503**, L1 (1998)

[9] D.N. Spergel and D.M. Golberg, Phys. Rev. D**59**, 103001 (1999)

[10] D.M. Golberg and D.N. Spergel, Phys. Rev. D**59**, 103002 (1999)

[11] P.S. Corasaniti, L. Amendola and F. Occhionero, MNRAS **323**, 677 (2001)

[12] P. De Bernardis et al., Nature **404**, 955 (2000); D.N. Spergel et al., ApJS **148**, 175 (2003),

[13] G. Efstathiou et al., MNRAS **330**, L29 (2002); Tegmark M. et al., PRD **69**, 103501 (2004)

[14] P. Astier, Astron. & Astrophys. **447**, 31 (2006)

[15] D. Clowe et al., ApJ **648**, L109 (2006)

[16] S.M. Carroll, Living Rev. Relativity, **4**, 1 (2001)

[17] M. Reuter and C. Wetterich, PLB **188**, 38 (1987); G. Dvali, S. Hofmann and J. Khoury, PRD **76**, 084006 (2007)

[18] T. Damour, G.W. Gibbons and C. Gundlach, Phys. Rev. Lett. **64**, 123 (1990); J.A. Casas, J. Garcia-Bellido and M. Quiros, Clas. Quant. Grav. 9, 1371 (1992); L. Amendola, Phys. Rev. D**62**, 043511 (2000); L. Amendola and D. Tocchini-Valentini, Phys. Rev. D**64**, 043509 (2001); D. Comelli, M. Pietroni and A. Riotto, Phys. Lett. B 571, 115 (2003); J.-M. Alimi and A. Fuzfa, JCAP, 014 (2008); A. Fuzfa and J.-M. Alimi, Phys. Rev. Lett. **97**, 061301 (2006).

[19] J. Khoury and A. Weltman, Phys. Rev. Lett. **93**, 172204 (2004); Phys. Rev. D**69**, 044026 (2004); S.S. Gubser and J. Khoury, Phys. Rev. D**70**, 104001 (2004).

[20] W.J. Percival et al., Mont. Not. Roy. Astron. Soc. **381**, 1053 (2007)

[21] P.A.R. Ade et al., arXiv:1303.5076 (2013)

[22] R.R. Caldwell, M. Kamionkowski and N.N. Weinberg, Phys. Rev. Lett. **91**, 071301 (2003)

[23] G. Huey, B.D. Wandelt, Phys. Rev. D**74**, 023519 (2006)

[24] S. Das, P.S. Corasaniti and J. Khoury, Phys. Rev. D**73**, 083509 (2006)

[25] R. Bean, E.E. Flanagan and M. Trodden, Phys. Rev. D**78**, 023009 (2008)

[26] J. Valiviita, E. Majerotto, R. Maartens, JCAP 0807, 020 (2008)

[27] M.C. Johnson and M. Kamionkoski, Phys. Rev. D**78**, 063010 (2008)

[28] P.S. Corasaniti, Phys. Rev. D**78**, 083538 (2008)

[29] M.M. Phillips, Astrophys. J., **413**, L105 (1993)

[30] M. Hamuy et al., Astrophys. J., **112**, 2391 (1996)

[31] V.N. Gamezo et al., Science, **299**, 77 (2003)

[32] V.N. Gamezo, A.M. Khokhlov, E.S. Oran, Phys. Rev. Lett., **92**, 211102 (2004)

[33] M. Kowalski et al., Astrophys. J., **686**, 749 (2008)

[34] I. Maor, R. Brustein, J. McMahon, and P.J. Steinhardt, Phys. Rev. D**65**, 123003 (2002)

[35] B.A. Bassett, P.S. Corasaniti, M. Kunz, Astrophys. J., **617**, L1 (2004)

[36] A.G. Kim, E.V. Linder, R. Miquel, N. Mostek, Mont. Not. Roy. Astron. Soc., **347**, 909 (2004)

[37] J. Weller, A. Albrecht, Phys. Rev. D**65**, 103512 (2002)

[38] P.S. Corasaniti, M. Loverde, A. Crotts, C. Blake, Mont. Not. Roy. Astron. Soc., **798**, 804 (2006)

[39] P.S. Corasaniti, Mont. Not. Roy. Astron. Soc., **372**, 191 (2006)

[40] D.A. Buote, ASSL Conference Proceedings, Vol. 281, Edited by J.L. Rosenberg and M.E. Putman, astro-ph/0210608.

[41] L.L Cowie, A. Songaila, T.S. Kim, E.M. Hu, Astron. J., **109**, 1522 (1995)

[42] R.C. Telfer, G.A. Kriss, W. Zheng, A.F. Davidsen, D. Tytler, Astrophys. J., **579**, 500 (2002)

[43] D. Chelouche, B.P. Koester, D.V. Bowen, Astrophys. J., **671**, L97 (2007)

[44] B. Menard et al., Mont. Not. Roy. Astron. Soc., **385**, 1053 (2008)

[45] B. Menard, R. Scranton, M. Fukugita, G. Richards, Mont. Not. Roy. Astron. Soc., **405**, 1025 (2010)

[46] S. Bianchi, A., Ferrara, Mont. Not. Roy. Astron. Soc., **358**, 379 (2005)

[47] A. Aguirre, Z. Haiman, Astrophys. J., **532**, 28 (2000)

[48] A.K. Inoue, H., Kamaya, Mont. Not. Roy. Astron. Soc., **341**, L7 (2003)

[49] F. Paerels, A. Petric, A. Telis, D.J. Helfand, BAAS, 201, 97.03 (2002)

[50] A.K. Inoue, H. Kamaya, H., Mont. Not. Roy. Astron. Soc., **350**, 729 (2004)

[51] A.J. Bunker, Proceedings of the IAU, IAU Symposium, Vol. 279, 224 (2012)

[52] A. Cooray, D.E. Holz, D. Huterer, Astrophys. J., **637**, L77 (2006)

[53] S. Dodelson, A. Vallinotto, Phys. Rev. D**74**, 063515 (2006)

[54] P. Whang, P.S. Corasaniti, Astrophys. J., **657**, 71 (2007)

[55] M. Bartelmann, P. Schneider, Phys. Rept., **340**, 291 (2001)

[56] M.J. Rees and D.W. Sciama, Nature 217, 511 (1968)

[57] T. Giannantonio et al., Phys. Rev. D**77**, 123520 (2008); S. Ho, C. Hirata, N. Padmanabhan, U. Seljak, N. Bahcall, Phys. Rev. D**78**, 043519 (2008)

[58] R.G. Crittenden and N. Turok, Phys. Rev. Lett., **76**, 575 (1996)

[59] P.S. Corasaniti, D. Huterer and A. Melchiorri, Phys. Rev. D**72**, 062001 (2007)

[60] L. Pogosian, P.S. Corasaniti. C. Stephan-Otto, R. Crittenden and R. Nichol, Phys. Rev. D**72**, 103519 (2005)

[61] E. Sefusatti and F. Vernizzi, F., JCAP, 1103, 047 (2011)

[62] C.P. Ma, R.R. Caldwell, P. Bode, L.-M. Wang, Astrophys. J., **521**, L1 (1999)

[63] A. Klypin, A. V. Maccio, R. Mainini, S. A. Bonometto, S. A., Astrophys. J., **521**, 31 (2003)

[64] A. Jenkins et al., Mon. Not. Roy. Astron. Soc., **321**, 372 (2001)

[65] J.-M. Alimi, A. Fuzfa, V. Boucher, Y. Rasera, J. Courtin, P.S. Corasaniti, Mont. Not. Roy. Astron. Soc., **401**, 775 (2010)

[66] Z. Ma, Astrophys. J., 665, 887 (2007)

[67] E. Jennings, C.M. Baugh, R.E. Angulo, S. Pascoli, Mont. Not. Roy. Astron. Soc., **401**, 2181 (2010)

[68] J. Courtin, Y. Rasera, J.-M. Alimi, P.S. Corasaniti, V. Boucher, A. Fuzfa, Mont. Not. Roy. Astron. Soc., **410**, 1911 (2011)

[69] R.K. Sheth and G. Tormen, Mont. Not. Roy. Astron. Soc., **308**, 119 (1999)

[70] W. H. Press and P. Schechter, Astrophys. J., **187**, 425 (1974)

[71] J.R. Bond, S. Cole, G. Efstathiou and G. Kaiser, Astrophys. J., **379**, 440 (1991)

[72] A.G. Doroshkevich, Astrophyzika **3**, 175 (1970)

[73] J.R. Bond and S. Myers, Astrophys. J. Supp., **103**, 1 (1996)

[74] R.K. Sheth, H.J. Mo and G. Tormen, Mont. Not. Roy. Astron. Soc., **323**, 1 (2001)

[75] M. Maggiore and A. Riotto, Astrophys. J. **711**, 907 (2010); M. Maggiore and A. Riotto, Astrophys. J. **717**, 515 (2010)

[76] P.S. Corasaniti and I. Achitouv, Phys. Rev. Lett. **106**, 241302 (2011); P.S. Corasaniti and I. Achitouv, Phys. Rev. D**84**, 023009 (2011)

[77] J. Tinker et al., Astrophys. J. **688**, 709 (2008).

[78] I. Achitouv and P.S. Corasaniti, JCAP **02**, 002 (2012); Erratum, JCAP **07** E01 (2012); I. Achitouv and P.S. Corasaniti, Phys. Rev. D**86**, 083011 (2012)

[79] I. Achitouv, Y. Rasera, R.K. Sheth, P.S. Corasaniti, arXiv:1212.1166

Appendix

Here are copies of the articles summarized in the HDR document.

Superacceleration as the signature of a dark sector interaction

Subinoy Das,[1,2] Pier Stefano Corasaniti,[1] and Justin Khoury[3]

[1]*ISCAP, Columbia University, New York, New York 10027, USA*
[2]*Center for Cosmology and Particle Physics, Department of Physics, New York University, New York, New York 10003, USA*
[3]*Center for Theoretical Physics, Massachusetts Institute of Technology, Cambridge, Massachusetts 02139, USA*

We show that an interaction between dark matter and dark energy generically results in an effective dark-energy equation of state of $w < -1$. This arises because the interaction alters the redshift dependence of the matter density. An observer who fits the data treating the dark matter as noninteracting will infer an effective dark-energy fluid with $w < -1$. We argue that the model is consistent with all current observations, the tightest constraint coming from estimates of the matter density at different redshifts. Comparing the luminosity and angular-diameter distance relations with ΛCDM and phantom models, we find that the three models are degenerate within current uncertainties but likely distinguishable by the next generation of dark-energy experiments.

I. INTRODUCTION

Nature would be cruel if dark energy were a cosmological constant. Unfortunately this daunting possibility is increasingly likely as observations converge towards an equation of state of $w = -1$. Combining galaxy, cosmic microwave background (CMB) and Type Ia supernovae (SNIa) data, Seljak *et al.* [1] recently found $-1.1 \lesssim w \lesssim -0.9$ at 1σ. On the one hand, a cosmological constant is theoretically simple as it involves only one parameter. However, observations would offer no further guidance to explain its minuteness, whether due to some physical mechanism or anthropic reasoning [2].

A more fertile outcome is $w \neq -1$. This implies dynamics—the vacuum energy is changing in a Hubble time—and hence, new physics. A well-studied candidate is quintessence [3,4], a scalar field ϕ rolling down a self-interaction potential $V(\phi)$. Its equation of state,

$$w_\phi = \frac{\dot{\phi}^2/2 - V(\phi)}{\dot{\phi}^2/2 + V(\phi)}, \tag{1}$$

can be $< -1/3$ for sufficiently flat $V(\phi)$ and thus lead to cosmic speed-up. Whether dark energy is quintessence or something else, this case offers hope that further observations, either cosmological or in the solar system, may unveil the underlying microphysics of the new sector.

An even more exciting possibility is $w < -1$. In fact there are already indications of this [5,6] from various independent analyses of the "Gold" SNIa data set [7]. Moreover, by constraining redshift parametrization of $w(z)$ they also exclude that this could result from assuming a constant w [8,9]. The $w < -1$ regime would rule out quintessence since $w_\phi \geq -1$ [see Eq. (1)], as well as most dark-energy models.

Devising consistent models with $w < -1$ has proven to be challenging. Existing theories generally involves ghosts, such as phantom models [10], resulting in instabilities and other pathologies [11]. Fields with nonminimal couplings to gravity, such as Brans-Dicke theory, can mimic $w < -1$ [12]. However, solar-system constraints render the Brans-Dicke scalar field nearly inert, thereby driving w indistinguishably close to -1. Other proposals for $w < -1$ include brane-world scenarios [13], quantum effects [14], quintessence-moduli interactions [15], and photon-axion conversion [16].

In this paper we show that $w < -1$ naturally arises if quintessence interacts with dark matter. The mechanism is simple. Because of the interaction, the mass of dark matter particles depends on ϕ. Consequently, in the recent past the dark matter energy density redshifts more slowly than the usual a^{-3}, which, for fixed present matter density, implies a smaller matter density in the past compared to normal cold dark matter (CDM).

An observer unaware of the interaction and fitting the data assuming normal CDM implicitly ascribes this dark matter deficit to the dark energy. The effective dark-energy fluid thus secretly receives two contributions: the quintessence part and the deficit in dark matter. The latter is growing in time, therefore causing the effective dark-energy density to also increase with time, hence $w < -1$.

Treating dark matter as noninteracting is a *sine qua non* for inferring $w < -1$. There are no wrong-sign kinetic terms in our model—in fact the combined dark matter plus dark-energy fluid satisfies $w > -1$. Hence the theory is well defined and free of instabilities.

Interacting dark matter/dark energy models have been studied in various contexts [17–23]. Huey and Wandelt [24] realized that coupled dark matter/quintessence can yield an effective $w < -1$. (See also [25] for similar ideas.) However, the dynamics in [24] are such that DM density becomes negligibly small for $z \gtrsim 1$, thereby forcing the addition of a second noninteracting DM component. In contrast, our model involves a single (interacting) DM component.

Given the lack of competing consistent models, we advocate that measuring $w < -1$ would hint at an interac-

083509-1

tion in the dark sector. More accurate observations could then search for direct evidence of this interaction. For instance, we show that the extra attractive force between dark matter particles enhances the growth of perturbations and leads to a few percent excess of power on small scales. Other possible signatures are discussed below.

II. DARK-SECTOR INTERACTION

Consider a quintessence scalar field ϕ which couples to the dark matter via, e.g., a Yukawa-like interaction

$$f(\phi/M_{\rm Pl})\bar{\psi}\psi, \tag{2}$$

where is f is an arbitrary function of ϕ and ψ is a dark matter Dirac spinor. In order to avoid constraints from solar-system tests of gravity, we do not couple ϕ to baryons. See [19], however, for an alternative approach.

In the presence of this dark-sector interaction, the energy density in the dark matter no longer redshifts as a^{-3} but instead scales as

$$\rho_{\rm DM} \sim \frac{f(\phi/M_{\rm Pl})}{a^3}. \tag{3}$$

This can be easily understood since the coupling in Eq. (2) implies a ϕ-dependent mass for the dark matter particles scaling as $f(\phi/M_{\rm Pl})$. Since the number density redshifts as a^{-3} as usual, Eq. (3) follows.

Thus the Friedmann equation reads

$$3H^2 M_{\rm Pl}^2 = \frac{\rho_{\rm DM}^{(0)}}{a^3} \frac{f(\phi/M_{\rm Pl})}{f_0} + \rho_\phi, \tag{4}$$

where $f_0 = f(\phi_0/M_{\rm Pl})$ with ϕ_0 the field value today, and

$$\rho_\phi = \tfrac{1}{2}\dot{\phi}^2 + V(\phi) \tag{5}$$

is the scalar field energy density. With $a = 1$ today, $\rho_{\rm DM}^{(0)}$ is identified as the present dark matter density.

Meanwhile, the scalar field evolution is governed by

$$\ddot{\phi} + 3H\dot{\phi} = -V_{,\phi} - \frac{\rho_{\rm DM}^{(0)}}{a^3} \frac{f_{,\phi}}{f_0}. \tag{6}$$

This differs from the usual Klein-Gordon equation for quintessence models by the last term on the right-hand side, arising from the interaction with dark matter.

The standard approach to constraining dark energy with experimental data assumes that it is a noninteracting perfect fluid, fully described by its equation of state, $w_{\rm eff}$. Given some $w_{\rm eff}(z)$, the evolution of the dark-energy density is then determined by the energy conservation equation:

$$\frac{d\rho_{\rm DE}^{\rm eff}}{dt} = -3H(1 + w_{\rm eff})\rho_{\rm DE}^{\rm eff}. \tag{7}$$

Meanwhile, the dark matter is generally assumed to be

noninteracting CDM, resulting in the Friedmann equation

$$3H^2 M_{\rm Pl}^2 = \frac{\rho_{\rm DM}^{(0)}}{a^3} + \rho_{\rm DE}^{\rm eff}. \tag{8}$$

An observer applying these assumptions to our model would infer an effective dark-energy fluid with

$$\rho_{\rm DE}^{\rm eff} \equiv \frac{\rho_{\rm DM}^{(0)}}{a^3}\left[\frac{f(\phi/M_{\rm Pl})}{f(\phi_0/M_{\rm Pl})} - 1\right] + \rho_\phi, \tag{9}$$

obtained by comparing Eqs. (4) and (8). The end result is to effectively ascribe part of the dark matter to dark energy. Notice that today the first term vanishes, hence the effective dark-energy density coincides with ρ_ϕ. In the past, however, $\phi \neq \phi_0$, and the two differ. In particular, we will find that the time-dependence of $\rho_{\rm DE}^{\rm eff}$ can be such that $w_{\rm eff} < -1$.

To show this explicitly requires an expression for $w_{\rm eff}$. Taking the time derivative of Eq. (9) and substituting the scalar equation of motion, Eq. (6), we obtain

$$\frac{d\rho_{\rm DE}^{\rm eff}}{dt} = -3H\left\{\frac{\rho_{\rm DM}^{(0)}}{a^3}\left[\frac{f(\phi/M_{\rm Pl})}{f(\phi_0/M_{\rm Pl})} - 1\right] + (1 + w_\phi)\rho_\phi\right\}. \tag{10}$$

Comparing with Eq. (7) allows us to read off $w_{\rm eff}$:

$$1 + w_{\rm eff} = \frac{1}{\rho_{\rm DE}^{\rm eff}}\left\{\left[\frac{f(\phi/M_{\rm Pl})}{f(\phi_0/M_{\rm Pl})} - 1\right]\frac{\rho_{\rm DM}^{(0)}}{a^3} + (1 + w_\phi)\rho_\phi\right\}. \tag{11}$$
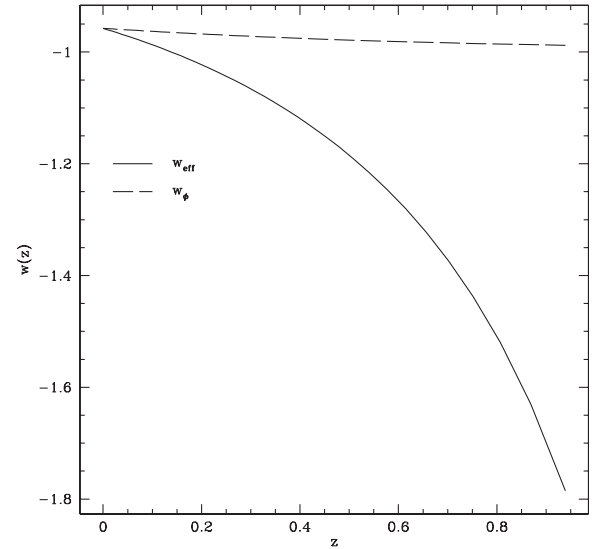
Now suppose that the dynamics of ϕ are such that

FIG. 1. Redshift evolution of $w_{\rm eff}$ (solid line) and w_ϕ (dash line). As advocated, $w_{\rm eff} < -1$ in the recent past due to the interaction with the dark matter.

$f(\phi/M_{\rm Pl})$ increases in time. This occurs in a wide class of models, as we will see in Sec. III. In this case,

$$x \equiv -\frac{\rho_{\rm DM}^{(0)}}{a^3 \rho_\phi}\left[\frac{f(\phi/M_{\rm Pl})}{f(\phi_0/M_{\rm Pl})} - 1\right] \geq 0 \qquad (12)$$

for all times until today, with equality holding at the present time. It is straightforward to show that $w_{\rm eff}$ takes a very simple form when expressed in terms of x:

$$w_{\rm eff} = \frac{w_\phi}{1 - x}. \qquad (13)$$

This is our main result. Since $x = 0$ today, one has $w_{\rm eff}^{(0)} = w_\phi^{(0)}$, which is greater than or equal to -1. In the past, however, $x > 0$. Moreover, for sufficiently flat potentials, $w_\phi \approx -1$. Hence it is possible to have $w_{\rm eff} < -1$ in the past. This is shown explicitly in Fig. 1 for a fiducial case: $f(\phi/M_{\rm Pl}) = \exp(\beta\phi/M_{\rm Pl})$ and $V(\phi) = M^4(M_{\rm Pl}/\phi)^\alpha$.

III. QUINTESSENCE DYNAMICS

We now come back to the equation of motion for ϕ, Eq. (6), and demonstrate that its dynamics can lead to $w_{\rm eff} < -1$. The scalar potential $V(\phi)$ is assumed to satisfy the tracker condition [26],

$$\Gamma \equiv \frac{V_{,\phi\phi}V}{V_{,\phi}^2} > 1. \qquad (14)$$

For an exponential potential, $\Gamma = 1$, while $\Gamma = 1 + \alpha^{-1}$ for $V(\phi) \sim \phi^{-\alpha}$. Moreover, we take the coupling function f to be monotonically increasing.

Without coupling to dark matter, the scalar field would run off to infinite values. Here, however, the interaction has a stabilizing effect since ϕ wants to minimize the effective potential

$$V^{\rm eff} = V(\phi) + \frac{\rho_{\rm DM}^{(0)}}{a^3}\frac{f(\phi/M_{\rm Pl})}{f(\phi_0/M_{\rm Pl})}. \qquad (15)$$

Indeed, it is easily seen that the right-hand side of Eq. (6) is just $-V_{,\phi}^{\rm eff}$. Similar stabilization mechanisms have been explored in other contexts, such as so-called VAMPS scenarios [27], string moduli [28,29], chameleon cosmology [19,20], interacting neutrino/dark-energy models [23], and other interacting dark matter/dark energy models [24,30], to name a few.

Having ϕ at the minimum of the effective potential is an attractor solution [20]: as the dark matter density redshifts due to cosmic expansion, ϕ adiabatically shifts to larger field values, always minimizing $V^{\rm eff}$. This is because the period of oscillations about the minimum, m^{-1}, is much shorter than a Hubble time, i.e., $m \gg H$. We show this for the present epoch, leaving the proof for all times as a straightforward exercise.

The mass of small fluctuations about the minimum is given as usual by

$$m^2 = V_{,\phi\phi}^{\rm eff} = \frac{\rho_{\rm DM}^{(0)}}{a^3}\frac{f_{,\phi\phi}}{f_0}\left\{1 + \frac{f_{,\phi}^2}{f_{,\phi\phi}f}\frac{\Gamma}{V}\frac{\rho_{\rm DM}^{(0)}}{a^3}\frac{f}{f_0}\right\}, \quad (16)$$

where we have substituted Γ using its definition, Eq. (14). Evaluating this today, and noting that $\rho_{\rm DM}^{(0)} = 3H_0^2 M_{\rm Pl}^2 \Omega_{\rm DM}^{(0)}$ and $V(\phi_0) < 3H_0^2 M_{\rm Pl}^2 \Omega_{\rm DE}^{(0)}$, we find

$$\frac{m_0^2}{H_0^2} > 3\Omega_{\rm DM}^{(0)} M_{\rm Pl}^2\left(\frac{f_{,\phi\phi}}{f}\right)_0\left\{1 + \Gamma\left(\frac{f_{,\phi}^2}{f_{,\phi\phi}f}\right)_0\frac{\Omega_{\rm DE}^{(0)}}{\Omega_{\rm DM}^{(0)}}\right\}. \quad (17)$$

The right-hand side is greater than unity for $M_{\rm Pl}^2 f_{,\phi\phi}/f \gtrsim 1$. In addition, as we will see later, $\Gamma \gg 1$ for consistency with observations of large-scale structure. These conditions guarantee that fluctuations about the minimum of the effective potential are small at the present time. For concreteness, let us evaluate this in the case of $f(\phi) = \exp(\beta\phi/M_{\rm Pl})$ and $V(\phi) = M^4(M_{\rm Pl}/\phi)^\alpha$:

$$\frac{m_0^2}{H_0^2} > 3\beta^2\Omega_{\rm DM}^{(0)}\left(1 + \frac{\alpha + 1}{\alpha}\frac{\Omega_{\rm DM}^{(0)}}{\Omega_{\rm DE}^{(0)}}\right). \qquad (18)$$

This is indeed larger than unity for $\alpha \lesssim 1$ and $\beta \gtrsim \mathcal{O}(1)$, the latter corresponding to a gravitational-strength interaction between dark matter and dark energy.

Next we show that the field is slow-rolling along this attractor solution. The proof is again straightforward. Differentiating the condition at the minimum, $V_{,\phi}^{\rm eff} = 0$, with respect to time, we obtain

$$\dot\phi = \frac{3H}{m^2}\frac{\rho_{\rm DM}^{(0)}}{a^3}\frac{f_{,\phi}}{f_0} = -\frac{3H}{m^2}V_{,\phi}, \qquad (19)$$

where in the last step we have used $V_{,\phi}^{\rm eff} = 0$. Thus,

$$\frac{\dot\phi^2}{2V} = \frac{9H^2}{2m^4}\frac{V_{,\phi}^2}{V} < \frac{9H^2}{2m^2}\frac{1}{\Gamma}. \qquad (20)$$

Since $m > H$ along the attractor, and since $\Gamma \gg 1$ as mentioned earlier, Eq. (20) implies that ϕ has negligible kinetic energy compared to potential energy, which is the definition of slow roll.

The slow-roll property has many virtues. First of all, it implies that our attractor solution is different than that derived by Amendola and collaborators [18]. In their case, during the matter-dominated era, the scalar field kinetic energy dominates over the potential energy and remains a fixed fraction of the critical density. This significantly alters the growth rate of perturbations. Microwave background anisotropy then constrains the dark matter–dark energy coupling to be less than gravitational strength: $\beta < 0.1$ for $f(\phi) = \exp(\beta\phi/M_{\rm Pl})$. In our case, as we will see in Sec. V C, slow roll implies a nearly identical growth rate to that in CDM models, even in the interesting regime $\beta \gtrsim 1$.

More importantly, slow roll means $w_\phi \approx -1$. As argued below Eq. (13), this facilitates obtaining $w_{\rm eff} < -1$.

In essence, slow roll is enhanced by the dark matter interaction term in Eq. (6) which acts to slow down the field. To see this explicitly, note that in usual quintessence models (without dark matter interaction), slow roll is achieved in the large Γ limit, for which

$$\frac{\dot{\phi}^2}{2V} \approx \frac{1}{4\Gamma}. \qquad (21)$$

Comparison with Eq. (20) shows that this ratio is further suppressed by $H^2/m^2 \ll 1$ in our case.

The attractor solution described here has a large basin of attraction. The covariant form of Eq. (6) involves T^{μ}_{μ}, the trace of the stress tensor of all fields coupled to ϕ. These do not exclusively consist of DM. For instance, in a supersymmetric model where the DM is the lightest supersymmetric particle, ϕ could conceivably couple to a host of superpartners. Deep in the radiation-dominated era, the T^{μ}_{μ} source term is generally negligible compared to the Hubble damping term, $3H\dot{\phi}$. However, they become comparable for about a Hubble time whenever a particle species coupled to ϕ becomes nonrelativistic [28], therefore driving ϕ towards the minimum of its effective potential. This provides an efficient mechanism for reaching the attractor [20].

IV. AN EXPLICIT EXAMPLE

In this section we illustrate our mechanism within a specific model. We consider an inverse power-law potential, $V(\phi) = M^4 (M_{\text{Pl}}/\phi)^{\alpha}$, where the mass scale M is tuned to $\sim 10^{-3}$ eV in order for acceleration to occur at the present epoch. This potential is a prototypical example of a tracker potential in quintessence scenarios. Its runaway form is in harmony with nonperturbative potentials for moduli in supergravity and string theories.

The coupling function is chosen to be $f(\phi) = \exp(\beta\phi/M_{\text{Pl}})$. The exponential form is generic in dimensional reduction in string theory where ϕ measures the volume of extra dimensions. Moreover, β is expected to be of order unity, corresponding to gravitational strength. While the coupling to matter exacerbates the fine-tuning of the quintessence potential [31], we find the phenomenological consequences of our model sufficiently interesting to warrant sweeping naturalness issues under the rug.

In this example, the condition at the minimum reads

$$-\frac{\alpha M^4 M_{\text{Pl}}^{\alpha}}{\phi^{\alpha+1}} + \frac{\beta}{M_{\text{Pl}}} \frac{\rho_{\text{DM}}^{(0)}}{a^3} e^{\beta(\phi-\phi_0)/M_{\text{Pl}}} = 0. \qquad (22)$$

Evaluating this today, and noting that $V_0 \approx 3H_0^2 M_{\text{Pl}}^2 \Omega_{\text{DE}}^{(0)}$ because of slow roll, we obtain

$$\frac{\phi_0}{M_{\text{Pl}}} \approx \frac{\alpha}{\beta} \frac{\Omega_{\text{DE}}^{(0)}}{\Omega_{\text{DM}}^{(0)}}. \qquad (23)$$

Equations (22) and (23) combine to provide a simple expression for the redshift evolution of ϕ as it follows the minimum of the effective potential:

$$\left(\frac{\phi}{\phi_0}\right)^{\alpha+1} = (1+z)^{-3} e^{\beta(\phi_0-\phi)/M_{\text{Pl}}}. \qquad (24)$$

Next we calculate the resulting effective equation of state. To do so, we first need an expression for ρ_{ϕ} as a function of redshift. Notice that in the slow-roll approximation, $\rho_{\phi} \approx V(\phi)$. This does not imply, however, that $\rho_{\phi} \approx \text{const}$, since ρ_{ϕ} does not obey the usual conservation equation. Using Eq. (22), we instead have

$$\rho_{\phi} \approx \frac{V}{V_{,\phi}} V_{,\phi} = \frac{\beta}{\alpha} \frac{\phi}{M_{\text{Pl}}} \frac{\rho_{\text{DM}}^{(0)}}{a^3} e^{\beta(\phi-\phi_0)/M_{\text{Pl}}}. \qquad (25)$$

Substituting this and Eq. (25) in the definition of x given in Eq. (12), we arrive at

$$x = \frac{\Omega_{\text{DM}}^{(0)}}{\Omega_{\text{DE}}^{(0)}} \frac{\phi_0}{\phi} \left\{ \exp\left[\alpha \frac{\Omega_{\text{DE}}^{(0)}}{\Omega_{\text{DM}}^{(0)}} \left(1 - \frac{\phi}{\phi_0} \right) \right] - 1 \right\}. \qquad (26)$$

This shows explicitly that x is a positive, monotonically increasing function of z which vanishes today. Moreover, since the field is slow rolling, we have $w_{\phi} \approx -1$. Therefore, Eq. (13) implies

$$w_{\text{eff}} \approx -\frac{1}{1-x} \leq -1, \qquad (27)$$

with the approximate equality holding today. Hence this yields an effective dark-energy fluid with $w < -1$ in the recent past.

Note from Eq. (26) that $x = 1$ at some time in the past, implying that $|w_{\text{eff}}|$ momentarily diverges and then becomes positive again at higher redshifts. This is because $\rho_{\text{DE}}^{\text{eff}}$ eventually becomes negative, at which point the effective dark-energy fluid has both negative pressure and energy density. As z increases further and x becomes large, one has $w_{\text{eff}} \approx 0$, and the fluid behaves like dust.

In Fig. 1 we plot the redshift evolution of w_{eff} and w_{ϕ} for $\alpha = 0.2$, $\beta = 1$ and $\Omega_{\text{DE}}^{(0)} = 0.7$. (As will be discussed in the next section, a small value for α is required for consistency with large-scale structure observations.) While w_{ϕ} remains bounded from below by -1, w_{eff} is less than -1 for $z \gtrsim 0.1$, as claimed above.

The evolution of $w_{\text{eff}}(z)$ shown in Fig. 1 is consistent with the observational limits on redshift dependent parametrizations of the dark-energy equation of state [6]. One way to see this is to consider the weighted average

$$\bar{w}_{\text{eff}} \equiv \frac{\int \Omega_{\text{eff}}(a) w_{\text{eff}}(a) da}{\int \Omega_{\text{eff}}(a) da}, \qquad (28)$$

where the integral runs from $z = 0$ up to the maximum redshift of current SN Ia data, $z \sim 1.5$. This gives $\bar{w}_{\text{eff}} \approx -1.1$, which lies within the allowed range of w found in [1]. Note that while Fig. 1 was derived using the above analytical expressions, we have checked these against

numerical solutions of the equations of motion and found very good agreement.

V. OBSERVATIONAL CONSTRAINTS AND CONSEQUENCES

We have shown that the interaction between quintessence and dark matter can mimic the cosmology of a phantom fluid. In this section we discuss some observational consequences of this scenario and argue that it is consistent with current observations. At the level of homogeneous cosmology this is certainly true, as long as parameters are chosen such that w_{eff} lies within the allowed range. We argue that this is also the case when considering inhomogeneities, at least at the linear level. The main effect here is the fifth force between dark matter particles mediated by ϕ, which enhances the growth rate of density perturbations.

A rigorous comparison with observations would require a full likelihood analysis including a host of cosmological probes, which is beyond the scope of this paper. We instead contend ourselves with a simplified (and perhaps more conservative) analysis to derive general constraints. As in Sec. IV, we focus on an exponential coupling function and inverse power-law potential.

A. Mass estimates from large-scale structure

The tightest constraint comes from various estimates of the dark matter density at different redshifts. Since the dark matter redshifts more slowly than a^{-3} in our model, then for fixed present matter density this implies a smaller matter density in the past compared to a CDM model. Indeed, at early times ($\phi \ll \phi_0$), the matter density differs from that of a usual dust CDM model by

$$\frac{\rho_{DM}}{\rho_{CDM}} \rightarrow e^{-\beta\phi_0/M_{Pl}} = \exp\left(-\alpha\frac{\Omega_{DE}^{(0)}}{\Omega_{DM}^{(0)}}\right), \qquad (29)$$

where in the last step we have used Eq. (23).

It is reasonable to assume that this ratio cannot deviate too much from unity, for otherwise we risk running into conflict with estimates of the matter density at various redshifts, e.g. from galaxy counts, Lyman-α forest, weak lensing, etc. This is supported by the fact that the allowed range of $\Omega_{DM}^{(0)}$ is almost independent of the specifics of the dark energy, as derived from a general analysis [6,32] of the combined SNIa Gold data [7], Wilkinson Anisotropy Microwave Probe (WMAP) power spectra [33] and Two-Degree Field (2dF) galaxy survey [34]. In particular $0.23 \lesssim \Omega_{DM}^{(0)} \lesssim 0.33$ at 2σ (see also [1,35]). Substituting $\Omega_{DM}^{(0)} = 0.33$ in Eq. (29), we obtain

$$\alpha \lesssim 0.2. \qquad (30)$$

Thus dark matter density estimates require the scalar field potential to be sufficiently flat, thereby making the attrac-

tor behavior and slow-roll condition discussed in Sec. III more easily satisfied.

Equation (29) shows that ρ_{DM} redshifts like normal CDM (i.e., $\rho_{DM} \sim a^{-3}$) for most of the cosmological history, except in the recent past. This is crucial in satisfying constraints on $\Omega_{DM}^{(0)}$ and traces back to our choice of inverse power-law potential. In contrast, the exponential potential studied in [24] has a very different attractor solution. In this case, dark energy remains a constant fraction of the total energy density and modifies the DM equation of state at all redshift. This in turn renders the matter density negligibly small for $z \gtrsim 1$. Therefore, in order to satisfy constraints on $\Omega_{DM}^{(0)}$ (as well as z_{eq}), one must introduce a second DM component, which is noninteracting and dominates for most of the history.

Finally, we note that while Eq. (30) is an extra tuning on $V(\phi)$, normal quintessence also suffers from the same constraint. Indeed, "tracker" quintessence with $V(\phi) = M^4(M_{Pl}/\phi)^\alpha$ leads to a dark-energy equation of state

$$w_\phi = -\frac{2}{\alpha + 2}. \qquad (31)$$

Imposing the current observational constraint $w < -0.9$ results in a bound on α identical to Eq. (30).

B. CMB and SNIa observables

We now focus on cosmological distance tests, in particular, the SNIa luminosity-distance relation and the angular-diameter distance to the last scattering surface as inferred from the position of CMB acoustic peaks. We wish to compare these observables for three different models, namely, the interacting scalar field dark matter model with $\alpha = 0.2$ and $\beta = 1$, a ΛCDM model, and a phantom model with $w = -1.2$.

The position of Doppler peaks depends on the angular-diameter distance to the last scattering surface,

$$d_A(z_{rec}) = (1 + z_{rec})^{-1} \int_0^{z_{rec}} \frac{dz}{H(z)}, \qquad (32)$$

where z_{rec} is the redshift at recombination. Observations of SNIa, on the other hand, probe the luminosity distance

$$d_L(z) = (1 + z) \int_0^z \frac{dz}{H(z)}. \qquad (33)$$

Figure 2(a) shows the luminosity distance for all three models with $\Omega_{DM}^{(0)} = 0.3$, while Fig. 2(b) gives their percentage difference. The difference between our model and ΛCDM is $\lesssim 4\%$ for $z < 1.5$; similarly the difference with respect to the phantom model is within $\lesssim 2\%$. Thus all three models are degenerate within the uncertainties of present SNIa data which determine $d_L(z)$ to no better than $\sim 7\%$. Furthermore, this suggests that percent-level accuracy from future SNIa experiments such as the Supernova Acceleration Probe (SNAP) [36], combined
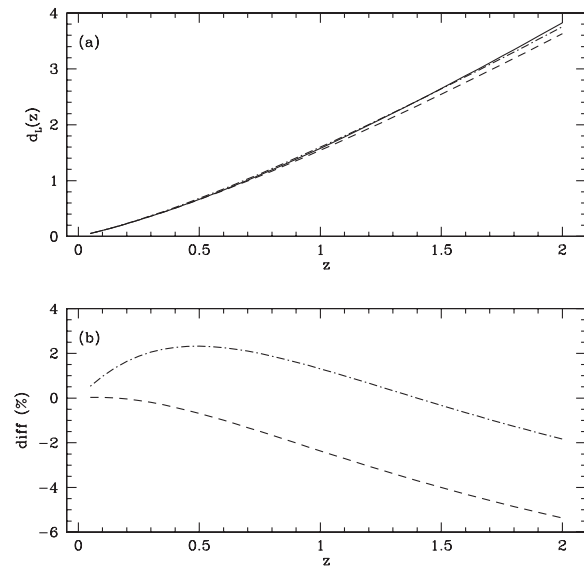
FIG. 2. Upper panel shows the luminosity distance (d_L) as a function of redshift for our model (solid) a phantom model with $w = -1.2$ (dash-dotted) and ΛCMD (dashed). We have fixed $\Omega_{DM}^{(0)} = 0.3$. Lower panel shows the percentage difference between our model and phantom (dash-dot), and between our model and ΛCDM (dashed), respectively.

with other cosmological probes, could distinguish between them.

Since $\Omega_{DM}^{(0)}$ is kept fixed in this case, the matter density in the interacting dark-energy model differs in the past from that in the ΛCDM and phantom cases, as seen from Eq. (29). This results in a 10% difference in $d_A(z_{rec})$, which is again within current CMB uncertainties.

Suppose we instead keep $d_A(z_{rec})$ fixed, which essentially amounts to fixing the matter density at high redshift. With $\Omega_{DM}^{(0)} = 0.3$ for both the ΛCDM and phantom models, this is achieved by setting $\Omega_{DM}^{(0)} = 0.4$ for our model. These values are compatible with current limits, as mentioned earlier. The resulting luminosity distances and percentage differences are plotted in Fig. 3. In this case we find that our model is nearly degenerate with ΛCDM. Since $\Omega_{DM}^{(0)}h^2$ is tightly constrained by CMB temperature anisotropy, however, such a difference in $\Omega_{DM}^{(0)}$ implies a 10% difference in h between our model and ΛCDM. This is comparable to the uncertainty in the measured value of h by the Hubble Key Project [37].

C. Growth of density perturbations

In the slow-roll approximation the evolution equation for dark matter inhomogeneities, $\delta = \delta\rho_{DM}/\rho_{DM}$, is given in synchronous gauge by [20]
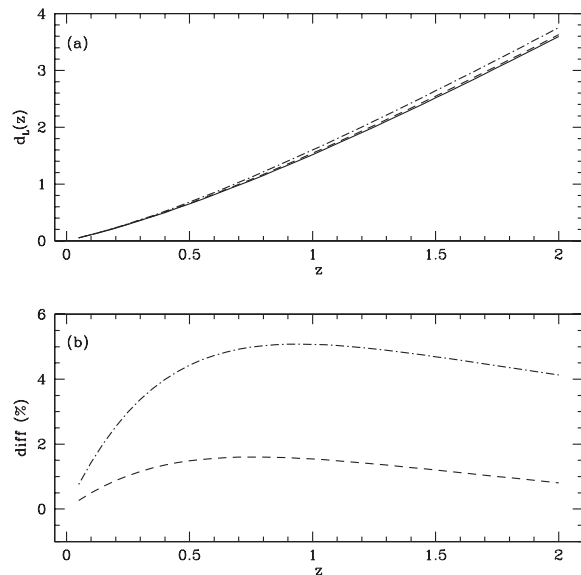

FIG. 3. Same as in Fig. 2, except $\Omega_{DM}^{(0)} = 0.4$ for the interacting scalar field dark matter model in this case. This gives equal $d_A(z_{rec})$ for all three models.

$$\delta'' + aH\delta' = \frac{3}{2}a^2H^2\left[1 + \frac{2\beta^2}{1 + a^2V_{,\phi\phi}/k^2}\right]\delta, \quad (34)$$

where primes denote differentiation with respect to conformal time. This differs from the corresponding expression in CDM models only through the factor in square brackets, normally equal to unity. Since this term accounts for the self-attractive force on the perturbation, the extra contribution proportional to β^2 arises from the attractive fifth force mediated by the scalar field. This force has a finite range, which for an inverse power-law potential is

$$\lambda = V_{,\phi\phi}^{-1/2} = \sqrt{\frac{\phi^{\alpha+2}}{\alpha(\alpha+1)M^4M_{Pl}^\alpha}}. \quad (35)$$

Perturbations with physical wavelength much larger than λ, i.e., $a/k \gg \lambda$, evolve as normal CDM. On the other hand, perturbations with $a/k \ll \lambda$, evolve as if Newton's constant were a factor of $1 + 2\beta^2$ larger. Thus the interaction with the quintessence field leads to an enhancement of power on small scales [38]. In particular, small-scale perturbations go nonlinear at higher redshift than in ΛCDM, as shown recently in a closely related context of chameleon cosmology [39]. (Numerical simulations have also found that a similar attractive scalar interaction for dark matter particles, albeit with a much smaller range of 1 Mpc, results in emptier voids between concentrations of large galaxies [40].)

Quantitatively, from Eqs. (23) and (24) in the limit $\alpha \ll 1$, we obtain

$$V_{,\phi\phi} \approx H_0^2(1+z)^6 e^{2\beta(\phi-\phi_0)/M_{Pl}} \frac{3\beta^2}{\alpha} \frac{(\Omega_{DM}^{(0)})^2}{\Omega_{DE}^{(0)}}, \quad (36)$$

where H_0 is the present value of the Hubble parameter. This implies, for instance, that at the present epoch

$$\lambda^{(0)} = H_0^{-1} \sqrt{\frac{\alpha \Omega_{DE}^{(0)}}{3\beta^2(\Omega_{DM}^{(0)})^2}} \approx 0.7 H_0^{-1}, \quad (37)$$

where in the last step we have taken $\alpha = 0.2$, $\beta = 1$ and $\Omega_{DM}^{(0)} = 0.3$. Hence the present range of this fifth force is comparable to the size of the observable universe. However, λ varies with redshift, and it is easily seen that $\lambda \ll H^{-1}$ in the past. In particular, we do not expect measurable effects in the CMB. This is in contrast with quintessence models [4], as well as the interacting dark matter/dark energy model of Amendola and collaborators [18], where $m \sim H$ along the attractor solution, leading to imprints in the CMB.

We solve numerically Eq. (34) and compute the linear matter power spectrum, $\Delta^2(k) \propto k^3 P(k)$, normalized to WMAP [33], where $P(k) = |\delta_k|^2$. In Fig. 4(a) we plot the resulting power spectrum for our model (solid line) and ΛCDM (dash line) with $\Omega_{DM}^{(0)} = 0.4$ and 0.3, respectively. The two curves are essentially indistinguishable by eye.

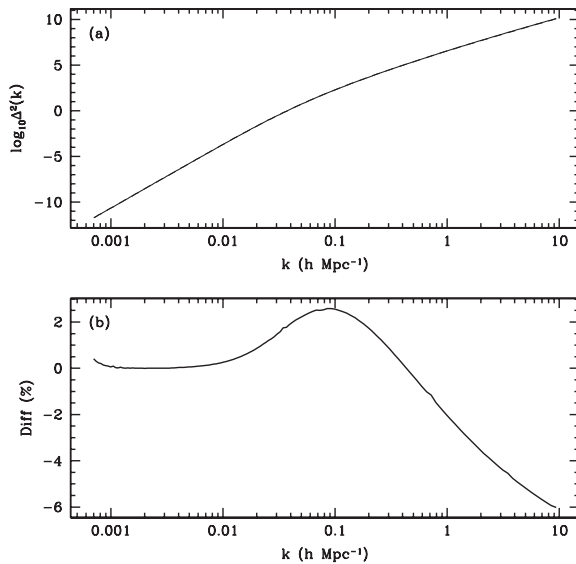In Fig. 4(b) we plot the fractional difference between the two spectra. The discrepancy is <2% on the scales probed

FIG. 4. The upper panel shows the matter power spectrum [$\Delta^2(k)$] over the relevant range of scales for our model (solid) and ΛCDM (dash) with $\Omega_{DM}^{(0)} = 0.4$ and 0.3, respectively. The lower panel shows the percentage difference between the two curves, which is well within current experimental accuracy.

by current large-scale structure surveys and consistent with the experimental accuracy of 2dF Galaxy Redshift Survey [34] and Sloan Digital Sky Survey (SDSS) [41]. On large scales the perturbations in the two models evolve in a similar way ($k < 0.01$ h Mpc^{-1}), while on intermediate scales ($0.01 < k < 0.4$ h Mpc^{-1}) the ΛCDM shows a few percent excess of power which is mostly due to small difference in the expansion rate of the two models after decoupling. Most importantly, on smaller scales ($k > 0.4$ h Mpc^{-1}) the power spectrum of ΛCDM is suppressed compared to our model. This is due to the fifth force which enhances the clustering of dark matter perturbations compared to the uncoupled case.

Thus deviations from ΛCDM are relevant only on small scales, well within the nonlinear regime. Therefore prospects for distinguishability using for instance the Lyman-α forest matter power spectrum requires accurate N-body simulations for this specific class of interacting dark matter/dark energy models. Another important probe is 21 cm tomography [42], which will allow to measure the power spectrum on very small scales and in a high enough redshift range ($30 \lesssim z \lesssim 200$) that linear analysis is valid.

D. Galaxy and cluster dynamics

Since the ϕ-mediated force is long-range today [see Eq. (37)], our model is subject to constraints from galaxy and cluster dynamics [38]. For instance, a fifth force in the dark sector leads to a discrepancy in mass estimates of a cluster acting as a strong lens for a high-redshift galaxy. Lensing measurements probe the actual mass since photons are oblivious to the fifth force, while dynamical observations are affected and would overestimate the mass of the cluster.

Other effects studied in [38] include mass-to-light ratios in the Local Group, rotation curves of galaxies in clusters, and dynamics of rich clusters. These combine to yield a constraint of $\beta \lesssim 0.8$, consistent with our assumption of $\beta \sim \mathcal{O}(1)$. This is consistent with generic string compactifications; if for instance ϕ is the radion field measuring the distance between two end-of-the-world branes, $\beta = 1/\sqrt{6}$ [20].

VI. DISCUSSION

In this paper we have shown that an interaction between dark matter and dark energy generically mimics $w < -1$ cosmology, provided that the observer treats the dark matter as noninteracting. Unlike phantom models, the theory is well defined and free of ghosts.

Our model is consistent with current observations provided the scalar potential is sufficiently flat. For our fiducial $V(\phi) = M^4/\phi^\alpha$, this translates into $\alpha \lesssim 0.2$. This is no worse than normal quintessence with tracker potential, where a nearly identical bound follows from observational constraints on w_ϕ.

In fact our scenario is less constrained than other interacting dark-energy/dark matter models studied in the literature. There is no need to introduce a noninteracting DM component, as in [24]; nor does the coupling strength need be much weaker than gravity, $\beta \lesssim 0.1$, as in [18]. Instead, our model allows for a single interacting DM species with gravitational-strength coupling to dark energy—$\beta \sim \mathcal{O}(1)$. In both cases this traces back to a difference in attractor solutions.

At the level of current uncertainties, the model is degenerate with both ΛCDM and phantom models. However, our calculations of luminosity and angular-diameter distances indicate that these models could be distinguished by the next generation of cosmological experiments devoted to the study of dark energy, such as SNAP, the Large Synoptic Survey Telescope [43], the Joint Efficient Dark-Energy Investigation (JEDI) [44], the Advanced Liquid-mirror Probe for Astrophysics, Cosmology and Asteroids (ALPACA) [45], and others.

A dark-sector interaction may reveal itself in various ways in the data. A strong hint would be a preference for $w < -1$ when fitting cosmological distance measurements assuming CDM. Another indication is a discrepancy between the clustering matter density at various redshifts and the expected $(1 + z)^3$ dependence in normal CDM models, which could appear as a discrepancy in the inferred value of $\Omega_M^{(0)}$.

We also uncovered modifications in the linear matter power spectrum and large-scale structure. These are primarily due to the attractive scalar-mediated force which enhances the growth of DM perturbations on small scales. Note that the opposite behavior obtains for a phantom scalar coupled to dark matter, resulting in a repulsive scalar force which damps perturbations [46]. As mentioned earlier, nonlinear effects are important for the relevant range of scales and would require N-body simulations. As an example it would be particularly useful to study the evolution of dark matter merging rates. Because of the fifth force, the gravitational interaction between dark matter halos is stronger than in standard CDM. This can potentially lead to higher halo merging events during structure formation and alleviate the so-called "dark matter halo problem." Other observational effects that could distinguish our model from ΛCDM and phantom include the bias parameter. Since baryons are unaffected by the fifth force, baryon fluctuations develop a constant large-scale bias [47] which could be observable. Similarly, comparison of the redshift dependence of the matter power spectrum, $P(k, z)$, may be useful to constrain the scale λ, which varies with z. The integrated Sachs-Wolfe effect is another mechanism worth studying. Since the present range of our scalar force is comparable to the size of the observable universe, it might account for the observed lack of power on large scales in the CMB.

ACKNOWLEDGMENTS

[1] U. Seljak *et al.*, Phys. Rev. D **71**, 103515 (2005).

[2] S. Weinberg, Phys. Rev. Lett. **59**, 2607 (1987).

[3] C. Wetterich, Nucl. Phys. **B302**, 668 (1988); P. J. E. Peebles and B. Ratra, Astrophys. J. **325**, L17 (1988).

[4] R. R. Caldwell, R. Dave, and P. J. Steinhardt, Phys. Rev. Lett. **80**, 1582 (1998).

[5] U. Alam, V. Sahni, T. D. Saini, and A. A. Starobinsky, Mon. Not. R. Astron. Soc. **354**, 275 (2004); D. Huterer and A. Cooray, Phys. Rev. D **71**, 023506 (2005); B. A. Bassett, P. S. Corasaniti, and M. Kunz, Astrophys. J. **617**, L1 (2004); E. Majerotto, D. Sapone, and L. Amendola, astro-ph/0410543.

[6] P. S. Corasaniti, M. Kunz, D. Parkinson, E. J. Copeland, and B. A. Bassett, Phys. Rev. D **70**, 083006 (2004).

[7] A. G. Riess *et al.*, Astrophys. J. **607**, 665 (2004).

[8] I. Maor, R. Brustein, J. McMahon, and P. J. Steinhardt, Phys. Rev. D **65**, 123003 (2002).

[9] C. Csaki, N. Kaloper, and J. Terning, astro-ph/0507148.

[10] R. R. Caldwell, M. Kamionkowski, and N. N. Weinberg, Phys. Rev. Lett. **91**, 071301 (2003).

[11] S. M. Carroll, M. Hoffman, and M. Trodden, Phys. Rev. D **68**, 023509 (2003); J. M. Cline, S. Y. Jeon, and G. D. Moore, Phys. Rev. D **70**, 043543 (2004); S. D. H. Hsu, A. Jenkins, and M. B. Wise, Phys. Lett. B **597**, 270 (2004).

[12] B. Boisseau, G. Esposito-Farese, D. Polarski, and Alexei A. Starobinsky, Phys. Rev. Lett. **85**, 2236 (2000); D. F. Torres, Phys. Rev. D **66**, 043522 (2002); S. Capozziello, Int. J. Mod. Phys. D **11**, 483 (2002); S. M. Carroll, A. De Felice, and M. Trodden, Phys. Rev. D **71**, 023525 (2005); V. Faraoni, Phys. Rev. D **68**, 063508 (2003); G. Allemandi, A. Borowiec, and M. Francaviglia, Phys. Rev. D **70**, 103503 (2004).

[13] V. Sahni and Y. Shtanov, J. Cosmol. Astropart. Phys. 11 (2003) 014.

[14] V. K. Onemli and R. P. Woodard, Classical Quantum Gravity **19**, 4607 (2002).

[15] D. J. H. Chung, L. L. Everett, and A. Riotto, Phys. Lett. B **556**, 61 (2003).

[16] C. Csaki, N. Kaloper, and J. Terning, Ann. Phys. (N.Y.) **317**, 410 (2005); **317**, 410 (2005).

[17] T. Damour, G. W. Gibbons, and C. Gundlach, Phys. Rev. Lett. **64**, 123 (1990); J. A. Casas, J. Garcia-Bellido, and M. Quiros, Classical Quantum Gravity **9**, 1371 (1992); R. Bean, Phys. Rev. D **64**, 123516 (2001); D. Comelli, M. Pietroni, and A. Riotto, Phys. Lett. B **571**, 115 (2003); U. Franca and R. Rosenfeld, Phys. Rev. D **69**, 063517 (2004); L. P. Chimento, A. S. Jakubi, D. Pavon, and W. Zimdahl, Phys. Rev. D **67**, 083513 (2003).

[18] L. Amendola, Phys. Rev. D **62**, 043511 (2000); L. Amendola and D. Tocchini-Valentini, Phys. Rev. D **64**, 043509 (2001); L. Amendola, C. Quercellini, D. Tocchini-Valentini, and A. Pasqui, Astrophys. J. **583**, L53 (2003); L. Amendola and C. Quercellini, Phys. Rev. D **68**, 023514 (2003); G. Olivares, F. Atrio-Barandela, and D. Pavon, Phys. Rev. D **71**, 063523 (2005).

[19] J. Khoury and A. Weltman, Phys. Rev. Lett. **93**, 171104 (2004); Phys. Rev. D **69**, 044026 (2004); S. S. Gubser and J. Khoury, Phys. Rev. D **70**, 104001 (2004).

[20] P. Brax, C. van de Bruck, A. C. Davis, J. Khoury, and A. Weltman, Phys. Rev. D **70**, 123518 (2004); in *Phi in the Sky: The Quest for Cosmological Scalar Fields*, AIP Conf. Proc. No. 736 (AIP, New York, 2005), pp. 105–110.

[21] H. Wei and R. G. Cai, Phys. Rev. D **71**, 043504 (2005).

[22] G. R. Farrar and P. J. E. Peebles, Astrophys. J. **604**, 1 (2004); S. S. Gubser and P. J. E. Peebles, Phys. Rev. D **70**, 123510 (2004).

[23] D. B. Kaplan, A. E. Nelson, and N. Weiner, Phys. Rev. Lett. **93**, 091801 (2004); R. D. Peccei, Phys. Rev. D **71**, 023527 (2005); R. Fardon, A. E. Nelson, and N. Weiner, hep-ph/0507235.

[24] G. Huey and B. D. Wandelt, astro-ph/0407196.

[25] H. Stefancic, Eur. Phys. J. C **36**, 523 (2004).

[26] P. J. Steinhardt, L. Wang, and I. Zlatev, Phys. Rev. D **59**, 123504 (1999).

[27] G. W. Anderson and S. M. Carroll, astro-ph/9711288.

[28] T. Damour and A. M. Polyakov, Nucl. Phys. **B423**, 532

(1994); T. Damour and A. M. Polyakov, Gen. Relativ. Gravit. **26**, 1171 (1994).

[29] G. Huey, P. J. Steinhardt, B. A. Ovrut, and D. Waldram, Phys. Lett. B **476**, 379 (2000); C. T. Hill and G. C. Ross, Nucl. Phys. **B311**, 253 (1988); J. Ellis, S. Kalara, K. A. Olive, and C. Wetterich, Phys. Lett. B **228**, 264 (1989).

[30] T. Biswas and A. Mazumdar, hep-th/0408026.

[31] S. M. Carroll, Phys. Rev. Lett. **81**, 3067 (1998); M. Doran and J. Jaeckel, Phys. Rev. D **66**, 043519 (2002).

[32] M. Kunz, P. S. Corasaniti, D. Parkinson, and E. J. Copeland, Phys. Rev. D **70**, 041301 (2004).

[33] H. V. Peiris *et al.*, Astrophys. J. Suppl. Ser. **148**, 213 (2003).

[34] W. J. Percival *et al.* (2dFGRS Collaboration), Mon. Not. R. Astron. Soc. **327**, 1297 (2001); S. Cole *et al.* (2dFGRS Collaboration), Mon. Not. R. Astron. Soc. **362**, 505 (2005).

[35] S. Hannestad and E. Mortsell, J. Cosmol. Astropart. Phys. 09 (2004) 001; D. Rapetti, S. W. Allen, and J. Weller, Mon. Not. R. Astron. Soc. **360**, 555 (2005).

[36] G. Aldering (SNAP Collaboration), astro-ph/0209550.

[37] W. L. Freedman *et al.*, Astrophys. J. **553**, 47 (2001).

[38] B. A. Gradwohl and J. A. Frieman, Astrophys. J. **398**, 407 (1992).

[39] P. Brax, C. van de Bruck, A. C. Davis, and A. M. Green, Phys. Lett. B **633**, 441 (2006).

[40] A. Nusser, S. S. Gubser, and P. J. E. Peebles, Phys. Rev. D **71**, 083505 (2005).

[41] M. Tegmark *et al.* (SDSS Collaboration), Astrophys. J. **606**, 702 (2004).

[42] A. Loeb and M. Zaldarriaga, Phys. Rev. Lett. **92**, 211301 (2004).

[43] See http://www.lsst.org.

[44] A. Crotts *et al.*, astro-ph/0507043.

[45] See http://www.astro.ubc.ca/LMT/alpaca/.

[46] L. Amendola, Phys. Rev. Lett. **93**, 181102 (2004); L. Amendola, S. Tsujikawa, and M. Sami, Phys. Lett. B **632**, 155 (2006).

[47] L. Amendola and D. Tocchini-Valentini, Phys. Rev. D **66**, 043528 (2002).

Slow-roll suppression of adiabatic instabilities in coupled scalar field-dark matter models

Pier Stefano Corasaniti

LUTH, Observatoire de Paris, CNRS UMR 8102, Université Paris Diderot, 5 Place Jules Janssen, 92195 Meudon Cedex, France
(Received 12 August 2008; published 27 October 2008)

We study the evolution of linear density perturbations in the context of interacting scalar field-dark matter cosmologies, where the presence of the coupling acts as a stabilization mechanism for the runaway behavior of the scalar self-interaction potential as in the case of the chameleon model. We show that, in the ''adiabatic'' background regime of the system, the rise of unstable growing modes of the perturbations is suppressed by the slow-roll dynamics of the field. Furthermore, the coupled system behaves as an inhomogeneous adiabatic fluid. In contrast, instabilities may develop for large values of the coupling constant, or along nonadiabatic solutions, characterized by a period of high-frequency dumped oscillations of the scalar field. In the latter case, the dynamical instabilities of the field fluctuations, which are typical of oscillatory scalar field regimes, are amplified and transmitted by the coupling to dark matter perturbations.

I. INTRODUCTION

Cosmology has provided evidence of a dark physics sector which is necessary to account for about 95% of the cosmic matter content [1]. Despite the success of the ΛCDM model to fit all cosmological observations, the existence of the dark energy phenomenon as well as its relation to the abundance and clustering of matter in the Universe still pose puzzling questions.

Models of interacting dark energy-dark matter have been proposed to address such problems. In this scenario, dark energy is a fundamental scalar field which directly couples to matter particles. This allows for a dynamical solution of the so-called ''coincidence'' problem, since independently of the initial conditions the scalar interaction drives the dark energy-to-matter ratio toward a constant value (see, e.g., [2–5]). These models are inspired by string and supergravity theories, where the compactification of extra dimensions in the low energy gives rise to massless scalars coupled to matter fields with gravitational strength. Therefore, a distinct feature of this scenario is that matter particles experience a long-range scalar force and acquire a time-dependent mass which cause violations of the equivalence principle (EP). The tight bounds imposed by EP tests are usually avoided as a consequence of other possible mechanisms. As an example, Damour and Polyakov have shown that in string theory the couplings between the dilaton and different matter fields can be dynamically suppressed [6]. An interesting possibility has been proposed in the ''chameleon'' model [7], where the mass of the scalar field is assumed to depend on the local matter density. In such a case, fifth-force effects can be strongly suppressed on Solar System scales, thus avoiding EP bounds. Another possibility has been explored in Ref. [8], where the authors consider a dilatonic field to be differently coupled to various matter species such that the system can naturally evolve toward a late time attractor solution where general

relativity is recovered. Nonminimally coupled models can successfully describe the background expansion of the Universe as probed by supernova type Ia luminosity distance or the position of the Doppler peaks in the cosmic microwave background anisotropy power spectrum (see, e.g., [9,10]). However, testing the formation of structure in the Universe more than standard cosmological tests may provide a key insight on this class of models. In fact, the scalar coupling contributes to modifying the clustering properties of matter, implying that an accurate study of the evolution of density fluctuations in both the linear and nonlinear phases of collapse can identify unique signatures of dark sector interactions [11]. In the context of linear perturbation theory, several interacting scalar field-dark matter models have been studied in the literature (see, e.g., [12]). In some specific realizations, it was found that the growth of linear density perturbations is spoiled by the presence of dangerous instabilities [13,14], as in the case of ''mass varying neutrino'' models [15]. Recently, a number of works have analyzed the stability of perturbations in more general setups. For instance, in Ref. [16] the authors have studied models with a background evolution characterized by an adiabatic regime and shown that unstable growing modes of the perturbations exist for couplings much greater than gravitational strength. On the other hand, the authors of Refs. [17,18] have considered the case of an interacting dark energy component with a constant equation of state and found that, for couplings proportional to the dark matter density, the perturbations are unstable.

In this paper, we provide a more detailed study of these instabilities, particularly in relation to the specificities of the background scalar field evolution. The paper is organized as follows: In Sec. II, we introduce the interacting scalar field-matter model as well as the background and perturbation equations; in Sec. III, we present the results of our analysis; finally, in Sec. IV, we present our conclusions.

083538-1

II. INTERACTING SCALAR FIELD-DARK MATTER MODEL

Let us consider a scalar field ϕ with direct coupling to matter particles via a Yukawa term $f(\phi/M_{\rm Pl})\bar{\psi}\psi$, where f is the coupling function and ψ is a Dirac spinor representing the matter field ($M_{\rm Pl} = 1/\sqrt{8\pi G}$ is the reduced Planck mass, with G being the Newton constant). The effect of the scalar-dependent coupling is to induce a time-varying mass of the matter particles, hence causing a violation of the EP. As mentioned in the previous section, there are several ways to evade the tight bounds from EP tests. Here we assume that the scalar field couples only to dark matter particles. Therefore, for the purposes of our analysis, we neglect the baryon contribution and focus only on the cosmological evolution of the coupled scalar field-dark matter system.

As in the case of the chameleon cosmology [19], we assume the ϕ field to have a self-interaction potential of runaway type in the form of an inverse power law:

$$V(\phi) = \frac{M^{4+\alpha}}{\phi^{\alpha}}, \tag{1}$$

where M is a mass scale and α is a positive constant. We consider a coupling function of dilatonic type, $f(\phi) = \exp(\beta\phi/M_{\rm Pl})$, with β a dimensionless coupling constant. The background evolution of this system has been studied in detail in [9].

A. Background and linear perturbation equations

Let assume a flat Friedmann-Lemaitre-Robertson-Walker metric $[ds^2 = -dt^2 + a(t)^2 d\mathbf{x}^2]$, and the evolution of the scalar factor is given by:

$$H^2 \equiv \left(\frac{\dot{a}}{a}\right)^2 = \frac{1}{3}[\rho_{\rm DM} + \dot{\phi}^2/2 + V(\phi)], \tag{2}$$

where $\rho_{\rm DM}$ is the dark matter density and we have adopted Planck units ($M_{\rm Pl} = 1$). The total energy momentum tensor of the system is conserved: $T^{\mu(T)}_{\nu;\mu} \equiv T^{\mu(\rm DM)}_{\nu;\mu} + T^{\mu(\phi)}_{\nu;\mu} = 0$. In contrast, the nonminimal coupling implies that the energy momentum tensor of each individual component is not conserved. In such a case, we can consider

$$T^{\mu(\rm DM)}_{\nu;\mu} = \beta\phi_{;\nu}T^{\gamma(\rm DM)}_{\gamma}, \tag{3}$$

$$T^{\mu(\phi)}_{\nu;\mu} = -\beta\phi_{;\nu}T^{\gamma(\rm DM)}_{\gamma}, \tag{4}$$

from which we obtain

$$\dot{\rho}_{\rm DM} + 3H\rho_{\rm DM} = \beta\dot{\phi}\rho_{\rm DM}, \tag{5}$$

$$\ddot{\phi} + 3H\dot{\phi} + V_{,\phi} = -\beta\rho_{\rm DM}. \tag{6}$$

Without loss of generality, we can rescale the coupling function $f(\phi)$ to its present value $f(\phi_0)$. Hence the solution to Eq. (5) is

$$\rho_{\rm DM} = \frac{\rho^{(0)}_{\rm DM}}{a^3} e^{\beta(\phi-\phi_0)}, \tag{7}$$

where $\rho^{(0)}_{\rm DM}$ is the present matter density. We may notice that as a consequence of the scalar interaction the dark matter density deviates from the standard scaling a^{-3}. Furthermore, for coupling values $\beta > 0$, the system of Eqs. (5) and (6) describes an energy transfer from the ϕ field to dark matter. In such a case, the scalar field evolves in an effective potential

$$V_{\rm eff}(\phi) = V(\phi) + \frac{\rho^{(0)}_{\rm DM}}{a^3} e^{\beta(\phi-\phi_0)}, \tag{8}$$

which is characterized by the presence of a minimum.

In Fig. 1, we plot the effective potential for $\beta = 1$ and $\alpha = 0.2$ at redshift $z = 1000$, 10, 3, and 0, respectively. For this choice of the model parameters, we have $\phi_0 \approx 0.7605$ as obtained by integrating numerically the system of Eqs. (2)–(5). The dashed line in Fig. 1 corresponds to the position of the minimum at different epochs.

In synchronous gauge, the linearized equations for the dark matter density contrast $\delta_{\rm DM}$, velocity gradient $\theta_{\rm DM}$, and field fluctuation $\delta\phi$ are given by

$$\dot{\delta}_{\rm DM} = -\left(\frac{\theta_{\rm DM}}{a} + \frac{\dot{h}}{2}\right) + \beta\delta\dot{\phi}, \tag{9}$$

$$\dot{\theta}_{\rm DM} = -H\theta_{\rm DM} + \beta\left(\frac{k^2}{a}\delta\phi - \dot{\phi}\theta_{\rm DM}\right), \tag{10}$$

$$\delta\ddot{\phi} + 3H\delta\dot{\phi} + \left(\frac{k^2}{a^2} + V_{,\phi\phi}\right)\delta\phi + \frac{1}{2}\dot{h}\dot{\phi} = -\beta\rho_{\rm DM}\delta_{\rm DM}, \tag{11}$$
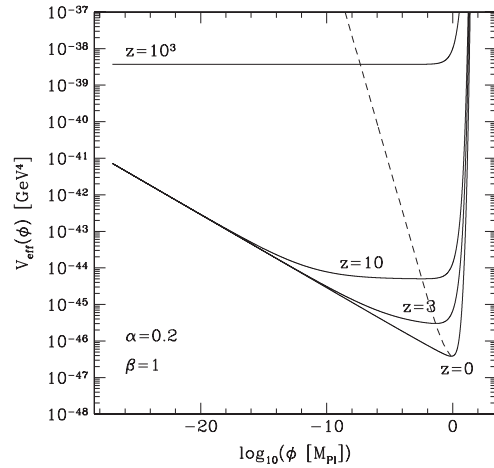

FIG. 1. Scalar field effective potential at $z = 10^3$, 10, 3, and 0 (solid lines) for $\alpha = 0.2$ and $\beta = 1$. The amplitude of the scalar potential M is set such that today $\Omega_{\rm DM} = 0.24$ ($\Omega_{\phi} = 1 - \Omega_{\rm DM}$). The dashed line corresponds to the position of the minimum of the effective potential at different epochs.

respectively, where h is the metric perturbation given by

$$h = \frac{2k^2\eta}{a^2 H} - \frac{8\pi G}{H}[\delta\rho_\phi + \rho_{DM}\delta_{DM}], \qquad (12)$$

with $\delta\rho_\phi = \dot{\phi}\delta\dot{\phi} + V_{,\phi}\delta\phi$ and

$$\dot{\eta} = \frac{4\pi G}{k^2} a[\rho_{DM}\theta_{DM} + ak^2\dot{\phi}\delta\phi]. \qquad (13)$$

In Sec. III, we will present the results of the numerical integration of this system of equations. However, for a qualitative understanding of the conditions which lead to the onset of instabilities during the growth of the density perturbations, it is useful to introduce an effective unified fluid description.

B. Effective unified fluid description

The conservation of the total energy momentum tensor allows us to describe the interacting scalar field-dark matter system as a single unified fluid. The equation for the background density is given by

$$\dot{\rho}_T = -3H(1 + w_T)\rho_T, \qquad (14)$$

with $\rho_T = \dot{\phi}^2/2 + V(\phi) + \rho_{DM}$ and $w_T = p_T/\rho_T$, where $p_T = \dot{\phi}^2/2 + V(\phi)$. Similarly, at linear order the perturbation equations in synchronous gauge read as

$$\dot{\delta}_T = -3H(c_{sT}^2 - w_T)\delta_T - (1 + w_T)$$
$$\times \left\{ \left[\frac{k^2}{a^2 H^2} + 9(c_{sT}^2 - c_{aT}^2) \right] \frac{aH^2}{k^2}\theta_T + \frac{\dot{h}}{2} \right\}, \quad (15)$$

$$\dot{\theta}_T = -H(1 - 3c_{sT}^2)\theta_T + \frac{c_{sT}^2 k^2}{a(1 + w_T)}\delta_T, \qquad (16)$$

where $c_{aT}^2 = \dot{p}_T/\dot{\rho}_T$ is the square of the adiabatic sound speed of the unified fluid and $c_{sT}^2 = \delta p_T/\delta\rho_T$ is the square of the speed at which pressure perturbations propagate in the fluid rest frame. For a barotropic fluid with a constant equation of state (e.g., matter, radiation), $c_s^2 = c_a^2 = w$. This is not the case for a generic fluid (e.g., scalar field), and for this reason we may expect the effective unified fluid to be nonbarotropic (i.e., $c_{sT}^2 \neq c_{aT}^2 \neq w_T$). In terms of the scalar field and dark matter variables, we have

$$c_{aT}^2 = \frac{3H\dot{\phi}^2 + \dot{\phi}[2V_{,\phi} + \beta\rho_{DM}]}{3H\dot{\phi}^2 + 3H\rho_{DM}}, \qquad (17)$$

$$c_{sT}^2 = \frac{\dot{\phi}\delta\dot{\phi} - V_{,\phi}\delta\phi}{\dot{\phi}\delta\dot{\phi} + V_{,\phi}\delta\phi + \rho_{DM}\delta_{DM}}. \qquad (18)$$

These relations provide us with a simple way of determining the properties of the perturbation in the coupled system. For example, in a given background regime, instabilities of the perturbations may develop if the adiabatic sound speed acquires sufficiently negative values.

III. SCALAR FIELD DYNAMICS AND EVOLUTION OF DENSITY PERTURBATIONS

The nonminimally coupled scalar field model described in Sec. II is characterized by the existence of an attractor solution which is set by the minimum of the effective potential. The minimum is given by $V_{eff}^{,\phi} = 0$; thus, along the attractor solution, the following condition is always satisfied:

$$V_{,\phi} = -\beta\frac{\rho_{DM}^{(0)}}{a^3}e^{\beta(\phi-\phi_0)}. \qquad (19)$$

Evaluating the derivative of Eq. (1) and substituting in Eq. (19), we obtain the time evolution of the field at the minimum:

$$\left(\frac{\phi_0}{\phi_{min}}\right)^{\alpha+1} = \frac{1}{a^3}e^{\beta(\phi_{min}-\phi_0)}, \qquad (20)$$

which depends on both the slope α and the coupling β. Equation (20) is a nonlinear algebraic equation which can be solved numerically through standard bisection methods (see dashed line in Fig. 1).

The field may reach the minimum from two different sets of initial conditions: $\phi_{ini} < \phi_{min}^{ini}$ (small field) or $\phi_{ini} > \phi_{min}^{ini}$ (large field). In the former case, ϕ evolves over the inverse power-law part of the effective potential, where it minimizes the potential by slow-rolling as shown in [9]. In fact, one can easily verify that throughout the cosmological evolution the field mass ($m^2 = V_{eff}^{,\phi\phi}$) as well as the ratio of its kinetic-to-potential energy satisfy the conditions $m > H$ and $\dot{\phi}^2/2V < 1$, respectively. In contrast, starting from large field values, ϕ rolls towards the minimum along the steep exponential part of $V_{eff}(\phi)$. Thus, it rapidly acquires kinetic energy which subsequently dissipates through large high-frequency damped oscillations around the minimum.

As we shall see next, the growth of linear perturbations in these two regimes is significantly different.

A. Adiabatic regime

As mentioned in Sec. II B, we can obtain a qualitative insight on the stability of the perturbations in the coupled system by considering the effective unified fluid description. Let us evaluate the adiabatic sound speed equation (17) along the adiabatic solution equation (19); after neglecting the term proportional to the kinetic energy of the scalar field, we have

$$c_{aT}^2 = -\beta\frac{\dot{\phi}}{3H}, \qquad (21)$$

and, since $\dot{\phi} > 0$, it then follows that $c_{aT}^2 < 0$, implying that adiabatic instabilities may indeed develop. However, we should remark that, during the adiabatic regime, the field is slow-rolling (i.e., $3H\dot{\phi} \approx 0$); hence, the term $\dot{\phi}/3H$ can be negligibly small compared to β, such that

$c_{aT}^2 \approx 0$, leading to a stable growth of the perturbations. In contrast, instabilities will occur if the coupling assumes extremely large values $\beta \gg 3H/\dot{\phi}$. This is consistent with the analysis presented in Ref. [16], where the authors have suggested that, during the adiabatic regime, perturbations suffer of instabilities provided that $\beta \gg 1$. Here we want to stress two main points which were not addressed in that study: first, that the rise of instabilities is suppressed by the slow-rolling of the field in the adiabatic regime and, second, that exactly because of the slow-roll condition, instabilities can spoil the growth of dark matter perturbations only for large unnatural values of the coupling. To give an example, let us assume that, for a given model along the adiabatic solution, the following condition occurs: $\dot{\phi}/3H \sim 10^{-2}$. In such a case, instabilities will develop only if the coupling constant $\beta > 100$, corresponding to a scalar fifth force which is 2000 times greater than the gravitational strength.[1]

Moreover, during the adiabatic evolution, Eq. (18) reads as

$$c_{sT}^2 = -\frac{1}{1 - \frac{1}{\beta}\frac{\delta_{\mathrm{DM}}}{\delta\phi}}, \tag{22}$$

and, assuming that the scalar field is nearly homogeneous, $\delta\phi \ll \delta_{\mathrm{DM}}$ (in Planck units), we have $c_{sT}^2 \approx \beta\delta\phi/\delta_{\mathrm{DM}}$; for $\beta \approx \mathcal{O}(1)$, this implies $c_{sT}^2 \approx 0$. In other words, if the scalar field fluctuations are small with respect to the dark matter density contrast, then the coupled system behaves has a single adiabatic inhomogeneous fluid ($c_{sT}^2 \approx c_{aT}^2 \approx 0$).

These results are supported by the numerical study of the system of Eqs. (9)–(13), with the scalar field evolution given by Eq. (20). We have set the model parameters to the following values: $\alpha = 0.2$ and $\beta = 1$, with $\Omega_{\mathrm{DM}} = 0.24$ and $H_0 = 70$ Km s^{-1} Mpc^{-1}. As shown in Ref. [9], this model has the interesting feature that the background dynamics can mimic that of a phantom cosmology corresponding to an uncoupled dark energy model with slightly constant supernegative equation of state $w_{\mathrm{DE}} = -1.1$.

The results of the numerical integration are shown in Fig. 2. In the upper left panel, we plot the scalar field equation of state w_ϕ (solid line) and the equation of state for the effective unified fluid w_T (dotted line). As we can see, $w_\phi = -1$, which is consistent with the fact that $\dot{\phi}/3H$ is negligible, as can be seen from the plot in the upper right panel. We can also notice that the unified fluid at early times behaves as a matter component ($w_T = 0$) and deviates toward negative values ($-1 < w_T < 0$) as the ϕ field becomes energetically dominant. In the lower left panel,

---

[1]As a consequence of the scalar interaction, dark matter particles experience a gravitational force with effective Newtonian constant $G_{\mathrm{eff}} = G(1 + 2\beta^2)$. In contrast, baryonic bodies may not experience such a modification due to the nonlinear nature of the scalar interaction [20].

we plot the absolute value of c_{aT}^2 and $c_{sT}^2(k)$ for three different scales $k = 10^{-3}$, 10^{-2}, and 0.1 Mpc^{-1}, respectively. The adiabatic sound speed has negligible negative values and evolves with a trend that matches that of $\dot{\phi}/3H$, which is consistent with Eq. (21). We can also notice that the speed of propagation of pressure perturbations in the unified fluid remains ≈ 0. Hence during the adiabatic regime the interacting system behaves as a single inhomogeneous adiabatic fluid. In the lower right panel, we plot the evolution of the dark matter density contrast normalized to the present value for $k = 10^{-3}$, 10^{-2}, and 0.1 Mpc^{-1}, respectively (for clarity, we have displaced by a constant factor the different curves which would otherwise nearly overlap). As expected, these different modes manifest a standard power-law growth, and no instabilities are present. These results have been obtained for an inverse power-law potential; nevertheless, they can be generalized to other scalar potentials—the only requirement is the existence of an adiabatic solution during which the slow-roll condition is satisfied.

B. Nonadiabatic regime: Large field oscillations

Starting from initially large field values, the system evolves along a nonadiabatic solution characterized by rapid dumped field oscillations around the minimum of the effective potential. We can see this explicitly in the upper left panel of Fig. 3, where we plot the evolution of the scalar field equation of state for the same model parameters as in Sec. III A and obtained by numerically integrating Eq. (6) with initial conditions: $\phi(a_{\mathrm{ini}} = 10^{-5}) = 0.15 > \phi_{\mathrm{min}}^{\mathrm{ini}}$ and $\dot{\phi}_{\mathrm{ini}} = 0$. We can infer the main features of the scalar field evolution from the behavior of its equation of state shown in the upper left panel of Fig. 3. As we can see, the field initially behaves as a stiff component with $w_\phi = 1$; this is because the field starts rolling on the steep exponential part of the potential, and consequently its energy is dominated by the kinetic term. As the field reaches the opposite side of the potential, it undergoes a series of high-frequency dumped oscillations around the minimum during which it dissipates most of its kinetic energy. It then sets on the inverse power-law part of the potential where it evolves along a tracker solution with $w_\phi \approx -2/(2 + \alpha) \approx -0.9$.

The evolution of density perturbations in the case of oscillating scalar fields has been widely studied in the literature, particularly in the context of inflation [21]. From these studies, it is well known that scalar field fluctuations are unstable during oscillatory regimes. In Ref. [22], the authors have presented a simple insightful explanation for the onset of such instabilities. The idea is to interpret the scalar fluctuation $\delta\phi$ as the separation between two particles whose dynamics is described by two coupled anharmonic oscillators. Then a simple stability criterion is given by the relation between the frequency of the oscillations ω and their amplitude $\tilde{\phi}$ [23]. Let us
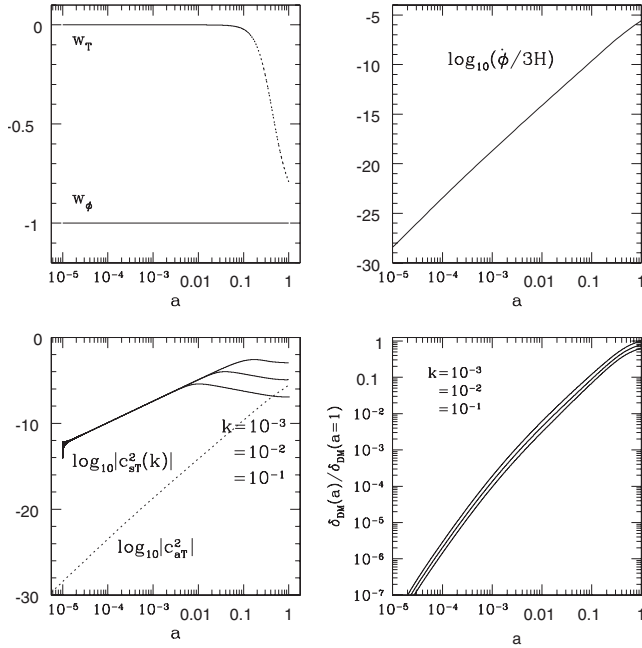
FIG. 2. Upper left panel: Evolution of the scalar field equation of state w_ϕ and effective unified fluid equation of state w_T; upper right panel: evolution of the scalar field velocity with respect to the Hubble rate. Lower left panel: Redshift evolution of the adiabatic sound speed c_{aT}^2 and propagation of pressure perturbations c_{sT}^2; lower right panel: linear growth factor of the dark matter density contrast at $k = 10^{-3}$, 10^{-2}, and 0.1 Mpc^{-1}.

suppose that the frequency increases as the amplitude of the oscillations diminishes; in such a case it has been shown that the distance between the two particles increases, thus causing the scalar field fluctuation to be unstable [22]. This is indeed what occurs in the interacting scalar field-dark matter system along the nonadiabatic solution we are considering. In fact, we can see in the

upper right panel of Fig. 3 that, as the field starts oscillating, the frequency of the oscillations increases as the field amplitude diminishes ($d\omega/d\tilde{\phi} < 0$). We can therefore expect the presence of instable modes. This is confirmed by the numerical solutions of $\delta\phi_k$ and δ_{DM} obtained from the integration of Eqs. (9)–(13). The evolution of the scalar field fluctuation $\delta\phi_k$ is shown in the lower left panel of
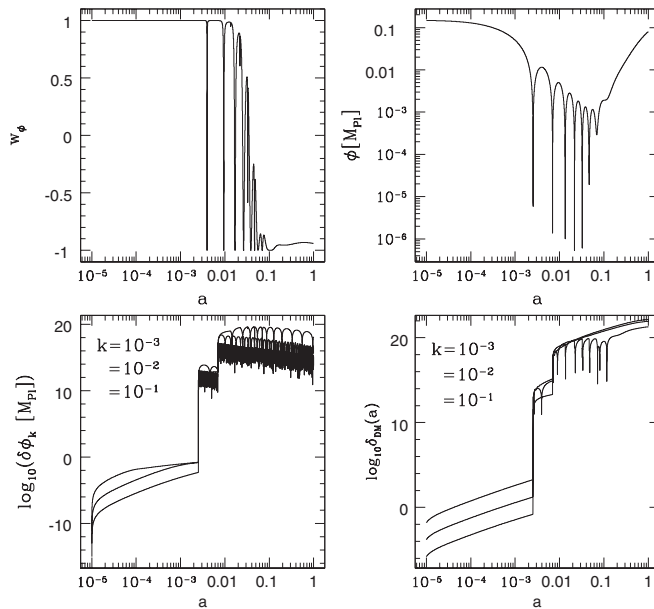
FIG. 3. Upper left panel: Evolution of the scalar field equation of state w_ϕ; upper right panel: evolution of the scalar field;. Lower left panel: Evolution of the field fluctuations $\delta\phi_k$ at $k = 10^{-3}$, 10^{-2}, and 0.1 Mpc^{-1}, respectively; lower right panel: evolution of dark matter density for k values as in the case of $\delta\phi_k$.

Fig. 3. We may notice the presence of an instability occurring roughly at the same time of the first oscillation, followed by a second stage of exponential growth at the beginning of the second oscillation. From the plot in the lower right panel, we can also see that the same instability is passed to the dark matter perturbation, which is a direct consequence of the coupling terms in Eqs. (9) and (10). Such unstable modes are similar to those found in Refs. [17,18]; in fact, by averaging over periods of time larger than the characteristic time of the oscillations, the scalar field behaves effectively as a dark energy component with a constant equation of state.

IV. CONCLUSIONS

We have studied the evolution of linear perturbations in the case of an interacting scalar field with runaway potential directly coupled to dark matter particles. We have specifically analyzed the stability of perturbations during the adiabatic evolution of the field and shown that, as a consequence of the slow-roll condition, the onset of instabilities is largely suppressed. This can be explained in terms of the adiabatic sound speed of the effective unified fluid. In fact, during the adiabatic regime, despite being negative, it assumes negligibly small values, and as a

consequence of this the growth of linear density perturbations remains stable. On the other hand, instabilities may develop in strongly coupled adiabatic regimes, with a coupling constant much greater than gravitational strength. Interestingly, during the adiabatic evolution of the field, the coupled system behaves as a single adiabatic inhomogeneous fluid. We have also shown that large instabilities can spoil the growth of linear perturbations in the case of nonadiabatic solutions characterized by large scalar field oscillations. It is well known that scalar field fluctuations are unstable during oscillatory regimes; in such a case, the scalar coupling amplifies and propagates such instabilities to the perturbations of the dark matter component.

Our analysis suggests that under minimal natural model assumptions chameleonlike cosmologies are not affected by instabilities of the perturbations and can provide a viable period of structure formation more than previously believed.

ACKNOWLEDGMENTS

[1] D. N. Spergel *et al.*, Astrophys. J. Suppl. Ser. **170**, 377 (2007); W. J. Percival *et al.*, Mon. Not. R. Astron. Soc. **327**, 1297 (2001); M. Tegmark *et al.*, Astrophys. J. **606**, 702 (2004); S. J. Perlmutter *et al.*, Astrophys. J. **517**, 565 (1999); A. Riess *et al.*, Astron. J. **116**, 1009 (1998).

[2] L. Amendola, Phys. Rev. D **62**, 043511 (2000); D. Tocchini-Valentini and L. Amendola, Phys. Rev. D **65**, 063508 (2002).

[3] L. P. Chimento, A. S. Jakubi, D. Pavon, and W. Zimdahl, Phys. Rev. D **67**, 083513 (2003).

[4] D. Comelli, M. Pietroni, and A. Riotto, Phys. Lett. B **571**, 115 (2003).

[5] A. Fuzfa and J.-M. Alimi, Phys. Rev. D **73**, 023520 (2006).

[6] T. Damour and A. M. Polyakov, Nucl. Phys. **B423**, 532 (1994).

[7] J. Khoury and A. Weltman, Phys. Rev. D **69**, 044026 (2004); Phys. Rev. Lett. **93**, 171104 (2004).

[8] A. Fuzfa and J.-M. Alimi, Phys. Rev. D **75**, 123007 (2007).

[9] S. Das, P. S. Corasaniti, and J. Khoury, Phys. Rev. D **73**, 083509 (2006).

[10] A. Fuzfa and J.-M. Alimi, Phys. Rev. Lett. **97**, 061301 (2006); G. Olivares, F. Atrio-Barandela, and D. Pavon, Phys. Rev. D **77**, 063513 (2008).

[11] G. R. Farrar and P. J. E. Peebles, Astrophys. J. **604**, 1

(2004); A. Nusser, S. S. Gubser, and P. J. E. Peebles, Phys. Rev. D **71**, 083505 (2005).

[12] L. Amendola, Phys. Rev. D **69**, 103524 (2004); P. Brax *et al.*, Phys. Rev. D **70**, 123518 (2004); G. Olivares, F. Atrio-Barandela, and D. Pavon, Phys. Rev. D **74**, 043521 (2006).

[13] T. Koivisto, Phys. Rev. D **72**, 043516 (2005).

[14] M. Kaplinghat and A. Rajaraman, Phys. Rev. D **75**, 103504 (2007).

[15] N. Afshordi, M. Zaldarriaga, and K. Kohri, Phys. Rev. D **72**, 065024 (2005).

[16] R. Bean, E. E. Flanagan, and M. Trodden, Phys. Rev. D **78**, 023009 (2008).

[17] J. Valiviita, E. Majerotto, and R. Maartens, J. Cosmol. Astropart. Phys. 07 (2008) 020.

[18] J.-H. He, B. Wang, and E. Abdalla, arXiv:0807.3471.

[19] P. Brax *et al.*, Phys. Rev. D **70**, 123518 (2004).

[20] D. F. Mota and D. J. Shaw, Phys. Rev. Lett. **97**, 151102 (2006).

[21] T. Damour and V. F. Mukhanov, Phys. Rev. Lett. **80**, 3440 (1998); A. Taruya, Phys. Rev. D **59**, 103505 (1999); S. Tsujikawa, Phys. Rev. D **61**, 083516 (2000).

[22] M. C. Johnson and M. Kamionkowski, Phys. Rev. D **78**, 063010 (2008).

[23] E. Masso, F. Rota, and G. Zsembinszki, Phys. Rev. D **72**, 084007 (2005).

The impact of cosmic dust on supernova cosmology

Pier Stefano Corasaniti[1,2]★

[1]*ISCAP, Columbia University, New York, NY 10027, USA*
[2]*Department of Astronomy, Columbia University, New York, NY 10027, USA*

ABSTRACT

Extinction by intergalactic grey dust introduces a magnitude redshift-dependent offset in the standard–candle relation of supernova Type Ia. This leads to overestimated luminosity distances compared to a dust-free universe. Quantifying the amplitude of this systematic effect is crucial for an accurate determination of the dark energy parameters. In this paper, we model the grey dust extinction in terms of the star formation history of the Universe and the physical properties of the dust grains. We focus on a class of cosmic dust models which satisfy current observational constraints. These can produce an extinction as large as 0.08 mag at $z = 1.7$ and potentially disrupt the dark energy parameter inference from future SN surveys. In particular depending on the dust model, we find that an unaccounted extinction can bias the estimation of a constant dark energy equation of state w by shifting its best-fitting value up to 20 per cent from its true value. Near-IR broad-band photometry will hardly detect this effect, while the induced decrement of the Balmer lines requires high signal-to-noise spectra. Indeed, IR-spectroscopy will be needed for high-redshift SNe. Cosmic dust extinction may also cause a detectable violation of the distance–duality relation. A more comprehensive knowledge of the physics of the intergalactic medium is necessary for an accurate modelling of intergalactic dust. Due to the large magnitude dispersion current luminosity distance measurements are insensitive to such possible extinction effects. In contrast, these must be taken into account if we hope to disclose the true nature of dark energy with the upcoming generation of SN Ia surveys.

Key words: dust, extinction – cosmology: theory.

1 INTRODUCTION

Dust particles are present in the interstellar medium causing the absorption of nearly 30–50 per cent of light emitted by stars in the Galaxy. On the other hand very little is known about dust particles which may exists outside our galactic environment. Metal lines are observed in the X-ray spectra of galaxy clusters (e.g. Buote 2002) and in high-redshift Lyman α clouds (Cowie et al. 1995; Telfer et al. 2002). Infrared (IR) emissions of distant quasars have been attributed to the presence of large amounts of dust (Bertoldi et al. 2003; Robson et al. 2004). Therefore, it has been speculated that some type of dust may be present in the low-density intergalactic medium (IGM). Since conditions in the IGM are unfavourable to the formation of dust grains, if such a component exists it originates in stars. However, it is unlikely that its properties are similar to those of interstellar grains. In fact because of the physical processes which expel dust from formation sites, intergalactic dust particles

may undergo very different selection effects (Shustov & Vibe 1995; Davies et al. 1998; Aguirre 1999).

Since the early search for distant supernovae Type Ia (SNe Ia) (Riess et al. 1998; Perlmutter et al. 1999), cosmic dust extinction was proposed to account for the observed dimming of SN luminosities at high redshift (Aguirre 1999). From several other observations, we have now compelling evidence of the cosmological nature of this signal (De Bernardis et al. 2000; Percival et al. 2001; Scranton et al. 2003; Spergel et al. 2003; Tegmark et al. 2004). There is a general consensus that it is caused by a recent accelerated phase of expansion driven by a dark energy component. This can be the manifestation of a cosmological constant, or an exotic specie of matter, or a different regime of gravity on the large scales. Distinguishing between these different scenarios has motivated a rich field of investigation.

Over the next decade, numerous experiments will test dark energy using a variety of techniques. Surveys of SN Ia such as the proposed *SNAP*, *JEDI* or ALPACA will play a leading role by providing very accurate luminosity distance measurements. The success of this programme will mostly depend on the ability to identify and reduce possible sources of systematic uncertainties affecting the SN Ia standard–candle relation.

★E-mail: pierste@astro.columbia.edu

Here, we address the impact of cosmic 'grey' dust. Our aim is to study this particular systematic effect from an astrophysical point of view. Differently from the original proposal by Aguirre (1999), we do not look for dust models which mimic the dimming of an accelerating universe. Instead, we estimate how an hypothetical cosmic grey dust model which satisfies existing astrophysical constraints may affect the dark energy parameter estimation from future SN observations. In order to do so, we evaluate the dust extinction from first principles by modelling the IGM dust in terms of the star formation history (SFH) of the Universe and the physical properties of the dust grains. This will allow us to establish how the uncertainties in the cosmic dust model, which depends on the complex physics of the IGM, relate to expected cosmological parameter errors.

This paper is organized as follows. In Section 2, we discuss the existing constraints on cosmic grey dust and evaluate the expected extinction for different IGM dust models. We evaluate the impact on the dark energy parameter inference and describe the results of our analysis in Section 3. In Section 4, we compute the signature of dust models in near-IR photometric measurements and the decrement of the Balmer lines. In Section 5, we discuss the violation of the distance–duality relation. Finally in Section 6 we present our conclusions.

2 COSMIC GREY DUST

2.1 Observational constraints

Typical dust extinction is correlated with reddening of incoming light, therefore it can be revealed by simple colour analysis. Using this technique, the interstellar extinction law has been estimated over a wide range of wavelengths (e.g. Cardelli, Clayton & Mathis 1989). However, this method is not effective for absorption caused by 'grey' dust. As suggested by Aguirre (1999), astrophysical processes which transfer dust into the IGM can preferentially destroy small grains over the large ones. Those surviving have radii $a \gtrsim 0.01 \, \mu$m. In such a case intergalactic dust may consist of particles which induce very little reddening (hence grey), while still able to cause large extinction effects.

The possibility of grey dust being entirely responsible for the dimming of high-redshift SN Ia has been now ruled out. For instance, Aguirre & Haiman (2000) showed that the density of dust necessary to reconcile SN data with a flat matter dominated universe is incompatible with the limits inferred from the far-infrared background (FIRB) as measured by the DIRBE/FIRAS experiment. Recently, Bassett & Kunz (2004b) have excluded this scenario at more than 4σ by testing the distance–duality relation. Nevertheless, the actual amount of dust in the IGM and its composition remain unknown.

Constraints on cosmic dust extinction have been inferred from colour analysis of distant quasars (Mortsell & Goobar 2003; Ostman & Mortsell 2005). Assuming the interstellar extinction law (Cardelli et al. 1989; Fitzpatrick 1999), these studies have confirmed that dust dimming cannot be larger than 0.2 mag at $z = 1$ and also indicated that if any grey dust component is present in the IGM it cannot induce extinction larger than 0.1 mag. For an early study of the effect of intergalactic extinction on cosmological expansion measurements see also Meinel (1981).

Indeed IR observations may turn out to be more informative. As an example, Aguirre & Haiman (2000) have suggested that resolving the FIRB will provide a definitive test of the IGM dust. Some

quantitative limits have also been derived from the thermal history of the IGM (Inoue & Kamaya 2003).

A more direct constraint on the density of cosmic dust particles has been obtained by Paerels et al. (2002) from the analysis of X-ray scattering halo around a distant quasar at $z = 4.30$. In particular for grains of size $\sim 1 \, \mu$m the total cosmic dust density is $\Omega_{\text{dust}}^{\text{IGM}} \lesssim 10^{-6}$, while for $0.1 \, \mu$m grains the constraint is one order of magnitude weaker. Compatible limits were also found by Inoue & Kamaya (2004) using existing bounds on SN Ia extinction and reddening.

As we will see in the next section a better knowledge of these quantities is necessary if we hope to measure the dark energy parameters with high accuracy.

2.2 Intergalactic dust extinction

In order to estimate the extinction from intergalactic grey dust, we need to determine the evolution of dust density in the IGM. Since dust particles are made of metals, the first step is to evaluate the evolution of the cosmic mean metallicity from the star formation history of the universe (Aguirre & Haiman 2000). For simplicity, we can assume that metals are instantaneously ejected from newly formed stars. In such a case, the metal ejection rate per unit comoving volume at redshift z can be written as (Tinsley 1980):

$$\dot{\rho}_Z(z) = \dot{\rho}_{\text{SFR}}(z) y_Z, \tag{1}$$

where $\dot{\rho}_{\text{SFR}}$ is the star formation rate and y_Z is the mean stellar yield, namely the average mass fraction of a star that is converted to metals. The value of y_Z is slightly sensitive to the initial mass function (IMF) and may also change with redshift if the IMF varies with time. For simplicity, we assume y_Z to be constant.

From equation (1) it follows that the mean cosmic metallicity is given by (Inoue & Kamaya 2004):

$$Z(z) = \frac{y_Z}{\Omega_{\text{b}} \rho_{\text{c}}} \int_z^{z_{\text{S}}} \dot{\rho}_{\text{SFR}}(z') \frac{dz'}{H(z')(1 + z')}, \tag{2}$$

where Ω_{b} is the baryon density, ρ_{c} is the current critical density, $H(z)$ is the Hubble rate and z_{S} redshift at which star formation began. There is little dependence on z_{S} for $z \lesssim 3$ provided that the star formation begin at $z_{\text{S}} \gtrsim 5$. Without loss of generality we set its value to $z_{\text{S}} = 10$.

Following the notation of Inoue & Kamaya (2004), we introduce a further parameter which describes the mass fraction of dust to the total metal mass, $\chi = \mathcal{D}/Z$ where $\mathcal{D}$ is the dust-to-gas ratio of the IGM. The latter depends on the mechanism which expel dust from galaxies and in principle may evolves with redshift according to the dominant process responsible for the transfer (e.g. stellar winds, SN II explosions and radiation pressure). Only recently, authors have began to study the metal enrichment of the IGM using numerical simulations (see for instance Bianchi & Ferrara 2005). As we lack of any guidance, we simply assume that the dust-to-gas ratio scales with the mean metallicity and consider χ as a constant free parameter.

Another open issue concerns the spatial distribution of dust particles in the IGM. It has been argued that a clumped grey dust would cause a dispersion of SN magnitudes larger than the observed one. Consequently if a grey dust component exists it must be nearly homogeneously distributed. However, this does not necessarily imply a strong constraint on the grey dust hypothesis. In fact, the overall dispersion at a given redshift goes roughly as $\Delta \propto 1/\sqrt{N}$ where N is the number of homogeneous dust patches along the line of sight (Aguirre 1999). Numerical simulations indicate that dust grains can diffuse in one billion years over scales of a few hundreds

Kpc (Aguirre et al. 2001). This corresponds to $N \gg 1$ for high-redshift SNe, in which case the dispersion would be small. Indeed more detailed studies are needed, but here we limit our analysis to a homogeneous dust distribution.

The differential number density of dust particles in a unit physical volume reads as

$$\frac{dn_d}{da}(z) = \frac{\chi \, Z(z) \, \Omega_b \rho_c (1+z)^3}{4\pi a^3 \varrho / 3} N(a), \qquad (3)$$

where ϱ is the grain material density and $N(a)$ is the grain size distribution normalized to unity.

The amount of cosmic dust extinction on a source at redshift z observed at the rest-frame wavelength λ integrated over the grain size distribution is then given by

$$\frac{A_\lambda(z)}{\text{mag}} = 1.086\pi \int_0^z \frac{c \, dz'}{(1+z')H(z')} \int a^2 Q_m^\lambda(a, z') \frac{dn_d}{da}(z') \, da, \quad (4)$$

where $Q_m^\lambda(a, z')$ is the extinction efficiency factor which depends on

the grain size a and complex refractive index m and c is the speed of light. Hence, the extinction at a given redshift depends on the dust properties and the metal content of the IGM. More specifically for a given cosmological background, a model of dust is specified by the grain composition, size distribution and material density, the mean interstellar yield, the star formation history and the IGM dust-to-total-metal mass ratio.

None of these parameters is precisely known, leaving us with a potentially large uncertainty about the level of cosmic dust extinction.

In the following, we assume a standard flat Λ cold dark matter (ΛCDM) model with Hubble constant $H_0 = 70$ km s^{-1} Mpc^{-1} matter density $\Omega_m = 0.30$ and baryon density $\Omega_b = 0.04$.

Several studies have suggested that the size of IGM dust grains varies in the range 0.05–0.2 μm (Ferrara et al. 1991; Shustov & Vibe 1995; Davies et al. 1998). Smaller grains ($a \lesssim 0.05$ μm) are either destroyed by sputtering or unable to travel far from formation sites as they are inefficiently pushed away by radiation pressure; in contrast grains larger than ~ 0.2 μm are too heavy and remain trapped in the gravitational field of the host galaxy. However, these analyses have provided no statistical description of the grain size abundance. A common assumption is to consider a power-law distribution, $N(a) \propto a^{-3.5}$ usually referred as the MRN model (Mathis, Rumpl & Nordsiek 1977). This describes the size distribution of dust grains in the Milky Way, but there is no guarantee that this model remains valid for IGM dust as well. On the other hand, Bianchi & Ferrara (2005) have studied through numerical simulation the size distribution of grains ejected into the IGM. Assuming an initial flat-size abundance they find that the post-processed distribution remains nearly flat and due to erosion sputtering the size range is slightly shifted towards smaller radii, 0.02–0.15 μm. We refer to this as the BF model and evaluate the grey dust extinction for both MRN and BF cases. We also consider a uniformly sized dust model corresponding to a distribution $N(a) = \delta(a)$ with $a = 0.1$ μm and for more descriptive purpose we also consider the less realistic value $a = 1.0$ μm.

The exact intergalactic dust composition is also not known, we focus silicate and graphite particles with material density
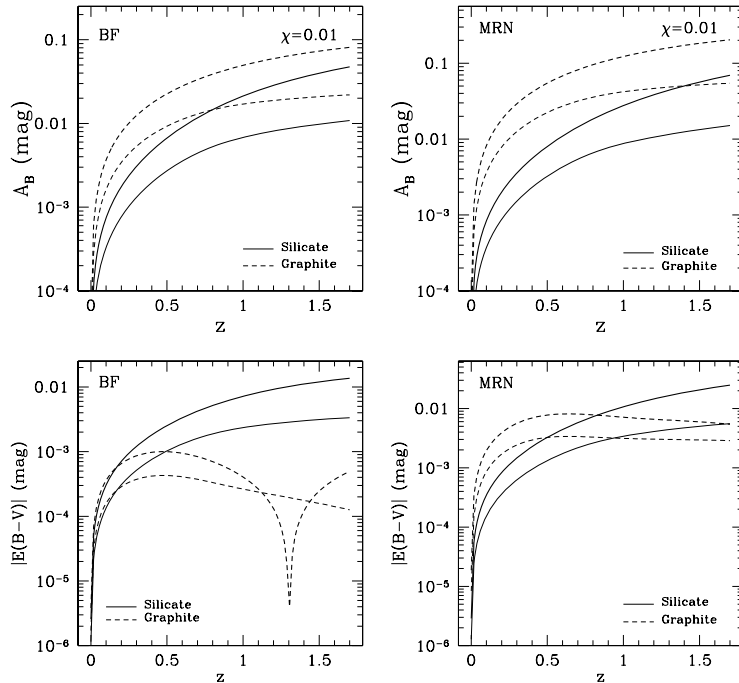
Figure 1. Cosmic grey dust extinction in the *B*-band (upper panels) and colour excess (lower panels) as function of redshift of the source for BF (left-hand panel) and MRN (right-hand panel) grain size distributions in the range 0.02–0.15 μm. Solid and dashed lines correspond to silicate and graphite grains, respectively. Thick (thin) lines correspond to high (low) SFH models.

$\varrho = 2\,\mathrm{g\,cm^{-3}}$ and optical properties specified as in Draine & Lee (1984). Using these specifications, we compute the extinction efficiency factor $Q_m^\lambda\,(a, z)$ by solving numerically the Mie equations for spherical grains (Barber & Hill 1990).

We set the mean interstellar yield to $y_Z = 0.024$ (Madau et al. 1996) corresponding to the value inferred from the Salpeter IMF (Salpeter 1955).

The star formation rate at different redshifts is known from a large body of measurements. The trend at redshifts $z \leqslant 1$ is well established with

$$\frac{\dot{\rho}_{\mathrm{SFR}}(z)}{\mathrm{M_\odot\,yr^{-1}\,Mpc^{-3}}} = 0.0158\,(1 + z)^{3.10}, \tag{5}$$

being the best fit to existing data (Hopkins 2004). On the other hand there is less agreement on the exact behaviour at higher redshifts, with recent observations favouring a flat redshift dependence (Giavalisco et al. 2004). We follow the analysis of Inoue & Kamaya (2004) and consider two possible star formation rates at $z > 1$:

$$\frac{\dot{\rho}_{\mathrm{SFR}}(z)}{\mathrm{M_\odot\,yr^{-1}\,Mpc^{-3}}} = \begin{cases} 0.156 & \text{(high SFH)} \\ 0.156\,(1 + z)^{-1.5} & \text{(low SFH)} \end{cases} \tag{6}$$

in units of solar mass $\mathrm{M_\odot}$ per year per Mpc volume.

Consistently with constraints derived in (Inoue & Kamaya 2004) we set $\chi = 0.01$. Since equation (4) is linear in this parameter the results can be simply rescaled for different values. For this particular choice, the total dust density up to $z = 4.3$ is $\Omega_{\mathrm{dust}}^{\mathrm{IGM}} \sim 10^{-6}$ which is consistent with the direct constraints found in Paerels et al. (2002). In addition, dust grains in the IGM can absorb the UV light in the Universe and re-emit in the far-IR contributing the FIRB. From the analysis of Aguirre & Haiman (2000), we find that for $\chi = 0.01$ cosmic grey dust would produce a background signal at $850\,\mu\mathrm{m}$

roughly 10 per cent of the FIRB and only 1 per cent at $200\,\mu\mathrm{m}$ thus well within the DIRBE/FIRAS limits.

In Fig. 1, we plot the *B*-band extinction (upper panels) and reddening (lower panels) as function of the redshift for BF (left-hand panels) and MRN (right-hand panels) grain size distributions. The solid and dashed lines correspond to silicate and graphite grains, respectively. Thick (thin) lines correspond to high (low) SFH models. Low SFH gives smaller extinction than the high case, consistently with the fact that low SFH produces a smaller amount of dust. The extinction is larger for graphite grains than silicate. Note also that the extinction for the BF distribution is smaller than for the MRN case. This is because in the *B*-band the efficiency factor is constant, thus equation (4) scales as $N(a)/a$. Since smaller grains are more abundant in the MRN model than in the BF case, the corresponding extinction is larger.

As it can be seen from the plots of the colour excess $|E(B - V)|$ these models cause very little reddening. Photometric measurements more accurate than 1 per cent would be needed to detect the imprint of grey dust at high redshift.

In Fig. 2, we plot the case of uniformly sized grains with radii $a = 0.1$ and $1.0\,\mu\mathrm{m}$. As expected $a = 0.1\,\mu\mathrm{m}$ grains cause an extinction nearly a factor of 10 larger than $1.0\,\mu\mathrm{m}$ particles, consistently with the $1/a$ dependence of A_B. Although these models are unrealistic from a purely astrophysical stand point, we can see that for $a = 0.1\,\mu\mathrm{m}$ the expected extinction and reddening are in agreement with those estimated assuming more realistic grain size distributions. Therefore without loss of generality we can use the uniform size approximation to study the effect of dust extinction on the dark energy parameter inference without the need to specify the exact form of $N(a)$. We can simply focusing on the typical size of grey particles and the other parameters specifying the IGM dust model.
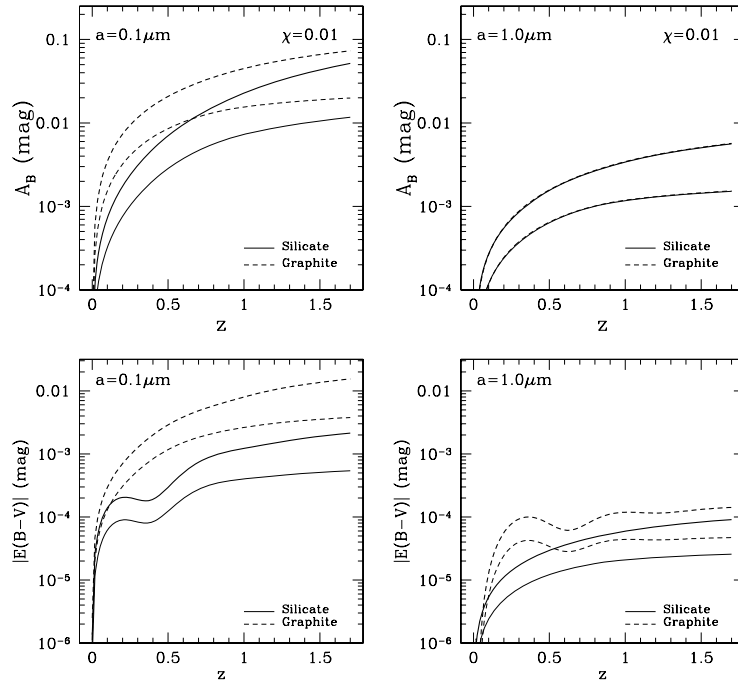
Figure 2. As in Fig. 1 for a uniform-sized grains with $a = 0.1\,\mu\mathrm{m}$ (left-hand panel) and $a = 1.0\,\mu\mathrm{m}$ (right-hand panel).

3 DARK ENERGY INFERENCE

SN Ia observations measure the luminosity distance through the standard–candle relation,

$$m_B(z) = \mathcal{M}_B + 5 \log H_0 \, d_L(z), \tag{7}$$

where $m_B(z)$ is the apparent SN magnitude in the B-band, $\mathcal{M}_B \equiv M_B - 5 \log H_0 + 25$ is the 'Hubble-constant-free' absolute magnitude and $d_L(z)$ is the luminosity distance.

Extinction modifies the standard–candle relation such that the observed SN magnitude is

$$\tilde{m}_B(z) = m_B(z) + A_B(z), \tag{8}$$

with $A_B(z)$ given by equation (4) evaluated at the B-band centre rest-frame wavelength, $\lambda = 0.44\,\mu$m. Hence SNe are systematically dimmer than in a dust-free universe, and overestimate luminosity distances. Note that the extinction term in equation (8) corresponds to a redshift-dependent magnitude offset. Previous studies of SN systematics have limited their analysis to a simple magnitude offset that linearly increases with redshift (Weller & Albrecht 2002; Kim et al. 2004). On the contrary here we approach this type of systematic from a physically motivated standpoint. Having modelled the grey dust extinction as in equation (4), we can determine how astrophysical uncertainties in the cosmic dust model parameters affect dark energy parameter inference.

3.1 Monte Carlo simulations

Using equation (8), we proceed by Monte Carlo simulating a sample of SN Ia data in the B band in a given cosmological background for dust models listed in Table 1. Then for each of these samples, we recover the background cosmology by inferring the best-fitting dark energy parameter values and uncertainties in a dust-free universe through standard likelihood analysis.

We consider a constant dark energy equation of state w and a time-varying equation of state of the form (Chevallier & Polarski 2001; Linder 2003):

$$w(z) = w_0 + w_1 \frac{z}{1+z}. \tag{9}$$

For simplicity, we focus on an SN experiment such as *SNAP* which goes very far in redshift. We assume the survey characteristics as specified in Kim et al. (2004). We consider a flat universe with $\Omega_m = 0.3$ and assume a Gaussian matter density prior $\sigma_{\Omega_m} = 0.01$.

First, we consider the case of a fiducial ΛCDM cosmology. In Fig. 3, we plot the marginalized 1 and 2σ contours in the $\Omega_m - w$ plane inferred from the data samples generated in models A (red dashed curve), B (red dotted curve) and C (black solid curve) for low (left-hand panel) and high SFH (right-hand panel). It can be seen that the overall effect of extinction is to shift the confidence regions towards more negative value of the dark energy equation of state. This is because the extinction dims SNe increasingly with the redshift. Thus inferred distances are bigger than in a dust-free universe mimicking a more rapid accelerating expansion. For fixed

Table 1. Grey dust models. For $a = 1.0\,\mu$m, we only consider silicate dust since graphite causes the same extinction.

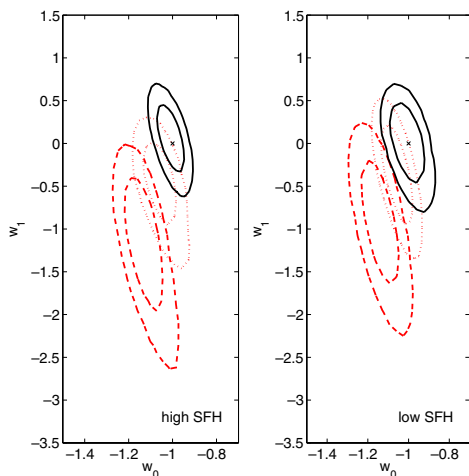|	χ	a	Type	SFH
A	0.01	0.1	Graphite	Low/high
B	0.01	0.1	Silicate	Low/high
C	0.01	1.0	Silicate	Low/high
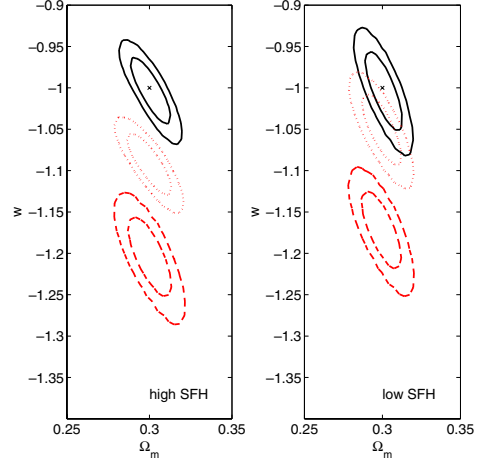
Figure 3. Marginalized 1 and 2σ confidence contours in the plane $\Omega_m - w$ plane inferred from data generated in models A (red dashed curve), B (red dotted curve) and C (black solid curve) in ΛCDM background. The left- and right-hand panels correspond to high- and low-SFH models, respectively. The cross point indicates the parameter values of the fiducial cosmology.
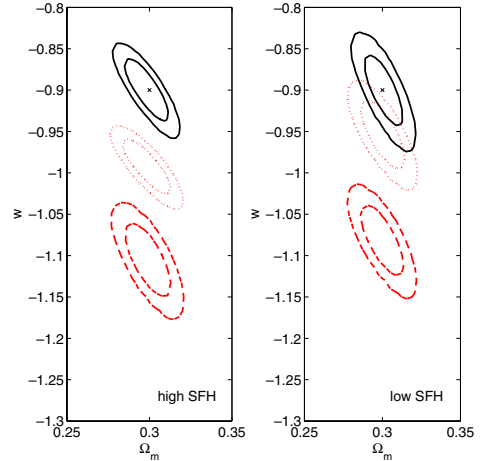
Figure 4. As in Fig. 3 with $w = -0.9$ dark energy fiducial cosmology.

values of Ω_m, this requires the dark energy equation of state to be < -1. As a result, an unaccounted extinction moves the best-fitting dark energy model many sigma away from the true one. The effect is more dramatic in model A since $A_B(z) \gtrsim 0.01$ at $z > 0.5$ while it is negligible in model C since the extinction is a factor of 10 smaller. From Fig. 3, it is evident that the existence of grey dust particles with size $\sim 0.1\,\mu$m and a dust-to-total-metal mass ratio of 0.01 in ΛCDM cosmology would cause an extinction that effectively mimic a phantom dark energy model, hence misleading us on the true nature of dark energy.

In the same manner, IGM dust may prevent us from detecting a quintessence-like dark energy. For instance in Fig. 4, we plot the confidence contours in the case of a fiducial dark energy cosmology with $w = -0.9$. Again the effect of dust extinction is to shift the confidence regions towards more negative values of w. The amplitude

**Figure 5.** Marginalized 1 and 2σ contours in the plane $w_0 - w_1$ for dust models as in Fig. 3.

Figure 6. Absolute value of colour excess $E(V-J)$, $E(R-J)$ and $E(I-J)$ versus redshift for models A (short-dashed line), B (solid line) and C (long-dashed line) in the case of high (left-hand panel) and low SFH (right-hand panel).

of this effect is similar to the previous ΛCDM case and therefore is fiducial cosmology independent.

To be quantitative, the extinction in model A causes a 20 per cent bias on the inferred values of w and 10 per cent in model B. On the contrary, model C does not affect the parameter inference.

A similar trend occurs for the constraints on the redshift parametrization (equation 9). We plot in Fig. 5 the marginalized 1 and 2σ contours in the $w_0 - w_1$ plane for a fiducial ΛCDM cosmology. Note that the size of the ellipses is altered, besides the amplitude of the shift is smaller than for the constant equation of state parameter. In fact while in model A the fiducial cosmology still lies many sigma away from the 95 per cent confidence region, it is within the 2σ contours for model B. This is because the effect of the extinction is spread over two degenerate equation of state parameters. Indeed IGM dust parameters should be included in the cosmological fit along the line suggested by Kim & Miquel (2006).

3.2 SN-gold data analysis

Can dust extinction affect the dark energy parameters inference from current SN Ia data? Despite the recent progress in the search for SN Ia, the magnitude dispersion is still large (~ 0.1 mag). Therefore, the extinction effect is well within the experimental errors. As an example, we consider the Gold sample (Riess et al. 2004) which extends up to $z_{max} \sim 1.7$ and therefore is more likely to be sensitive to grey dust extinction than the SNLS data set (Astier et al. 2006) for which $z_{max} \sim 1$. In addition, the estimated SN extinctions in the Gold data set appear to be correlated with the magnitude dispersion (Jain & Ralston 2006). We assume a flat universe with prior $\Omega_m = 0.27 \pm 0.04$. Using equation (8), we fit the Gold data accounting for the extinction of dust model A. We find $w = -0.90 \pm^{0.17}_{0.21}$ at 1σ. On the contrary, the fit without extinction gives $w = -0.96 \pm^{0.18}_{0.16}$. Thus the shift is less than 1σ. The fact that the best-fitting value is slightly > -1 should not be surprising. Comparison with the SNLS data shows that SNe in the Gold sample are slightly brighter. Nevertheless the ΛCDM is within 1σ uncertainty. Note that the direction of the shift is consistent with the result of the Monte Carlo analysis. In fact accounting for the extinction term allows models with a larger value of w to be consistent with the data.
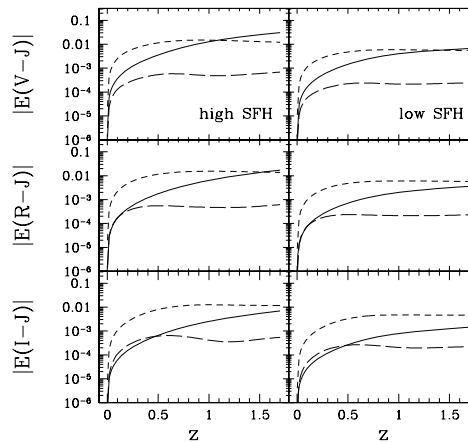
4 NEAR-IR COLOUR ANALYSIS AND DECREMENT OF BALMER LINES

As we have seen in Section 2.2, it is very difficult to detect the signature of grey dust through reddening analysis in the optical wavelengths. It has been suggested that broad-band photometry in the near-IR could be more effective. For instance, Goobar, Bergstrom & Mortsell (2002) estimated in 1 per cent the spectrophotometric accuracy necessary to detect the dust reddening in the I, J and R bands. In Fig. 6, we plot the colour excess $|E(V-J)|$, $|E(R-J)|$ and $|E(I-J)|$ for our test-bed of cosmic dust models. For low-SFH models, the colour excess is too small to be detectable with 1 per cent photometry. Only model A in the high-SFH case would be marginally distinguishable. In general, we find that our estimates are a factor of 2 smaller than those in Goobar et al. (2002). Given the difficulty of performing such accurate near-IR measurements, distinguishing the effect of cosmic dust will be a challenging task.

A possible alternative is to consider the decrement in the relative strength of the Balmer lines in the host galaxy spectrum. The recombination of ionized hydrogen atoms causes the well-known Hα and Hβ emission lines at 6563 and 4861 Å respectively, with intensity ratio $r_{H\alpha/H\beta} = 2.86$. Deviations from this value are indicative of selective absorption. For instance in the case of an extinction law with negative slope, the blue light is dimmed more than the red one, hence causing $r_{H\alpha/H\beta} > 2.86$. In Fig. 7 we plot the absolute value of the relative decrement of the Balmer lines as function of redshift for models A, B and C. We may notice that the amplitude of the decrement for models A and B is within standard accuracy of high signal-to-noise spectroscopy. It is also worth noticing that for 1.0-μm silicate grains (model C) the extinction law at $z > 0.4$ changes slope, thus causing $r_{H\alpha/H\beta} < 2.86$. Deep redshift spectroscopic surveys can in principle be used to track the trend of the Balmer line decrement and provide a complementary method to test the cosmic dust extinction. However, IR observations are necessary in order to measure the Hα emission of high-redshift sources. As an example, the SDSS catalogue of galaxy and quasar spectra spans the range $3800 < \lambda < 9200$ Å therefore the Hα cannot be detected for objects at $z \gtrsim 0.25$. The next generation of satellite surveyors will be equipped for IR-spectroscopy and capable to provide such measurements.
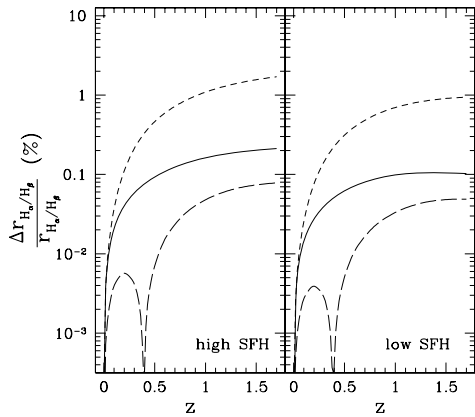
Figure 7. Relative decrement of Balmer lines for dust models as in Fig. 6.

5 TESTING DISTANCE–DUALITY RELATION

A well-known result of metric theories of gravity is the uniqueness of cosmological distances (Etherington 1933). Thus measurements of the luminosity distance $d_L(z)$ and angular diameter distance $d_A(z)$ at redshift z are linked through the duality relation (Linder 1988; Schneider, Ehlers & Falco 1992):

$$Y \equiv \frac{d_L(z)}{d_A(z)(1+z)^2} = 1. \tag{10}$$

As discussed in (Bassett & Kunz 2004b) testing this equality with high accuracy can be a powerful probe of exotic physics. Violations of the duality relation are predicted by non-metric theories of gravity, varying fundamental constants and axion–photon mixing (Bassett & Kunz 2004a; Uzan, Aghanim & Mellier 2004) just to mention a few. Also astrophysical mechanisms such as gravitational lensing and dust extinction can cause deviation from equation (10).

From equations (7) and (8), it is easy to show that in the presence of dust extinction the deviation from equation (10) is given by

$$\Delta Y(z) = 10^{1/5 A_B(z)} - 1. \tag{11}$$

Therefore if SN Ia are dimmed by intergalactic dust absorption, this would be manifested in the violation of the duality relation.

The distance–duality relation can be tested using SN Ia data and angular diameter distance measurements from detection of baryon acoustic oscillations (BAOs) in the galaxy power spectrum (Bassett & Kunz 2004b; Linder 2005). Over the next decade, several surveys of the large-scale structures will measure $d_A(z)$ with a few per cent of accuracy over a wide range of redshifts. Similarly future SN Ia surveys such as *SNAP* are designed to control intrinsic SN systematics within a few per cent which would provide luminosity distances measurements with 1–2 per cent accuracy.

We forecast the sensitivity of future distance–duality test by error propagation of equation (10). We assume the expected errors on the angular diameter distance for a galaxy survey of 10 000 deg^2 with spectroscopic redshifts as quoted in (Glazebrook & Blake 2005).

In Fig. 8, we plot equation (11) for dust models A and B in the case of high (thick lines) and low SFH (thin lines). The error bars correspond to the expected uncertainty of the distance–duality test. It can be seen that for high SFH, silicate and graphite particles of size 0.1 μm would cause a clearly detectable violation of the distance–duality relation.
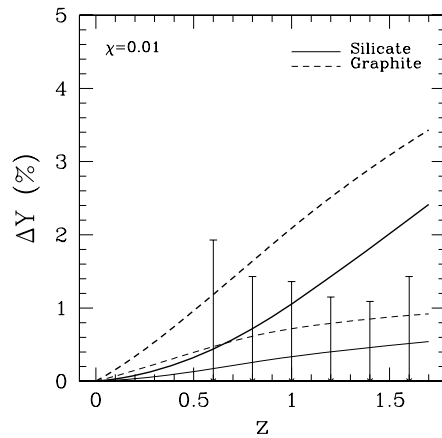

Figure 8. Percentage deviation from the distance–duality relation as function of redshift. The dashed and solid lines represent the violation caused by dust extinction for 0.1 μm graphite and silicate grains, respectively. Thick (thin) lines correspond to high (low) SFH. The error bars are the errors on the duality test as expected from upcoming SN Ia and BAO surveys. At $z < 0.5$, the errors on angular diameter distance measurements are not accurate enough for testing the duality.

6 CONCLUSION

The goal of the next generation of SN Ia experiments is to determine the dark energy parameters with high accuracy. For this to be possible, systematic effects must be carefully taken into account. Here, we have studied the impact of intergalactic grey dust extinction. We have used an astrophysical-motivated modelling of the IGM dust in terms of the star formation history of the Universe and the physical properties of the dust grains. We have identified a number of models, which satisfy current astrophysical constraints such as those inferred from X-ray quasar halo scattering and the amplitude of the FIRB emission. Although characterized by negligible reddening IGM dust may cause large extinction effects and strongly affect the dark energy parameter estimation. In particular for high star formation history, we find that dust particles with size ~0.1 μm and a total dust density $\Omega_{dust}^{IGM} \sim 10^{-6}$ may bias the inferred values of a constant dark energy equation of state up to 20 per cent. Current SN Ia data are insensitive to such effects since the amplitude of the induced extinction is well within the SN magnitude dispersion. Near-IR colour analysis would require an accuracy better than 1 per cent to detect the signature of these IGM dust particles. On the other hand, IGM dust arising from high SFH can be distinguished from the decrement of Balmer lines with high signal-to-noise spectroscopy. We have also shown that cosmic dust violates the distance–duality relation, and depending on the dust model this may be detected with future SN Ia and BAO data.

It is worth remarking that a number of caveats concerning the physics of the IGM have been assumed throughout this analysis. Specifically, we have considered a redshift-independent dust-to-total-metal mass ratio. Unfortunately, we are still lack of a satisfactory understanding of the intergalactic medium both theoretically and observationally which would allow us to make more robust prediction about IGM dust extinction. Indeed if we happen to live in a Universe with a total grey dust density $\Omega_{dust}^{IGM} \sim 10^{-6}$, extinction effects on SN Ia observations must be considered more than previously thought. The risk is to miss the discovery of the real nature of dark energy.

REFERENCES

Aguirre A., 1999, ApJ, 525, 583
Aguirre A., Haiman Z., 2000, ApJ, 532, 28
Aguirre A., Hernquist L., Katz N., Gardner J., Weinberg D., 2001, ApJ, 561, 521
Astier P. et al., 2006, A&A, 447, 31
Barber P. W., Hill S. C., 1990, Light Scattering by Particles: Computational Methods. World Scientific Publishing, Singapore
Bassett B. A., Kunz M., 2004a, ApJ, 607, 661
Bassett B. A., Kunz M., 2004b, Phys. Rev. D, 69, 101305
Bertoldi F., Carilli C. L., Cox P., Fan X., Strauss M. A., Beelen A., Omont A., Zylka R., 2003, A&A, 406, L55
Bianchi S., Ferrara A., 2005, MNRAS, 358, 379
Buote D. A., 2002, preprint (astro-ph/0210608)
Cardelli J. A., Clayton G. C., Mathis J. S., 1989, ApJ, 345, 245
Chevallier M., Polarski D., 2001, Int. J. Mod. Phys., D10, 713
Cowie L. L., Songaila A., Kim T. S., Hu E. M., 1995, AJ, 109, 1522
Davies J. I., Alton P. B., Bianchi S., Trewhella M., 1998, MNRAS, 300, 1006
De Bernardis P. et al., 2000, Nat, 404, 955
Draine T. B., Lee H. M., 1984, ApJ, 285, 89
Etherington J. M. H., 1933, Phil. Mag., 15, 761
Ferrara A., Ferrini F., Barsella B., Franco J., 1991, ApJ, 381, 137
Fitzpatrick E., 1999, PASP, 111, 755
Giavalisco M. et al., 2004, ApJ, 600, L103
Glazebrook K., Blake C., 2005, ApJ, 631, 1
Goobar A., Bergstrom L., Mortsell E., 2002, A&A, 384, 1

Hopkins A. M., 2004, ApJ, 615, 209
Inoue A. K., Kamaya H., 2003, MNRAS, 341, L7
Inoue A. K., Kamaya H., 2004, MNRAS, 350, 729
Jain P., Ralston J. P., 2006, ApJ, 637, 91
Kim A. G., Linder E. V., Miquel R., Mostek N., 2004, MNRAS, 347, 909
Kim A. G., Miquel R., 2006, Astropart. Phys., 24, 451
Linder E. V., 1988, A&A, 206, 190
Linder E. V., 2003, Phys. Rev. Lett., 90, 091301
Linder E. V., 2005, preprint (astro-ph/0507308)
Madau P., Ferguson H. C., Dickinson M. E., Giavalisco M., Steidel C. C., Fruchter A., 1996, MNRAS, 263, 1388
Mathis J. S., Rumpl W., Nordsiek K. H., 1977, ApJ, 217, 425
Mortsell E., Goobar A., 2003, JCAP, 09, 009
Ostman L., Mortsell E., 2005, JCAP, 02, 005
Paerels F., Petric A., Telis A., Helfand D. J., 2002, BAAS, 201, 97.03
Percival W. J. et al., 2001, MNRAS, 327, 1297
Perlmutter S. et al., 1999, ApJ, 517, 565
Riess A. G. et al., 1998, AJ, 116, 1009
Riess G. et al., 2004, ApJ, 607, 665
Robson I., Priddey R. S., Isaak K. G., McMahon R. G., 2004, MNRAS, 351, L29
Salpeter E. E., 1955, ApJ, 121, 161
Schneider P., Ehlers J., Falco E. E., 1992, Gravitational Lenses. Springer-Verlag, Berlin
Scranton R. et al., 2003, preprint (astro-ph/0307335)
Shustov B. M., Vibe D. Z., 1995, Astron. Rep., 39, 579
Spergel D. N. et al., 2003, ApJS, 148, 175
Tegmark M. et al., 2004, ApJ, 606, 70
Telfer R. C., Kriss G. A., Zheng W., Davidsen A. F., Tytler D., 2002, ApJ, 579, 500
Tinsley B. M., 1980, Fundam. Cosmic. Phys., 5, 287
Uzan J.-P., Aghanim N., Mellier Y., 2004, PRD, 70, 083533
Weller J., Albrecht A., 2002, PRD, 65, 103512

This paper has been typeset from a TEX/LATEX file prepared by the author.

Ⓔ

COSMIC DUST INDUCED FLUX FLUCTUATIONS: BAD AND GOOD ASPECTS

Pengjie Zhang[1,2] and Pier Stefano Corasaniti[3,4]
Received 2006 August 2; accepted 2006 November 9

ABSTRACT

Cosmic dust extinction alters the flux of Type Ia supernovae (SNe Ia). Inhomogeneities in the dust distribution induce correlated fluctuations of the SN fluxes. We find that such correlation can be up to 60% of the signal caused by gravitational lensing magnification, with an opposite sign. Therefore, if not corrected, cosmic dust extinction is the dominant source of systematic uncertainty for future SNe Ia lensing measurement, limiting the overall S/N to be ≲10. On the other hand, SN flux correlation measurements can be used in combination with other lensing data to infer the level of dust extinction. This will provide a viable method to eliminate gray dust contamination from the SN Ia Hubble diagram.

Subject headings: dust, extinction — gravitational lensing — large-scale structure of universe — supernovae: general

Online material: color figures

1. INTRODUCTION

Gravitational lensing causes several observable effects, such as distortion of galaxy shape ("cosmic shear"), variation of galaxy number density ("cosmic magnification"), and mode coupling in cosmic backgrounds. Over the coming years, measurements of these effects will provide an accurate mapping of the matter distribution in the universe (for reviews, see Bartelmann & Schneider 2001; Refregier 2003).

Recently, several other lensing reconstruction methods have been proposed. One possibility is to measure the spatial correlation of lensing-induced supernova (SN) flux fluctuations. In fact, due to lensing magnification,[5] the SN flux is altered such that $F \rightarrow F\mu \simeq F(1 + 2\kappa)$, where F is the intrinsic SN flux, μ is the lensing magnification, and κ is the lensing convergence. Intrinsic fluctuations of the SN flux are random (analogous to intrinsic galaxy ellipticities in cosmic shear measurement). In contrast, those induced by lensing magnification (see, e.g., Kantowski et al. 1995; Frieman 1996; Holz 1998; Dalal et al. 2003) are correlated with the overall matter distribution (analogous to the shear signal). Therefore, the lensing signature can be inferred either from spatial correlation measurements of SN fluxes (Cooray et al. 2006a) or from the rms of flux fluctuations of high-redshift SNe for which the lensing signal is dominant (Dodelson & Vallinotto 2006).

Gravitational lensing also induces scatter in the galaxy fundamental plane through magnification of the effective radius, $R_e \rightarrow R_e\mu^{1/2} \simeq R_e(1 + \kappa)$. Since intrinsic scatters in the fundamental plane are random, spatial correlation measurements can be used to infer the lensing signal (Bertin & Lombardi 2006). A similar analysis can be applied to the Tully-Fisher relation as well.

Astrophysical effects may limit the accuracy of these methods. For instance, extinction by cosmic gray dust can be an important

source of systematic uncertainty. This is because dust absorption changes the apparent SN flux and may induce correlation of the flux fluctuations. It also induces scatters in the fundamental plane by dimming the galaxy surface brightness and affects the Tully-Fisher relation through dimming the galaxy flux. These effects potentially cause nonnegligible systematics in the corresponding lensing measurements.

Although the existence of gray dust in the intergalactic medium (IGM) remains untested, this scenario could account for the metal enrichment of the IGM (Bianchi & Ferrara 2005, and references therein). Testing the gray dust hypothesis is also relevant for cosmological parameter inference from Type Ia supernova (SN Ia) luminosity distance measurements. Recently, Corasaniti (2006) has pointed out that gray dust models that pass current astrophysical constraints can induce a ~20% bias in the estimate of the dark energy equation of state w using the Hubble diagram of future SN Ia experiments.

In this paper, we study the impact of cosmic gray dust on SN lensing measurements, under the optimistic assumption that contaminations of reddening dust can be perfectly corrected. The effects on lensing reconstruction based on the fundamental plane and the Tully-Fisher relation can be estimated similarly. For supernovae, the key point is that extinction caused by dust inhomogeneities along the line of sight causes flux fluctuations that are anticorrelated with the lensing magnification signal and thus wash out its imprint. In particular, we find that dust-induced correlation can bias SN lensing measurements by 10%–60%. Therefore, this effect is likely to be the dominant source of systematics for future SN surveys characterized by large sky coverage and sufficiently high surface number density. If not corrected, the dust-induced correlation would limit the signal-to-noise ratio (S/N) to ≲10. This is low compared to the S/N achieved by current cosmic shear measurements (e.g., Jarvis et al. 2005; Van Waerbeke et al. 2005; Hoekstra et al. 2006) and that of proposed methods such as cosmic microwave background (CMB) lensing (Seljak & Zaldarriaga 1999; Zaldarriaga & Seljak 1999; Hu 2001; Hu & Okamoto 2002), 21 cm background lensing (Cooray 2004; Pen 2004; Zahn & Zaldarriaga 2005; Mandel & Zaldarriaga 2005), and cosmic magnification of 21 cm emitting galaxies (Zhang & Pen 2005, 2006).

Nevertheless, we suggest that measurements of the SN flux correlation still carry valuable information. In fact, in combination

---

[1] Shanghai Astronomical Observatory, Chinese Academy of Science, Shanghai, China; pjzhang@shao.ac.cn.
[2] Joint Institute for Galaxies and Cosmology (JOINGC) of SHAO and USTC.
[3] Institute for Strings, Cosmology, and Astroparticle Physics (ISCAP), Columbia University, New York, NY; pierste@astro.columbia.edu.
[4] Department of Astronomy, Columbia University, New York, NY.
[5] Throughout this paper, the term "lensing magnification" refers to both the cases of magnification ($\mu > 1$) and demagnification ($\mu < 1$). To be more specific, the spatial correlation functions and the corresponding power spectra (C_κ and $C_{\kappa\delta\tau}$) investigated hereafter are averaged over the full distribution of μ.

with other lensing data they will provide a viable method to detect and eliminate cosmic gray dust contamination from future SN Ia luminosity distance measurements.

2. DUST-INDUCED FLUX FLUCTUATIONS

The observed flux of a SN Ia at redshift z in the direction $\hat{n}$ of the sky is

$$F^{\text{obs}}(\hat{n}, z) = F \mu e^{-\tau}, \qquad (1)$$

where F is the intrinsic flux and τ is the optical depth caused by dust extinction along the line of sight. The lensing magnification can be written as $\mu \equiv 1/[(1 - \kappa)^2 - \gamma^2] \simeq 1 + 2\kappa$, with κ and γ being the lensing convergence and shear, respectively. In the presence of dust density inhomogeneities, the optical depth can be decomposed into a homogeneous and isotropic part $\bar{\tau}$ and a fluctuation $\delta\tau$ ($\tau \equiv \bar{\tau} + \delta\tau$). To first order, equation (1) reads

$$F^{\text{obs}}(\hat{n}, z) \simeq F e^{-\bar{\tau}(z)}[1 + 2\kappa(\hat{n}, z) - \delta\tau(\hat{n}, z)]. \qquad (2)$$

It is worth noting that the lensing and dust extinction terms have opposite sign. Since $\bar{\mu} = 0$ (ensemble average) and $\bar{\kappa} = 0$, the average flux of a SN Ia sample in a given redshift bin is $\bar{F}^{\text{obs}}(z) \simeq \bar{F} e^{-\bar{\tau}(z)}$.

The angular correlation of the flux fluctuations can be inferred from the estimator $\delta_F(\hat{n}, z) \equiv F^{\text{obs}}/\bar{F}^{\text{obs}} - 1$ (Cooray et al. 2006a). From equation (2) we then have $\delta_F = 2\kappa - \delta\tau$; hence, δ_F provides an estimate of the gravitational lensing only if fluctuations in the optical depth are negligible.

The lensing convergence κ is related to the three-dimensional (3D) matter overdensity δ_m by

$$\kappa = \frac{3}{2} \Omega_m \frac{H_0^2}{c^2} \int \delta_m W(\chi, \chi_s) \, d\chi, \qquad (3)$$

where $W(\chi, \chi_s)$ is the lensing geometry function. For a flat universe $W(\chi, \chi_s) = (1 + z)\chi(1 - \chi/\chi_s)$, with χ and χ_s the comoving diameter distance to the lens and source, respectively.

Following the derivation of Corasaniti (2006), the average optical depth to redshift z is

$$\bar{\tau}(z) = \frac{1}{2.5 \log e} \int_0^z \frac{d\bar{A}}{dz'} c \, dz', \qquad (4)$$

where c is the speed of light and

$$\frac{1}{2.5 \log e} \frac{d\bar{A}}{dz} = \frac{3}{4\varrho} \frac{\bar{\rho}_d(z)}{(1 + z)H(z)} \int Q_m^\lambda(a, z) N(a) \frac{da}{a}, \qquad (5)$$

where $\bar{\rho}_d$ is the average dust density, ϱ is the grain material density, a is the grain size, Q_m^λ is the extinction efficiency factor at the rest-frame wavelength λ that depends on the grain size and complex refractive index m, and $N(a)$ is the size distribution of dust particles. The extinction efficiency factor is computed by numerically solving the Mie equations for spherical grains (Barber & Hill 1990). Since dust particles are made of metals, we estimate the evolution of the average cosmic dust density $\bar{\rho}_d$ from the redshift dependence of the average cosmic metallicity as inferred by integrating the star formation history (SFH) of the universe. Such a modeling is an extension of that presented in Aguirre (1999) and Aguirre & Haiman (2000), since, in addition to estimating the amount of cosmic dust density in terms of the measured SFH, it accounts for the physical and optical properties of the dust grains.

This approach differs from that used in some of the SN Ia literature (see for instance Riess et al. 2004). In these studies the cosmic dust dimming is estimated by modeling the evolution of dust density as a redshift power law with different slopes corresponding to different cosmic dust models. More importantly, these studies assume the empirical interstellar extinction law, typically in the form inferred by Cardelli et al. (1989). However, cosmic dust particles undergo very different selection mechanisms from those of interstellar grains and therefore are unlikely to cause a similar extinction.

In this perspective, our modeling is rather robust, since the cosmic dust absorption is computed from first principles and in terms of astrophysical parameters that can be measured through several observations, such as X-ray quasar halo scattering (see Paerels et al. 2002) or high-resolution measurements of the far-infrared background (FIRB; Aguirre & Haiman 2000). For more details on these cosmic dust models and their cosmological impact, see Corasaniti (2006).

The fluctuation in the optical depth is then given by

$$\delta\tau = \frac{1}{2.5 \log e} \int_0^z \frac{d\bar{A}}{dz'} \delta_d(z') c \, dz', \qquad (6)$$

where δ_d is the fractional dust density perturbation. The resulting autocorrelation power spectrum of δ_F is

$$\frac{1}{4} C_{\delta_F}(l) = C_\kappa + \frac{1}{4} C_{\delta\tau} - C_{\kappa\delta\tau}, \qquad (7)$$

where C_κ, $C_{\delta\tau}$, and $C_{\kappa\delta\tau}$ are the angular power spectra of κ, $\delta\tau$, and the κ-$\delta\tau$ cross correlation. Using the Limber's approximation, these read (Limber 1954; Kaiser 1998)

$$\frac{l^2 C_\kappa}{2\pi} = \frac{\pi}{l} \left(\frac{3\Omega_m H_0^2}{2c^2} \right)^2 \int \Delta_\delta^2 \left(\frac{l}{\chi}, z \right) W^2(\chi, \chi_s) \chi \, d\chi, \quad (8)$$

$$\frac{l^2 C_{\delta\tau}}{2\pi} = \frac{\pi}{l} \left(\frac{1}{2.5 \log e} \right)^2 \int \Delta_{\delta_d}^2 \left(\frac{l}{\chi}, z \right) \left(\frac{d\bar{A}}{d\chi} \right)^2 \chi \, d\chi, \quad (9)$$

and

$$\frac{l^2 C_{\kappa\delta\tau}}{2\pi} = \frac{\pi}{l} \frac{3\Omega_m H_0^2}{5c^2 \log e} \int \Delta_{\delta\delta_d}^2 \left(\frac{l}{\chi}, z \right) W(\chi, \chi_s) \frac{d\bar{A}}{d\chi} \chi \, d\chi, \quad (10)$$

where $\Delta_\delta^2 \equiv k^3 P_\delta(k)/2\pi^2$ is the dimensionless matter density variance and P_δ is the matter density power spectrum. The nonlinear Δ_δ^2 is calculated using the Peacock-Dodds fitting formula (Peacock & Dodds 1996); $\Delta_{\delta\delta_d}^2$ and $\Delta_{\delta_d}^2$ are defined analogously. The spatial distribution of IGM dust is not known; the simplest assumption is that dust traces the total mass distribution. In such a case, $\Delta_{\delta_d}^2 = b_d^2 \Delta_\delta^2$ and $\Delta_{\delta\delta_d} = b_d \Delta_\delta^2$, where b_d is the dust bias. Defining $\Sigma_L \equiv (3/2)\Omega_m(H_0^2/c^2) \int W(\chi, \chi_s) \, d\chi$, one has $\delta\tau/\kappa \sim b_d \bar{A}/\Sigma_L$, and hence, $C_{\delta\tau}/C_\kappa \sim b_d^2 (\bar{A}/\Sigma_L)^2$ and $C_{\kappa\delta\tau}/C_\kappa \sim b_d(\bar{A}/\Sigma_L)$. This indicates that cosmic dust contamination is negligible only if $\bar{A}(z) \ll \Sigma_L(z)$.

We adopt a flat ΛCDM cosmology, with $\Omega_m = 0.3$, $\Omega_\Lambda = 0.7$, $h = 0.7$, $\Omega_b = 0.04$, $\sigma_8 = 0.9$, and the primordial power index $n = 1$. We assume the BBKS transfer function (Bardeen et al. 1986). For the dust extinction we limit our analysis to a test bed of four cosmic dust models studied in Corasaniti (2006). These are characterized by model parameter values motivated by astrophysical considerations. In particular, the particle size distribution is in the range 0.05–0.2 μm, consistent with the fact that smaller
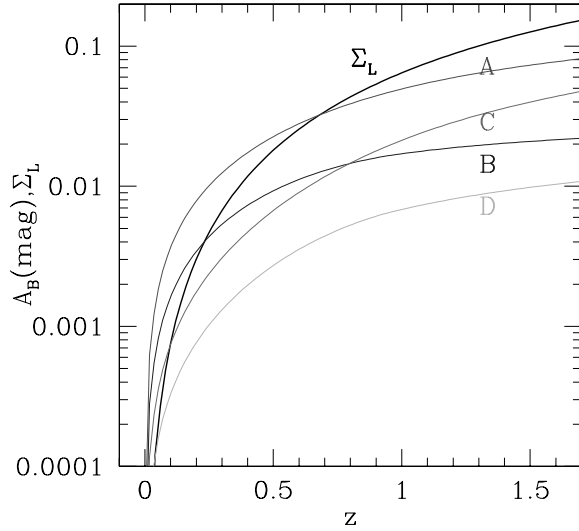
Fig. 1.—Lensing normalized matter surface density Σ_L and the B-band dust extinction A_B for different dust models (see text). Since A_B and Σ_L are comparable, dust extinction effects cannot be neglected in lensing measurements of SN flux correlation. [*See the electronic edition of the Journal for a color version of this figure.*]

Fig. 2.—Lensing and dust contamination power spectra. The upper line is the lensing convergence $l^2 C_\kappa/2\pi$. Other lines are $C_{\kappa\delta\tau} - C_{\delta\tau}/4$ for dust model A, B, C, and D, respectively, with $b_d = 1$. We have assumed all SNe to be at $z_s = 1$. Clearly, the existence of cosmic dust would degrade or even prohibit measurement of the lensing signal. [*See the electronic edition of the Journal for a color version of this figure.*]

grains are destroyed by sputtering, while larger ones remain trapped in the gravitational potential of the host galaxy (Ferrara et al. 1991; Shustov & Vibe 1995; Davies et al. 1998). The grain composition consists of silicate or graphite particles, and we consider both low and high star formation history scenarios.

Models A and B assume graphite particles with low and high SFH, respectively, while models C and D use silicate grains. The total dust density for these models is within the limits imposed by the DIRBE/FIRAS data (Aguirre & Haiman 2000) and coincides with the upper limit obtained from the analysis of X-ray quasar halo scattering (Paerels et al. 2002). These gray dust models cause little reddening of the incoming light and induce a color excess in the optical and near-IR bands smaller than 0.01 mag.

A further assumption concerns the gray dust spatial distribution, of which we have little knowledge. This model uncertainty may affect the results presented in this paper significantly. One can imagine an extreme case where gray dust distributes homogeneously. Then there will be no fluctuations in τ and thus no induced correlation in SN flux fluctuations. However, current understanding of gray dust formation implies that gray dust is associated with the overall matter distribution. So a more appropriate treatment of gray dust distribution is the bias model $\delta_d = b_d \delta_m$, as adopted in this paper. Although it is natural to expect b_d to be redshift- and scale-dependent, since we have little knowledge of it, for simplicity we assume $b_d = 1$.

From Figure 1 we can see that Σ_L is comparable to the B-band dust extinction $\bar{A}$; hence, dust contamination cannot be neglected. Therefore, $C_{\delta\tau}$ and $C_{\kappa\delta\tau}$ in equation (7) are sources of systematic errors that need to be corrected if we want to measure the convergence power spectrum.

In Figure 2 we plot the lensing convergence power spectrum $l^2 C_\kappa/2\pi$ and the dust contamination power spectrum $C_{\kappa\delta\tau} - C_{\delta\tau}/4$ for our test bed of dust models for sources at $z_s = 1$. We find that $C_{\delta\tau}$ is smaller than $C_{\kappa\delta\tau}$, mainly due to the 1/4 prefactor. Since $C_{\kappa\delta\tau}$ has a sign opposite that of the lensing signal in equation (7), its overall effect is to suppress the spatial correlation of SN Ia flux fluctuations and consequently diminish the variance and covariance of
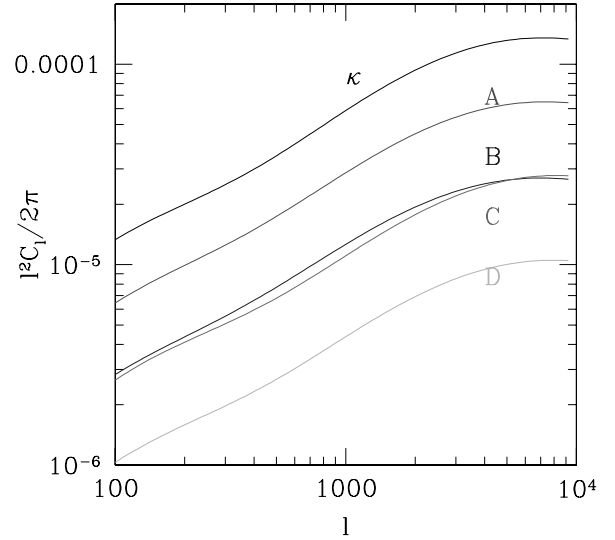
flux fluctuations. Since statistical errors on cosmological parameter constraints from SNe Ia Hubble diagram are proportional to the square root of the variance and covariance (see, e.g., Cooray et al. [2006b] for discussions), the existence of cosmic dust extinction fluctuations decreases the statistical uncertainties, although the mean dust extinction will induce a systematic bias unless corrected.

Dust contamination can be quantified by the ratio $\eta \equiv |C_{\kappa\delta\tau} - C_{\delta\tau}/4|/C_\kappa$. Since both κ and $\delta\tau$ trace the same large-scale structure (enforced by the simplification $b_d = $ constant), the multipole dependence of C_κ, $C_{\delta\tau}$, and $C_{\kappa\delta\tau}$ are similar, such that η is roughly constant. In Table 1 we list its values for sources at redshift $z_s = $ 0.5, 1.0, and 1.7, respectively. As can be seen, model A causes the largest contamination, inducing a systematic error as large as 60% of the lensing signal. Even for model D the contamination is still $\sim$10%, which is comparable to the statistical error expected from future SN Ia lensing measurements. Consequently, dust-induced systematics will be the dominant source of uncertainty for this type of measurement.

Furthermore, we find that the relative error can be approximated by $\eta = \beta b_d \bar{A}/\Sigma_L$, where $\beta \simeq 0.7$ with a dispersion <0.1 over the redshifts investigated for our test bed of dust models. This relation suggests that if we can measure η in combination with an independent lensing measurement, it would be possible to infer $\bar{A}$ given knowledge of b_d. In § 3 we discuss how these type of measurements can be used to remove cosmic dust contamination in the SN Ia Hubble diagram.

3. REMOVING COSMIC DUST CONTAMINATION

Flux fluctuations induced by lensing and extinction are small compared to intrinsic SN flux fluctuations and therefore can only be extracted statistically, except for the strongly lensed or heavily extinced SNe. Accurate lensing measurements can be obtained from a variety of astrophysical observations of cosmic shear and cosmic magnification. In combination with correlation measurements of SN fluxes, these can be used to quantify the level of cosmic

SOURCE REDSHIFT (z_s)	GRAPHITE		SILICATE	
	High SFH Model A	Low SFH Model B	High SFH Model C	Low SFH Model D
0.5......................	0.65	0.33	0.24	0.11
1.0......................	0.45	0.20	0.21	0.08
1.7......................	0.36	0.13	0.19	0.06

NOTE.—The relative error caused by extinction with respect to lensing, $\eta = |C_{\kappa\delta\tau} - C_{\delta\tau}/4|/C_\kappa$, at different source redshifts for our test bed of dust models. Here, η is roughly independent of multipole l, since shapes of C_κ, $C_{\kappa\delta\tau}$, and $C_{\delta\tau}$ are very similar.

dust extinction and provide a viable method of removing dust systematics from the SN Ia Hubble diagram. The idea is to infer η from the comparison of C_{δ_F} and C_κ. As discussed before, $\eta \simeq 0.7 b_d \bar{A}/\Sigma_L$ would allow us to measure $\bar{A}$ up to model uncertainties in b_d and measurement errors in C_{δ_F}. The estimated value of $\bar{A}$ can then be used to correct the standard candle relation of SNe Ia.

The efficiency of this method depends on the sky coverage and the SN number density of the survey. For instance, in order to measure $\bar{A}$ to 10% accuracy, the overall S/N of C_{δ_F} must be $\gtrsim 10$ $(1/\eta - 1)$. This implies that for model A, C_{δ_F} should be measured with S/N of ~ 10, while for model B, C, and D, it would require a S/N ≥ 40–100. In the case of a survey with 10^4 SNe and covering 20 deg^2 of the sky, the S/N is ~ 10 (Cooray et al. 2006a). Since S/N $\propto f_{sky}^{1/2}$, reaching S/N = 40–100 requires a factor of 20–100 times higher in sky coverage and total number of observed SNe. This could be achieved by the proposed Advanced Liquid-mirror Probe for Astrophysics, Cosmology, and Asteroids (ALPACA) experiment (Corasaniti et al. 2006).

Galaxy-quasar correlation measurements provide another method of estimating the level of cosmic dust extinction. For a given line of sight, dust extinction reduces the observed number of galaxies above flux F from $N(>F)$ to $N(>F \exp[\bar{\tau} + \delta\tau]) \simeq N(>F)[1 - \alpha(\bar{\tau} + \delta\tau)]$. Here, $\alpha = -d \ln N/d \ln F$ is the (negative) slope of the intrinsic galaxy luminosity function $N(>F)$, and we have assumed $\tau \ll 1$. Thus, dust inhomogeneities induce a fractional fluctuation $-\alpha\delta\tau$ in the galaxy number density. Since $\delta\tau$ is correlated with the matter density field, dust extinction induces a correlation between foreground galaxies and background galaxies (quasars) such that $w_{fb}(\theta) = -\alpha\langle\delta\tau(\boldsymbol{\theta}')\delta_g^f(\boldsymbol{\theta}' + \boldsymbol{\theta})\rangle$, where, δ_g^f is the foreground galaxy number overdensity. On the other hand, lensing-induced fluctuations in galaxy number density are $2(\alpha - 1)\kappa$ (Bartelmann & Schneider 2001), where the -1 term accounts for the fact that lensing magnifies the surface area and thus decreases the number density. Because of the different dependence on the slope α, the signal of extinction and lensing can be separated simultaneously.

The Sloan Digital Sky Survey (SDSS) galaxy-quasar cross correlation measurement (Scranton et al. 2005) is consistent with the $\alpha - 1$ scaling and thus the dust contamination, if any, remains subdominant. Our dust models are consistent with this measurement, since the expected fractional contribution from dust extinction is

$$-\frac{\alpha}{2(\alpha - 1)}\frac{\langle\delta\tau\delta_g^f\rangle}{\langle\kappa\delta_g^f\rangle} \sim -\frac{\alpha}{(\alpha - 1)} \times (0.27, 0.11, 0.08, 0.03)$$

for dust model A, B, C, and D, respectively. However, such measurement is already at the edge of providing interesting dust

constraints. For instance, model A induces, at $\theta = 0.01°$, a negative correlation with amplitude $\sim 0.003\alpha b_g$, where b_g is the SDSS galaxy bias. This signal is already very close to the measurement uncertainty (Fig. 7 of Scranton et al. [2005], and the averaged $\langle\alpha\rangle \simeq 1$ from their Table 2). In principle, by combining color and flux dependences of the galaxy-quasar cross correlation and the color-galaxy cross correlation, it will be possible to separate the contribution of lensing magnification, gray, and reddening simultaneously (B. Menard 2006, private communication). The next generation of galaxy surveys, such as the Large Synoptic Survey Telescope (LSST), ALPACA, or PanSTARRS will provide foreground galaxy-quasar measurements that can achieve a S/N $\gg 10$. This will allow us to discriminate the above dust models unambiguously, thus providing accurate constraints on the cosmic dust extinction and clustering properties.

4. CONCLUSIONS

Several new methods have been proposed for inferring the lensing magnification signal from a variety of correlation measurements. These involve SN Ia flux, the fundamental plane, and Tully-Fisher relation of optical galaxies. In this paper we have shown that contamination of cosmic dust extinction may severely degrade such measurements. As an example, inhomogeneities in the cosmic dust distribution may limit the S/N of SN lensing measurements to the $\lesssim 10$ level.

Billions of galaxies can be detected/resolved by the Square Kilometer Array[6] through the 21 cm hyperfine transition line emission, which is not affected by dust extinction. In such a case the only scatters other than intrinsic ones in the Tully-Fisher relation ($L \propto v_c^4$) are induced by lensing magnification, $L \to L(1 + 2\kappa)$. Therefore, lensing reconstruction using these galaxies is an attractive possibility, since it is free of some systematics associated with cosmic shear, such as shape distortion induced by the point-spread function.

On the other hand, measurements of SN flux spatial correlation or galaxy-quasar cross-correlation will constrain the amount of cosmic gray dust and its clustering properties to high accuracy. This will provide not only a better understanding of IGM dust physics, but also a valuable handing of dust contamination in the SN Ia Hubble diagram.

[6] SKA, see: http://www.skatelescope.org/.

REFERENCES

Aguirre, A. 1999, ApJ, 525, 583
Aguirre, A., & Haiman, Z. 2000, ApJ, 532, 28
Barber, P. W., & Hill, S. C. 1990, Light Scattering by Particles: Computational Methods (Singapore: World Scientific)
Bardeen, J. M., Bond, J. R., Kaiser, N., & Szalay, A. S. 1986, ApJ, 304, 15
Bartelmann, M., & Schneider, P. 2001, Phys. Rep., 340, 291
Bertin, G., & Lombardi, M. 2006, ApJ, 648, L17
Bianchi, S., & Ferrara, A. 2005, MNRAS, 358, 379
Cardelli, J. A., Clayton, G. C., & Mathis, J. S. 1989, ApJ, 345, 245
Cooray, A. 2004, NewA, 9, 173
Cooray, A., Holz, D. E., & Huterer, D. 2006a, ApJ, 637, L77
Cooray, A., Huterer, D., & Holz, D. E. 2006b, Phys. Rev. Lett., 96, 021301
Corasaniti, P. S. 2006, MNRAS, 372, 191
Corasaniti, P. S., LoVerde, M., Blake, C., & Crotts, A. 2006, MNRAS, 369, 798
Dalal, N., Holz, D. E., Chen, X., & Frieman, J. A. 2003, ApJ, 585, L11
Davies, J. I., Alton, P. B., Bianchi, S., & Trewhella, M. 1998, MNRAS, 300, 1006
Dodelson, S., & Vallinotto, A. 2006, Phys. Rev. D, 74, 063515
Ferrara, A., Ferrini, F., Barsella, B., & Franco, J. 1991, ApJ, 381, 137
Frieman, J. 1996, preprint (astro-ph/9608068)
Hoekstra, H., et al. 2006, ApJ, 647, 116

Holz, D. E. 1998, ApJ, 506, L1
Hu, W. 2001, Phys. Rev. D, 64, 083005
Hu, W., & Okamoto, T. 2002, ApJ, 574, 566
Jarvis, M., Jain, B., Bernstein, G., & Dolney, D. 2006, ApJ, 644, 71
Kaiser, N. 1998, ApJ, 498, 26
Kantowski, R., Vaughan, T., & Branch, D. 1995, ApJ, 447, 35
Limber, D. N. 1954, ApJ, 119, 655
Mandel, K. S., & Zaldarriaga, M. 2006, ApJ, 647, 719
Paerels, F., Petric, A., Telis, A., & Helfand, D. J. 2002, BAAS, 34, 1264
Peacock, J. A., & Dodds, S. J. 1996, MNRAS, 280, L19
Pen, U. 2004, NewA, 9, 417
Refregier, A. 2003, ARA&A, 41, 645
Riess, A. G., et al. 2004, ApJ, 607, 665
Scranton, R., et al. 2005, ApJ, 633, 589
Seljak, U., M. Zaldarriaga 1999, Phys. Rev. Lett., 82, 2636
Shustov, B. M., & Vibe, D. Z. 1995, Astron. Rep., 39, 578
Van Waerbeke, L., Mellier, Y., & Hoekstra, H. 2005, A&A, 429, 75
Zahn, O., & Zaldarriaga, M. 2006, ApJ, 653, 922
Zaldarriaga, M., & Seljak, U. 1999, Phys. Rev. D, 59, 123507
Zhang, P. J., & Pen, U. L. 2005, Phys. Rev. Lett., 95, 241302
———. 2006, MNRAS, 367, 169

P H Y S I C A L   R E V I E W   L E T T E R S

Toward a Universal Formulation of the Halo Mass Function

P. S. Corasaniti[1] and I. Achitouv[1]

[1]*Laboratoire Univers et Théories (LUTh), UMR 8102 CNRS, Observatoire de Paris, Université Paris Diderot,
5 Place Jules Janssen, 92190 Meudon, France*

We compute the dark matter halo mass function using the excursion set formalism for a diffusive barrier with linearly drifting average which captures the main features of the ellipsoidal collapse model. We evaluate the non-Markovian corrections due to the sharp filtering of the linear density field in real space with a path-integral method. We find an unprecedented agreement with N-body simulation data with deviations $\lesssim 5\%$ over the range of masses probed by the simulations. This indicates that the excursion set in combination with a realistic modeling of the collapse threshold can provide a robust estimation of the halo mass function.

A large body of evidence suggests that dark matter (DM) plays a crucial role in the formation, evolution, and spatial distribution of cosmic structures [1–4]. Central to the DM paradigm is the idea that initial density fluctuations grow under gravitational instability eventually collapsing into virialized objects, the halos. It is inside these gravitationally bounded structures that cooling baryonic gas falls in to form the stars and galaxies we observe today. Consequently, the study of the halo mass distribution is of primary importance in cosmology. In the Press-Schechter approach [5], the number of halos in the mass range $[M, M + dM]$ can be written as

$$\frac{dn}{dM} = f(\sigma) \frac{\bar{\rho}}{M^2} \frac{d\log\sigma^{-1}}{d\log M}, \qquad (1)$$

where $\bar{\rho}$ is the background matter density and $\sigma(M)$ is the root-mean-square fluctuation of the linear dark matter density field smoothed on a scale $R(M)$ (containing a mass M), with

$$\sigma^2(M) \equiv S(M) = \frac{1}{2\pi^2} \int dk k^2 P(k) \tilde{W}^2[k, R(M)], \qquad (2)$$

where $P(k)$ is the linear DM power spectrum and $\tilde{W}(k, R)$ is the Fourier transform of the smoothing (filter) function in real space. In Eq. (1), the function $f(\sigma) = 2\sigma^2 \mathcal{F}(\sigma^2)$, known as "multiplicity function," encodes the effects of the gravitational processes responsible for the formation of halos through its dependence on $\mathcal{F}(S) \equiv dF/dS$, with $F(S)$ being the fraction of mass elements in halos of mass $>M(S)$. Hereafter, we will refer to $f(\sigma)$ simply as the halo mass function.

The collapse of halos is a highly nonlinear gravitational process that has been primarily investigated using numerical N-body simulations. Over the past few years several numerical studies have measured $f(\sigma)$ at few percent uncertainty level for various cosmologies and using different halo detection algorithms (see, e.g., [6–9]). On the other hand, we still lack an accurate theoretical estimation of the halo mass function. Following the seminal work by

Press and Schechter [5], the excursion set theory [10] has provided us with a consistent mathematical framework for computing $f(\sigma)$ from the statistical properties of the initial DM density field (for a review, see [11]). Nevertheless, an analytical derivation of $f(\sigma)$ can be obtained only for a top-hat filter in Fourier space (sharp-k filter). Although Monte Carlo simulations can be used in the case of generic filters (see, e.g., [10,12]), most of the work in the literature has focused on the modeling of the halo collapse conditions and the comparison with N-body simulations using numerical and semianalytical techniques which assume the sharp-k filter (see, e.g., [13–16]). However, such a smoothing function does not correspond to any realistic halo mass definition. The issue has been recently addressed by Maggiore and Riotto [17] who made a major contribution by introducing a path-integral method that extends the analytical computation to generic filters.

In this Letter we present the first thorough comparison against N-body simulation data of the excursion set mass function with top-hat filter in real space for a stochastic barrier model which encapsulates the main characteristics of the ellipsoidal collapse of dark matter. A detailed derivation of these results is given in a companion paper [18].

Let us consider the DM density contrast, $\delta(\mathbf{x})$, smoothed on the scale R,

$$\delta(\mathbf{x}, R) = \int d^3 y W(|\mathbf{x} - \mathbf{y}|, R)\delta(\mathbf{y}), \qquad (3)$$

where $W(\mathbf{x}, R)$ is the smoothing function in real space. Bond *et al.* [10] have shown that at any given point in space, $\delta(\mathbf{x}, R)$ performs a random walk as a function of the variance of the smoothed linear density field $S(R)$. The formation of halos of mass M corresponds to trajectories $\delta(S)$ crossing for the first time a barrier B at $S(M)$, i.e., $\delta(S) = B$, where the value of B depends on the assumed gravitational collapse criterion. In the case of the spherical collapse model [19] $B = \delta_c$, that is the linearly extrapolated density of a top-hat spherical perturbation at the time of collapse. Then, the evaluation of $f(\sigma)$

is reduced to computing the rate at which the random walks hit the barrier for the first time, i.e., $\mathcal{F}(S) = dF/dS$.

The nature of the random walk depends on the filtering procedure, which specifies the relation between the smoothing scale R and the halo mass definition M. For a sharp-k filter, $\tilde{W}(k, R) = \theta(1/R - k)$, and Gaussian initial conditions, $\delta(S)$ performs a Markov random walk described by the Langevin equation:

$$\frac{\partial \delta}{\partial S} = \eta_\delta(S), \qquad (4)$$

with noise $\eta_\delta(S)$ such that $\langle \eta_\delta(S) \rangle = 0$ and $\langle \eta_\delta(S) \eta_\delta(S') \rangle = \delta_D(S - S')$, where δ_D is the Dirac function (for the full derivation, see, e.g., [11,17]). As first shown in [10], the probability distribution of the trajectories satisfies a simple Fokker-Planck equation with absorbing boundary at $\delta(S) = \delta_c$. The resulting first-crossing distribution gives the Press-Schechter formula [5] with the correct normalization factor (the so called "extended Press-Schechter").

However, the spherical collapse model is a simplistic approximation of the nonlinear evolution of matter density fluctuations. As shown in [20], initial Gaussian perturbations are highly nonspherical. Hence, the collapse of a homogeneous ellipsoid (see, e.g., [21]) should provide a far better description. In such a model the critical density threshold depends on the eigenvalues of the deformation tensor, which are random variables with probability distributions that depend on the statistics of the linear density field [14,20,22–26]. Because of this, the barrier behaves as a stochastic variable itself, performing a random walk whose properties depend on the specificities of the collapse model considered. For example, Sheth *et al.* [14] showed that the average of the barrier is $\langle B(S) \rangle = \delta_c[1 + \beta(S/\delta_c^2)^\gamma]$, with $\beta = 0.47$ and $\gamma = 0.615$.

The recent analysis of halos in N-body simulations has confirmed the stochastic barrier hypothesis [27]. Maggiore and Riotto [28] have modeled these features assuming a stochastic barrier with average $\langle B(S) \rangle = \delta_c$ and variance $\langle (B - \langle B(S) \rangle)^2 \rangle = SD_B$, where D_B is a constant diffusion coefficient. Here, we improve their barrier model by assuming a Gaussian diffusion with linearly drifting average $\langle B(S) \rangle = \delta_c + \beta S$ [13] which approximates the ellipsoidal collapse prediction [14]. Recently, a general analysis of nondiffusive moving barriers has been presented in [29]. However, this work has mainly focused on the mass function in the presence of non-Gaussian initial conditions rather than the comparison with Gaussian N-body simulations. The Langevin equation for this barrier model reads as

$$\frac{\partial B}{\partial S} = \beta + \eta_B(S), \qquad (5)$$

where the noise $\eta_B(S)$ is characterized by $\langle \eta_B(S) \rangle = 0$ and $\langle \eta_B(S) \eta_B(S') \rangle = D_B \delta_D(S - S')$. Without loss of generality we can assume that $\eta_B(S)$ and $\eta_\delta(S)$ are uncorrelated. It is convenient to introduce $Y = B - \delta$ and rewrite Eqs. (4) and (5) as a single Langevin equation:

$$\frac{\partial Y}{\partial S} = \beta + \eta(S), \qquad (6)$$

with white noise $\eta(S) = \eta_\delta(S) + \eta_B(S)$ such that $\langle \eta(S) \rangle = 0$ and $\langle \eta(S) \eta(S') \rangle = (1 + D_B) \delta(S - S')$. The Fokker-Planck equation associated with Eq. (6) and describing the probability $\Pi_0(Y_0, Y, S)$ reads as

$$\frac{\partial \Pi_0}{\partial S} = -\beta \frac{\partial \Pi_0}{\partial Y} + \frac{1 + D_B}{2} \frac{\partial^2 \Pi_0}{\partial Y^2}, \qquad (7)$$

where we indicate with the "0" underscore the fact that Π_0 is associated to a Markov process.

The system starts at $\{\delta(0) = 0, B(0) = \delta_c\}$; hence, we solve Eq. (7) with initial condition $Y_0 = \delta_c$ and impose the absorbing boundary condition at $Y = 0$, i.e., $\Pi_0(0, S) = 0$. For a concise notation we omit the dependence on Y_0 and simply refer to $\Pi_0(Y, S)$. By rescaling the variable $Y \to \tilde{Y} = Y/\sqrt{1 + D_B}$, a factorizable solution can be found in the form $\Pi_0(\tilde{Y}, S) = U(\tilde{Y}, S) \exp[c(\tilde{Y} - cS/2)]$, where $c = \beta/\sqrt{1 + D_B}$ and $U(\tilde{Y}, S)$ satisfies a diffusion equation. Using the above initial condition, the latter can be solved with the image method [30] or by Fourier transform. Thus, we obtain

$$\Pi_0(Y, S) = \frac{e^{(\beta/1 + D_B)(Y - Y_0 - \beta(S/2))}}{\sqrt{2\pi S(1 + D_B)}}$$
$$\times \left[e^{-(Y - Y_0)^2/(2S(1 + D_B))} - e^{-(Y + Y_0)^2/(2S(1 + D_B))} \right].$$
$$(8)$$

In general the Fokker-Planck equation for random walks with nonlinear biased diffusion and absorbing boundary condition does not have an exact analytic solution. This is why we have assumed the linearly drifting average barrier rather than the prediction of the ellipsoidal collapse model [14]. As we will see later, having an exact analytical solution greatly simplify the evaluation of the corrections due to the smoothing function. We should remark that the above solution is defined only for $Y > 0$. Since the number of trajectories is conserved, then the first-crossing distribution is obtained by deriving $\int_0^S \mathcal{F}_0(S') dS' = 1 - \int_0^\infty \Pi_0(Y, S) dY$ from which we finally obtain the Markovian mass function

$$f_0(\sigma) = \frac{\delta_c}{\sigma \sqrt{1 + D_B}} \sqrt{\frac{2}{\pi}} e^{-(\delta_c + \beta \sigma^2)^2/(2\sigma^2(1 + D_B))}, \quad (9)$$

for $\beta = 0$ and $D_B = 0$ this coincides with the standard Markovian solution that gives the extended Press-Schechter formula, while for $D_B = 0$ we recover the solution for the nondiffusive linearly drifting barrier [11].

As mentioned earlier, a crucial point of this derivation is the assumption of the sharp-k filter. In numerical N-body simulations the mass definition depends on the halo detection algorithm. For instance, the spherical overdensity (SOD) halo finder detects halos as groups of particles in a spherical regions of radius R_Δ containing a density

$\rho_\Delta = \Delta\bar\rho$, with Δ an overdensity parameter usually fixed to $\Delta = 200$. Thus, the halo mass is $M = 4/3\pi R_\Delta^3 \rho_\Delta$, which is equivalent to having a sharp-x filter, or $\tilde{W}(k, R) = 3/(kR)^3[\sin(kR) - kR\cos(kR)]$. However, in this case the stochastic evolution of the system is no longer Markovian. Hence, in order to consistently compare the excursion set mass function with SOD estimates of $f(\sigma)$ it is necessary to account for the correlations induced by $\tilde{W}(k, R)$.

Maggiore and Riotto [17] have shown that these correlations can be treated as perturbations about the "zero"-order Markovian solution. More specifically, the noise variable $\eta(S)$ acquires a perturbative correction, $\langle\eta(S)\eta(S')\rangle = (1 + D_B)\delta_D(S - S') + \Delta(S, S')$, which in the case of the sharp-x filter can be approximated by $\Delta(S, S') \approx \kappa S(S' - S)/S'$. For the concordance Λ cold DM model we find $\kappa \approx 0.47$. Using the path-integral technique described in [17], we compute the corrections to $\Pi_0(Y, S)$ to first order in κ. These consist of a "memory" term,

$$\Pi_1^m = -\partial_Y \int_0^S dS' \Delta(S', S)\Pi_0^f(Y_0, 0, S')\Pi_0^f(0, Y, S - S'),$$
(10)

and a "memory-of-memory" term

$$\Pi_1^{m-m} = \int_0^S dS' \int_{S''}^S dS'' \Delta(S', S'')\Pi_0^f(Y_0, 0, S')$$
$$\times \Pi_0^f(0, 0, S'' - S')\Pi_0^f(0, Y, S - S'),$$
(11)

where $\Pi_0^f(Y_0, 0, S)$, $\Pi_0^f(0, Y, S)$ and $\Pi_0^f(0, 0, S)$ in Eqs. (10) and (11) are given by the finite time corrections of the Markovian solution near the barrier (see [18]). We find

$$\Pi_0^f(Y_0, 0, S) = \frac{aY_0}{S^{3/2}\sqrt{\pi}} e^{-(a(Y_0 + \beta S)^2)/(2S)},$$
(12)

$$\Pi_0^f(0, Y, S) = \frac{aY}{S^{3/2}\sqrt{\pi}} e^{-(a(Y - \beta S)^2)/(2S)},$$
(13)

$$\Pi_0^f(0, 0, S) = \frac{1}{S^{3/2}}\sqrt{\frac{a}{2\pi}},$$
(14)

where $a \equiv 1/(1 + D_B)$. Equation (10) can be computed analytically, we find

$$\Pi_1^m = -\tilde\kappa aY_0 \partial_Y\left\{Ye^{a\beta(Y - Y_0 - \beta(S/2))}\mathrm{Erfc}\left[\sqrt{\frac{a}{2S}}(Y_0 + Y)\right]\right\},$$
(15)

where $\tilde\kappa = \kappa/(1 + D_B)$. Since Eq. (15) is linear in Y, the integration of $\mathcal{F}_1^m(S) = -\partial/\partial S \int_0^\infty \Pi_1^m dY$ vanishes. Thus, the memory term does not contribute to the mass function independently of the barrier behavior (in agreement with [17]). The double integral in the memory-of-memory term cannot be computed analytically, in such a case we expand the integrands in powers of β (given that from the ellipsoidal collapse we expect $\beta < 1$). By computing $\mathcal{F}_1^{m-m}(S) = -\partial/\partial S \int_0^\infty \Pi_1^{m-m} dY$ and expressing the results directly in terms of $f(\sigma)$, we find the non-Markovian correction to zero order in β (i.e., $\beta = 0$) to be

$$f_{(1),\beta=0}^{m-m}(\sigma) = -\tilde\kappa\frac{\delta_c}{\sigma}\sqrt{\frac{2a}{\pi}}\left[e^{-(a\delta_c^2)/(2\sigma^2)} - \frac{1}{2}\Gamma\left(0, \frac{a\delta_c^2}{2\sigma^2}\right)\right],$$
(16)

where $\Gamma(0, z)$ is the incomplete Gamma function. Not surprisingly this expression coincides with the memory-of-memory term in [17]. The first order correction in β is given by

$$f_{1,\beta^{(1)}}^{m-m}(\sigma) = -\beta a\delta_c\left[f_{1,\beta=0}^{m-m}(\sigma) + \tilde\kappa\mathrm{Erfc}\left(\frac{\delta_c}{\sigma}\sqrt{\frac{a}{2}}\right)\right],$$
(17)

and the second order reads

$$f_{1,\beta^{(2)}}^{m-m}(\sigma) = \beta^2 a\delta_c\tilde\kappa\left\{a\delta_c\mathrm{Erfc}\left(\frac{\delta_c}{\sigma}\sqrt{\frac{a}{2}}\right)\right.$$
$$+ \sigma\sqrt{\frac{a}{2\pi}}\left[e^{-(a\delta_c^2)/(2\sigma^2)}\left(\frac{1}{2} - \frac{a\delta_c^2}{\sigma^2}\right)\right.$$
$$\left.\left. + \frac{3}{4}\frac{a\delta_c^2}{\sigma^2}\Gamma\left(0, \frac{a\delta_c^2}{2\sigma^2}\right)\right]\right\}.$$
(18)

For $\beta/(1 + D_B) < 1$, corrections $\mathcal{O}(>\beta^2)$ are negligible (see, e.g., Fig. 1); hence, Eqs. (9) and (16)–(18) give the relevant contributions to the mass function.

In principle the values of β and D_B as well as their redshift and cosmology dependence can be predicted in a given halo collapse model by computing the average and variance of the probability distribution of the collapse density threshold. However, this requires a dedicated study which should also include environmental effects that have been shown to play an important role in determining the
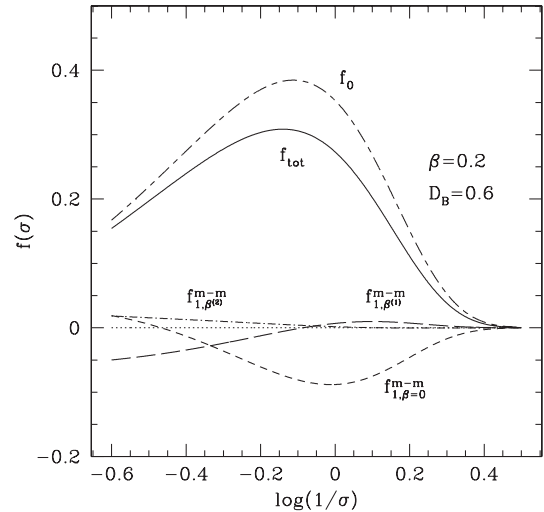

FIG. 1. Contributions to the halo mass function f_{tot} (solid line) for $\beta = 0.2$ and $D_B = 0.6$. The different curves correspond to the Markovian mass function f_0 (dotted line), $f_{1,\beta=0}^{m-m}$ (short-dashed line), $f_{1,\beta^{(1)}}^{m-m}$ (long-dashed line), $f_{1,\beta^{(2)}}^{m-m}$ (dot–short dashed line), $f_{1,\beta^{(3)}}^{m-m}$ (dot–long dashed line).
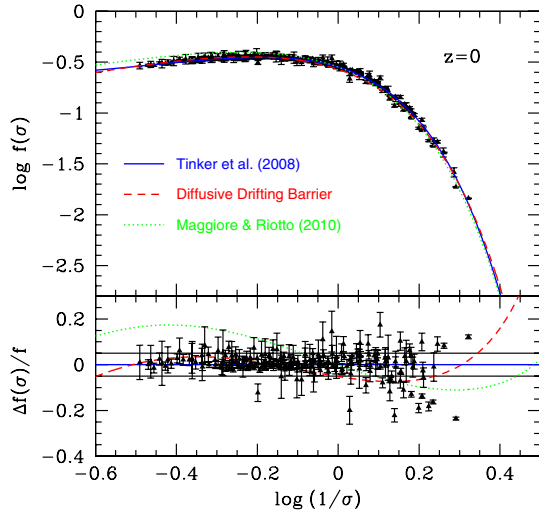
FIG. 2 (color online).   Halo mass function at $z = 0$ given by the Tinker *et al.* fitting formula for $\Delta = 200$ (solid blue line), diffusing drifting barrier with $\beta = 0.057$ and $D_b = 0.294$ (red dashed line) and Maggiore and Riotto [28] with $D_B = 0.235$ (green dotted line). Data points are from [6]. (Lower panel) Relative difference with respect to the Tinker *et al.* fitting formula. The thin black solid lines indicates 5% deviations.

properties of the halo mass distribution [26]. This goes beyond the scope of this Letter.

Here, we take a different approach. β and D_B are physical motivated model parameters which we can calibrate against N-body simulation data, and test whether the mass function derived above provides an acceptable description of the data. To this purpose we use the measurements of the halo mass function obtained by Tinker *et al.* [6] using SOD(200) on a set of WMAP–1 yr and WMAP–3 yr cosmological N-body simulations. For these cosmological models the spherical collapse predicts $\delta_c = 1.673$ at $z = 0$ (for a detailed calculation see [8]). Using such a value, we run a likelihood Markov chain Monte Carlo analysis to confront the mass function previously computed against the data at $z = 0$. We find the best fit values to be $\beta = 0.057$ and $D_b = 0.294$. The data strongly constrain these parameters, with errors $\sigma_\beta = 0.001$ and $\sigma_{D_B} = 0.001$, respectively. In Fig. 2 (upper panel) we plot the corresponding mass function (red dash line) against the simulation data together with the four-parameter fitting formula by Tinker *et al.* [6] for $\Delta = 200$ (solid blue line). For comparison we also plot the diffusive barrier case by Maggiore and Riotto [28] which best fit the data with $D_B = 0.235$ (green dotted line). In Fig. 2 (lower panel) we plot the relative differences with respect to the Tinker *et al.* formula. We may notice the remarkable agreement of the diffusive drifting barrier with the data. Deviations with respect to Tinker *et al.* (2008) are $\lesssim 5\%$ level over the range of masses probed by the simulations. This is quite impressive given the fact that our

model depends only on two physically motivated parameters.

In the upcoming years a variety of astrophysical observations will directly probe dn/dM. The halo mass function we have derived here can provide the base for a through cosmological model comparison. In a companion paper we will describe in detail the derivation of these results, as well as extensive discussion on the redshift evolution of the mass function and halo bias.

[1] D. N. Spergel *et al.*, Astrophys. J. Suppl. Ser. **148**, 175 (2003).
[2] M. Tegmark *et al.*, Phys. Rev. D **69**, 103501 (2004).
[3] D. Clowe *et al.*, Astrophys. J. **648**, L109 (2006).
[4] R. Massey *et al.*, Nature (London) **445**, 286 (2007).
[5] W. H. Press and P. Schechter, Astrophys. J. **187**, 425 (1974).
[6] J. Tinker *et al.*, Astrophys. J. **688**, 709 (2008).
[7] M. Crocce *et al.*, Mon. Not. R. Astron. Soc. **403**, 1353 (2010).
[8] S. Courtin *et al.*, Mon. Not. R. Astron. Soc. **410**, 1911 (2011).
[9] S. Bhattacharya *et al.*, Astrophys. J. **732**, 122 (2011).
[10] J. R. Bond, S. Cole, G. Efstathiou, and G. Kaiser, Astrophys. J. **379**, 440 (1991).
[11] A. R. Zentner, Int. J. Mod. Phys. D **16**, 763 (2007).
[12] W. J. Percival, Mon. Not. R. Astron. Soc. **327**, 1313 (2001).
[13] R. K. Sheth, Mon. Not. R. Astron. Soc. **300**, 1057 (1998).
[14] R. K. Sheth, H. J. Mo, and G. Tormen, Mon. Not. R. Astron. Soc. **323**, 1 (2001).
[15] J. Shen, T. Abel, H. J. Mo, and R. K. Sheth, Astrophys. J. **645**, 783 (2006).
[16] J. Zhang and L. Hui, Astrophys. J. **641**, 641 (2006).
[17] M. Maggiore and A. Riotto, Astrophys. J. **711**, 907 (2010).
[18] P. S. Corasaniti and I. Achitouv (unpublished).
[19] J. E. Gunn and J. R. Gott III, Astrophys. J. **176**, 1 (1972).
[20] A. G. Doroshkevich, Astrophyzika **3**, 175 (1970).
[21] D. J. Eisenstein and A. Loeb, Astrophys. J. **439**, 520 (1995).
[22] J. M. Bardeen, J. R. Bond, N. Kaiser, and A. Szalay, Astrophys. J. **304**, 15 (1986).
[23] P. Monaco, Astrophys. J. **447**, 23 (1995).
[24] E. Audit, R. Teyssier, and J.-M. Alimi, Astron. Astrophys. **325**, 439 (1997).
[25] J. Lee and S. Shandarin, Astrophys. J. **500**, 14 (1998).
[26] V. Desjacques, Mon. Not. R. Astron. Soc. **388**, 638 (2008).
[27] B. Robertson, A. Kravtsov, J. Tinker, and A. Zentner, Astrophys. J. **696**, 636 (2009).
[28] M. Maggiore and A. Riotto, Astrophys. J. **717**, 515 (2010).
[29] A. De Simone, M. Magiore, and A. Riotto, Mon. Not. R. Astron. Soc. **412**, 2587 (2011).
[30] S. Redner, *A Guide to First-Passage Processes* (Cambridge University Press, Cambridge, U.K., 2001).